Thèse N°41077 présentée pour obtenir le grade de

DOCTEUR DE L'UNIVERSITE LILLE1
Spécialité : Ingénierie des Fonctions Biologiques

École Doctorale
Sciences de la Matière, du Rayonnement et de l'environnement

Par
Guillaume Bastin

RGS4 Cysteine Residues at Positions 2 and 12 Influence its Intracellular Trafficking and Function

Les Résidus Cystéines en Positions 2 et 12 de RGS4 Influencent son Trafic Intracellulaire et ses Fonctions

Thèse co-dirigée par :
Dr. Christian Rolando, Docteur à l'université Lille1
Pr. Scott Heximer, Professeur à l'université de Toronto

Soutenue le 29janvier 2013, devant le jury composé de :

Dr. Xavier Coumoul	**Rapporteur**
Dr. Philippe Chavrier	**Rapporteur**
Dr. Christian Rolando	**Co-Directeur de thèse**
Pr. Scott Heximer	**Co-Directeur de thèse**
Dr. Caroline Tokarski	**Examinateur**

À ma soeur,

Acknowledgments

First I would like to thank Scott Heximer for teaching me the underwear of science, what is required to make your way up to the lasts floors. How writing a paper, importance of functional assays. I have to salute him for keeping me as he, for the most, funded my entire project; the way we made that happening allowed me having a normal life while regular international students barely can afford a beer to cheers on weekends. Finally, beyond a lot of things I could thank him for giving credit to my ideas and my way to think science.

En deuxième lieu, je remercie Christian Rolando car ce doctorat n'aurait pas été possible sans lui. Je désire aussi le remercier pour m'avoir accueilli à bras ouverts et de manière répétée. Il fut présent à chaque étapes importantes de mon cursus… les premiers pas dans une équipe de recherche, la confirmation quelques années plus tard et dernièrement le doctorat. Je pense que peu d'étudiants eurent le privilège d'observer l'évolution d'une équipe de recherche et leurs projets sur une telle période. Croyez bien que cela m'apporte une idée claire me permettant d'imaginer le futur sereinement. Enfin, merci pour les conseils, simples, clairs et bien placés.

Je désire remercier mes parents. Je pense que leur éducation me sert énormément aujourd'hui, la rigueur et la simplicité y sont importantes. Ils m'ont aussi supporté à tous les niveaux du doctorat. Leur présence même éloignée fut très importante.

La famille proche, le fréro et min oncle, les grand mères pour toujours prendre l'opportunité de partager de bons repas en famille, couscous, lapin ou carbonnade flamande. Vive eul ch'nor. Mi jm'in fou ch'pe dire ch'que j've dans s'te partie.

Les amis proches. Le nombre de fêtes, repas et sorties organisés lors de mes retours fut autant indécent que remarquable. Nous n'en avons pas fini. Merci à la LDC team association, son président, secrétaire et trésorier, Pulp, Pek, Tom, PO, Languette, Piquette ainsi que pôle Brest, Paris et Réunion. Pour les autres, Mathilde d'amour, Capucine, Steph, Bib, Léo-nore, Thibault, Julie, Julien, Gus et Déborah.

Enfin je voudrai remercier les personnes m'ayant fait passer de bons moments au Canada, principalement Victor, mon colloque, Antonin, célèbre malgrès lui, Cheyanne, longue histoire, Stéphanie, mémé, Anja, Roxy, Matthieu, Vahideh, Avais, Mélanie, Fran.

I would like to thank the twelve undergrad students I had the chance to supervise. They did much as they both abrogated my working limits and provided me fun. Finally I liked having the privilege to be part of your evolution. Hope you all reach your goals guys. Special mention to Kevin Singh and Aliya Nurmohamed.

I wanted to end in thanking particularly KavEsh Dissanayake for whom I have much pleasure misspelling his name. Very much fun having you around in the lab buddy, smart, good and fun guy. Hey dude, so much fun in L.A. huh! Let's rent a car and play American football on Santa Monica's beaches! See you soon in London.

Résumé

Les protéines RGS (Regulator of G-protein Signaling) sont des inhibiteurs des voies de signalisation des protéines G. RGS4 atténue l'activité de protéines G dans plusieurs tissus tel que la diminution de son activité peut conduire à la bradycardie, cardiomyopathie diabétique, l'invasion de cellule cancéreuse du sein, résistance à l'insuline, intolérance au glucose et inflammation intestinale. RGS4 est localisé à la membrane plasmique ainsi que dans des compartiments intracellulaires, cependant, son mode de trafique intracellulaire reste méconnu. Il est important de noter que la présence de RGS4 dans les compartiments intracellulaires n'est pas expliquée alors que l'inhibition des protéines G nécessite la présence de RGS4 à la membrane plasmique. En utilisant 2-BP- un inhibiteur de palmitoylation, nous avons empêché RGS4 d'atteindre la membrane cytoplasmique et compartiments intracellulaires. Nous avons donc muté Cystéine2 et 12, deux principaux sites de palmitoylation de RGS4, et montré que Cys2 participe à la localisation aux compartiments intracellulaires et Cys12 contribue à la localisation à la membrane cellulaire. En utilisant l'imagerie de cellule vivante par microscopie confocale, nous avons pu comparer la localisation de RGS4 avec TGN38, un marqueur du trans-Golgi. Nous observons que RGS4WT colocalize de manière modérée avec TGN38, que la mutation de Cys2 empêche RGS4 de s'associer aux endosomes alors que la mutation de Cys12 a cantonné RGS4 aux endosomes contenant TGN38. Ces données suggèrent que Cys2 et 12 affectent la localisation et le mode de trafique intracellulaire de RGS4. Confirmant l'importance des palmitoylations dans la régulation des fonctions de RGS4, la mutation de Cys2 diminua l'inhibition de la voie de signalisation dirigée par Gq alors que la mutation de Cys12 empêcha totalement RGS4 de fonctionner. La diminution de l'expression de DHHC3 et 7, deux enzymes de palmitoylation connues pour réguler RGS4, modifie la localisation de RGS4 aux endosomes et membrane cytoplasmique ainsi que sa fonctionnalité. L'expression de DHHC3 et 7 dominants négatifs mit en évidence le rôle de DHHC3 et 7 pour amener RGS4 dans les compartiments intracellulaires en interagissant avec Cys2. Pour finir, la famille des protéines Rab est connue pour faciliter le trafic intracellulaire de protéines à travers divers compartiments vésiculaires et endosomaux par migration rétrograde et antérograde. En utilisant l'imagerie de cellule vivante par microscopie confocale, nous

avons mis à jour une forte colocalisation entre RGS4 et Rab11 au niveau des compartiments intracellulaires. Puis, nous nous sommes demandé si Rab11, un élément important de l'exocytose et recyclage protéique, pouvait être important dans la localisation de RGS4 à la membrane plasmique. En effet, l'expression de Rab11 dominant négatif diminua la présence de RGS4 à la membrane plasmique ainsi que sa capacité à inhiber la voie de signalisation du récepteur muscarinique M1. En parallèle, nous avons montré que la quantité de RGS4 présent à la membrane plasmique était régulée par les méchanismes d'endocytose. Précisément, la surexpression de Rab5a, responsable de l'endocytose dépendante des protéines clathrines, diminua la présence de RGS4 à la membrane plasmique et sa capacité à inhiber la voie de signalisation du récepteur muscarinique M1. Ensemble, ces résultats sont la première étude démontrant l'importance des protéines Rab dans le trafic intracellulaire de RGS4 avec la participation de DHHC3 et 7 ainsi que de ses sites de palmitoylation N-terminaux. Ces travaux confèrent une base de données pour des études ultérieures visant à développer des stratégies permettant d'accroître les fonctionnalités de RGS4. En espérant traiter des pathologies associées à la diminution de son expression et présence à la membrane cytoplasmique.

Abstract

RGS proteins (Regulator of G-protein Signaling) are potent inhibitors of heterotrimeric G-protein signaling. RGS4 attenuates G-protein activity in several tissues such that loss of its function may lead to bradycardia, diabetic cardiomyopathy, breast cancer cell invasion, insulin resistance, glucose intolerance, and intestinal inflammation. RGS4 has been localized to both plasma membrane and intracellular pools, however, the nature of its intracellular trafficking remains to be elucidated. G-protein inhibition requires the presence of RGS4 at the plasma membrane. Interestingly, we prevented both endosomal and plasma membrane targeting with the addition of 2-BP, an inhibitor of palmitoylation. Following introduction of mutations at Cysteine2 and Cysteine12, two putatively important palmitoylation sites in RGS4, we show Cys2 palmitoylation contributes to RGS4 localization on intracellular endosomes and Cys12 palmitoylation contributes to its plasma membrane targeting. Using live cell confocal microscopy, we set out to compare the localization of RGS4 with TGN38, a trans-Golgi and endosomal marker. We found that RGS4WT only partially colocalized with TGN38 on endosomal structures. Notably, the Cys2 mutant completely prevented RGS4 association with endosomal structures whereas Cys12 mutant was found to be exclusively RGS4 endosomal colocalized with TGN38. These data suggest palmitoylation of Cys2 and Cys12 differentially affects the localization and trafficking of RGS4. Consistent with a role for palmitoylation in regulating RGS4 function mutation of Cys2 reduced RGS4 inhibition of Gq mediated signaling whereas the Cys12 mutation completely abrogated RGS4 function. Knock downs of DHHC3 and 7, two palmitoylating enzymes known to regulate RGS4, impaired RGS4 endosomal, plasma membrane targeting and function. The expression of DHHC3 and 7 dominant negatives highlighted the role of DHHC3 and 7 to direct RGS4 to endosomal compartments via Cys2. Lastly, the Rab family of proteins is known to facilitate intracellular trafficking of proteins through various vesicular and endosomal compartments via both retrograde and anterograde pathways. We used live cell imaging confocal microscopy to uncover marked colocalization between RGS4 and Rab11 on intracellular endosomes. We asked whether Rab11, a key element in endosomal protein recycling and exocytosis, may be important for

plasma membrane targeting of RGS4. Indeed, when co-expressed dominant negative Rab11, RGS4 showed reduced plasma membrane targeting and an impaired ability to inhibit M1 muscarinic receptor mediated signaling. In parallel, we showed that RGS4 plasma membrane levels could also be regulated at the level of the endocytic machinery. Specifically, overexpression of Rab5a, the Rab family member required for clathrin-mediated endocytosis, decreased the presence of RGS4 at the plasma membrane and impaired its M1 muscarinic receptor inhibitory function. Taken together, these data provide the first evidence of Rab-dependent intracellular trafficking of RGS4 with the participation of DHHC3 and 7, and its N-terminal palmitoylation sites. These novel findings provide a strong rationale for future studies aimed at developing new strategies to increase the function of RGS4.

Table of content

Abbreviations

Arf: ADP Ribosylation Factor

Cys: Cysteine

DEP/DHEX: Dishevelled, Egl-10 and Pleckstrin domain/ DEP+Helix

DHHC: Asp-His-His-Cys

DNA: Deoxyribo Nucleic Acid

Dpc: (embryo time)

e-NOS: endothelial-Nitric Oxide Synthase

ERK: Extracellular Regulated Signals

GAP: GTPase Activating Protein

GDP: Guanosine DiPhosphate

GEF: GDP/GTP Exchange Factor

GGT-I: GernaylGeranyl Transferase-I

GIRK: G protein-coupled Inwardly-Rectifying potassium channels

GPCR: G-Protein Coupled Receptor

GTP: Guanosine TriPhosphate

GTPase: GTP hydrolase

Hpf: (embryo time)

Il: Interleukin

IRI: Ischemic Reperfusion Injury

KO: Knocked Out

MAPK: Mitogen-Activated Protein Kinases

MHC: Major Histocompatibility Complex

NMDA: *N*-Methyl-D-aspartic Acid

N-terminal: Protein NH2- terminal

PD: Parkinson Disease

PI: phosphoinositide

PSD-95: Postsynaptic Density Protein 95

REP: Rab Escort Proteins

RGS: Regulator of G-protein Signaling

RNA: Ribo Nucleic Acid

SNARE: Soluble N-tehylmaleimide-sensitive factor Attachment protein REceptor

TGN: Trans Golgi Network

WT: Wild Type

PartI

1. GPCR generalities

G protein coupled receptors are the most commonly targeted entities by pharmaceutical companies, they represent up to one third of drugs on the market and generate over 100 billion euros in sales revenues per year[1]. Their agonists are as diversified as their functions; they can be, for example, peptides, hormones, growth factors, odorants, neurotransmitters and light. Studying and characterizing GPCRs and the pathways they regulate is therefore of significant academic interest.

1.1. GPCR structures and signaling

Heterotrimeric G-proteins are made up of one α subunit and a stable βɣ heterodimer. They are responsible for transducing an extracellular signal received by 7-transmembrane domain receptors (7TDMRs) to the inside of the cell. Transmembrane domains are helical in nature and anchor the receptors to membranes (Figure1. Page15). A 7TDMR is activated by the binding of an agonist to its extracellular domain[2]. The conformational changes of the receptor in response to agonist promote its guanine nucleotide exchange factor (GEF) activity toward the coupled Gα subunit to result in replacement of GDP by a GTP moiety[3]. The rate-limiting step in the sequence is the release of GDP from the Gα subunit[4], whereas GTP-binding occurs efficiently due to its higher intracellular concentrations. The Gβɣ heterodimer is displaced from GαGTP; so that GαGTP and Gβɣ may separate to interact with their respective downstream effectors[5] (figure2.page16). This is the starting point of signaling pathways and cascades.

1.2. G-proteins and their main signaling pathways activation

GPCRs couple to four main classes of Gα subunits that determine the functional cellular response. The different subclasses are Gαs, Gαi/o, Gαq/11, Gα12/13[6] accordingly

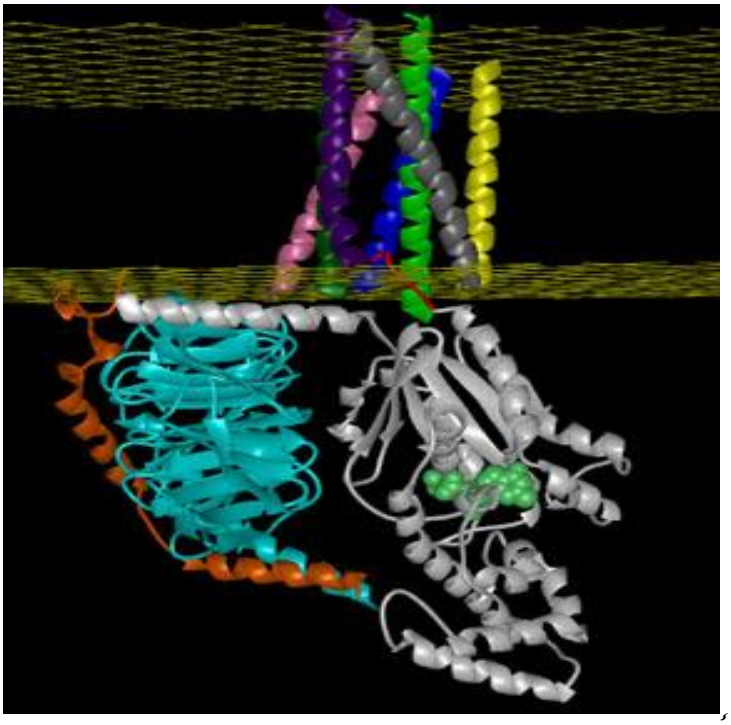

Figure1: Ribbon schematic representation of a complete GPCR including the 7transmembrane receptor coupled to intracellular Gα itself bound by Gβɣ protein. 7transmembrane receptor's N-terminal tail is extracellular and responsible for agonist binding. C-terminal is intracellular and conjugate with interacting protein such as Gα protein.

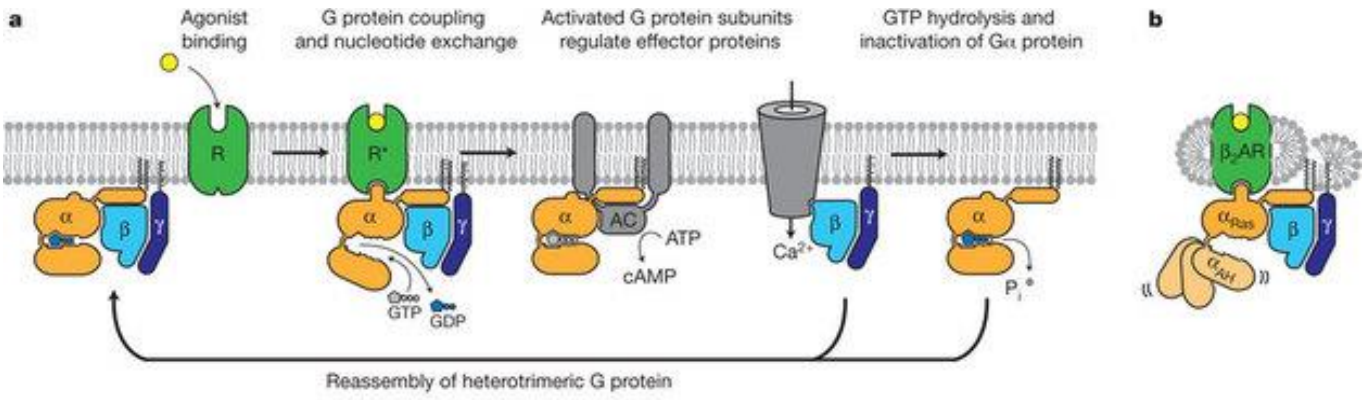

Figure2: G protein cycle for the β2AR–Gs complex. a) Extracellular agonist binding to the β2AR leads to conformational rearrangements of the cytoplasmic ends of transmembrane segments that enable the Gs heterotrimer (α, β, and ɣ) to bind the receptor. GDP is released from the α subunit upon formation of β2AR–Gs complex. The GTP binds to the nucleotide-free α subunit resulting in dissociation of the α and βɣ subunits from the receptor. The subunits regulate their respective effector proteins adenylyl cyclase (AC) and Ca2+ channels. The Gs heterotrimer reassembles from a and βɣ subunits following hydrolysis of GTP to GDP in the α subunit. b) The purified nucleotide-free β2AR–Gs protein complex maintained in detergent micelles. The Gαs subunit consists of two domains, the Ras domain (αRas) and the α-helical domain (αAH). Both are involved in nucleotide binding. In the nucleotide-free state, the αAH domain has a variable position relative the αRas domain. From Søren G. F. Rasmussen et al. 2011.

to primary amino acid sequence and each subclass activates relatively unique set of downstream effector pathways. For instance Gαs-type (stimulatory) activates different ACs while Gαi-type (inhibitory) inhibits AC function[7]. Gαq/11-type activates PLCβ leading to hydrolysis of PIP2 into DAG and IP3, the second messenger that leads to activation of intracellular calcium channel (IP3R)[7]. Gα12/13-type activation leads to Rho and Rho kinase activation[7]. As described above many of the known signals are mediated by the Gα subunit, however Gβɣ released from the activated heterotrimer is also capable of activating a wide number downstream effectors such as PLA, PLC and ion channels including K^+ and Ca^{2+} channels[8;9]. The downstream pathway activated can be specific to the nature of the βɣ subunit. Notably many combinations are possible as since there exist 12ɣ and 5β different subunits that may combine in numerous different heterodimer pairs[10]. Not all the combinations are compatible due to affinities or lack of stabilities.

1.3. GPCR desensitization

After GPCR activation and once the Gα-GTP protein away, G-protein receptor kinase (GRK) proteins phosphorylate the C-terminal tail of the receptor, such that it becomes a binding target for arrestins which promote internalization, and receptor inactivation[11]. However, once activated the G-proteins continue to signal until they are deactivated. The duration of G-protein activation determines the duration of its signaling activity. Thus, the signal activation by Gα-GTP and Gβɣ will be terminated once the herotrimer reforms which requires Gα-GDP binding Gβɣ. Gα subunit is a natural GTP hydrolyzing enzyme, it is therefore a matter of time for Gα-GTP to be converted to the inactive Gα-GDP. However, the intrinsic rate of GTP hydrolysis is relatively slow so that G-α can spend minutes to hydrolyze GTP into GDP+ Pi[12]. The RGS superfamily of proteins act as specific GTPase Activating Proteins (GAPs) for G-protein α-subunits and thus promote an accelerated rate of GTP hydrolysis by up to 2000-fold (Figure3.p18)[13]. As will be discussed in detail later, the GAP activity is a crucial factor in the ability of RGS proteins to terminate GPCR signaling. Thus, most RGS proteins act as potent inhibitors of GPCRs function and as such represent important targets of therapeutic strategies in the treatment and prevention of diseases that are associated with increased GPCR signaling.

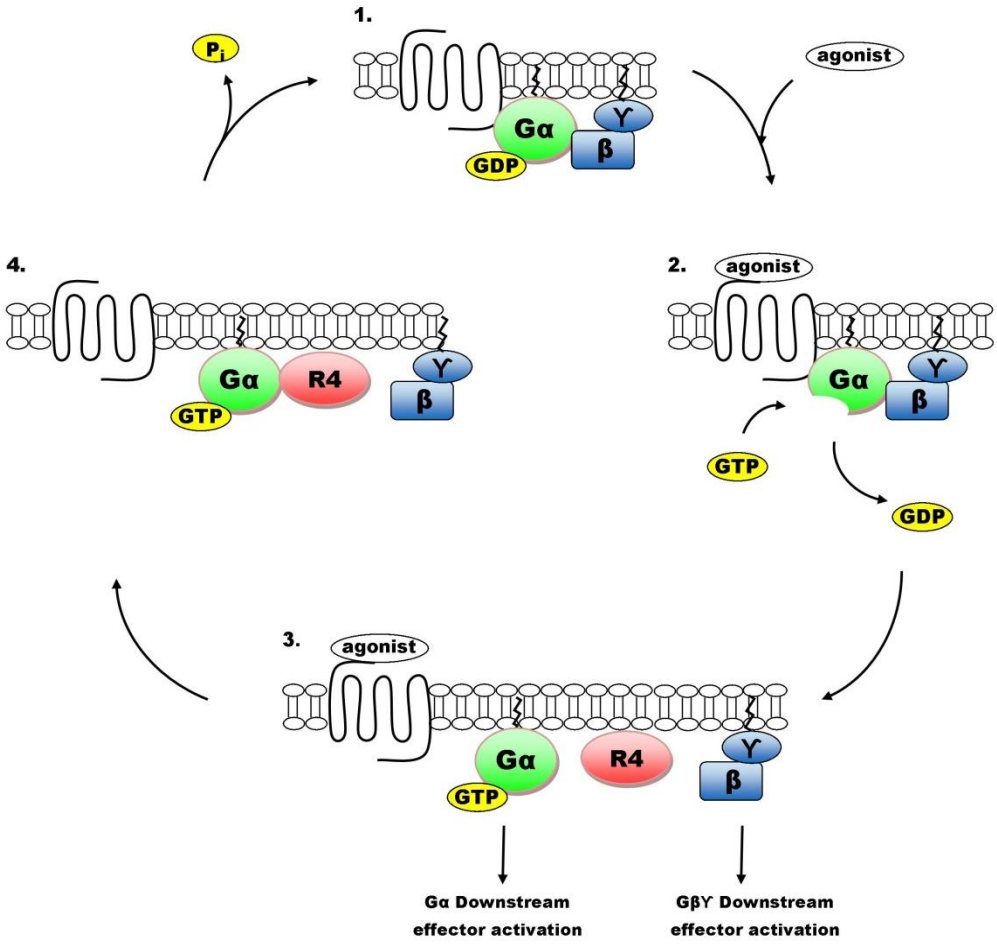

Figure3: G-Protein Coupled Receptor Cycle (GPCR). This cycle is schematically divided in 4 steps. 1. GPCR is in resting state, no agonist. The GDP-α form of the G-protein is having a high affinity to the β-Ɣ subunit, therefore they are forming one unique entity and are binding to a 7-transmembrane domain receptor. 2. The receptor is activated by an agonist, this changes its conformation and induces the release of GDP of the G protein α-subunit. In the cytosol, GTP is present in a higher concentration than GDP, as a consequence GTP will preferentially replace the expelled GDP. GTP-α form of the G-protein shows a lower affinity to β-Ɣ. 3. β-Ɣ subunits separate from GTP-α and are activating respectively their downstream effector. Note that β and Ɣ stay bound to each other. 4. The cycle terminates when the α-subunit of the G-protein hydrolyzes the GTP in GDP+ Pi. The α-subunit hydrolyzes spontaneously the GTP in GDP+ Pi, although in stabilizing the reaction, RGS proteins allows the speed of the reaction increasing by 2000fold. In binding to GDP, the α-subunit recovers a high affinity to β-Ɣ. Thus they stop activating their downstream effector and come back together to reform the GDP-α-β-Ɣ entity. The GPCR is now capable of processing a new external signal. From Bastin. G et al. 2010.

1.4. G-protein trafficking

The intracellular trafficking of the G-proteins is not well understood. The majority of data so far has focused on G-protein localization to the plasma membrane[14] since their main function are thought to require signal transduction from the plasma membrane. Since neither Gα nor Gβɣ have a transmembrane domain, they require lipid modification in order to anchor to the plasma membrane[15]. βɣ is capable of binding the plasma membrane due to farnesylation (-C15 unsaturated fatty acid) or geranylgeranylation (-C20 unsaturated fatty acid) on the ɣ subunit. These lipids modifications are stable, linked via a covalent thioether bond, and provide a constitutive binding of the βɣ subunit to plasma membrane or endomembranes. Gα subunits show a higher degree of heterogeneity with respect to their lipid modifications. Gαi are myristoylated (-C14) and palmitoylated (-C16) while Gαq/11 may be twice palmitoylated, but in both cases palmitoylation is the prerequisite for plasma membrane targeting. Interestingly, since palmitoylation is reversible it is possible to regulate G-protein binding to the plasma membrane. Gα-GDP and βɣ subunits undergoing compartmentalized specific lipid modifications may not be obligatory partners inside the cell. Moreover, G-βɣ and Gα have been shown to activate distinct downstream effectors in the cell, leading to the hypothesis that Gα and βɣ may not traffic together through the same endo-compartments.

2. RGS family

The RGS protein superfamily consists of about 35 proteins in the mammalian genome, all of which contain a well-conserved 120 amino acid region[16], the “RGS-box”, that is responsible for Gα-GTP-binding and markedly accelerated GTP hydrolysis[17;18]. The RGS-box that embodies the RGS protein GAP activity is found rarely in the absence of other regulatory protein modules. Similarities among regulatory modules among RGS family members have allowed definition of multiple subfamily groups within the RGS superfamily. The RGS subgroups are as follows: A/RZ, B/R4, C/R7, D/R12, E/RA, F/GEF, G/GRK, H/SNX (Figure4. Page 21). A description of the main subfamilies follows below.

2.1 A/RZ Subfamily

The RZ subfamily is made up of RGS17, RGS19 and RGS20. They have a cysteine rich domain at the N-terminal side of the RGS-box[19]. These cysteines are thought to be heavily palmitoylated, leading to tight membrane association. Their GAP activities have been characterized as Gαz and Gαo specific in bovine brain and Gαi3 in yeast[16;20;21]. RGS19 is also called GAIP (Gα interacting protein), which was among the first mammalian RGS proteins to be discovered.

2.2 B/R4 Subfamily

The R4 subfamily is made up of RGS1, RGS2, RGS3, RGS4, RGS5, RGS8, RGS13, RGS16 and RGS18. This is the largest group of RGS proteins; they have some of the shortest flanking sequences on either side of the RGS-box[22]. But just because these flanking domains are small in size, does not mean they are unimportant. For example, RGS2, RGS3 and RGS5 all have an RGS-box capable of inhibiting Gαq but do not appear to inhibit the same receptors coupled to Gαq[23]. Thus, determinants outside of the RGS-box appear to play a role in targeting the Gα GAP activity of these RGS proteins. This notion is central to our work; in this thesis where we will define and characterize some of the important residues outside of the RGS4 GAP domain that are determinants for its proper localization, trafficking, and function.

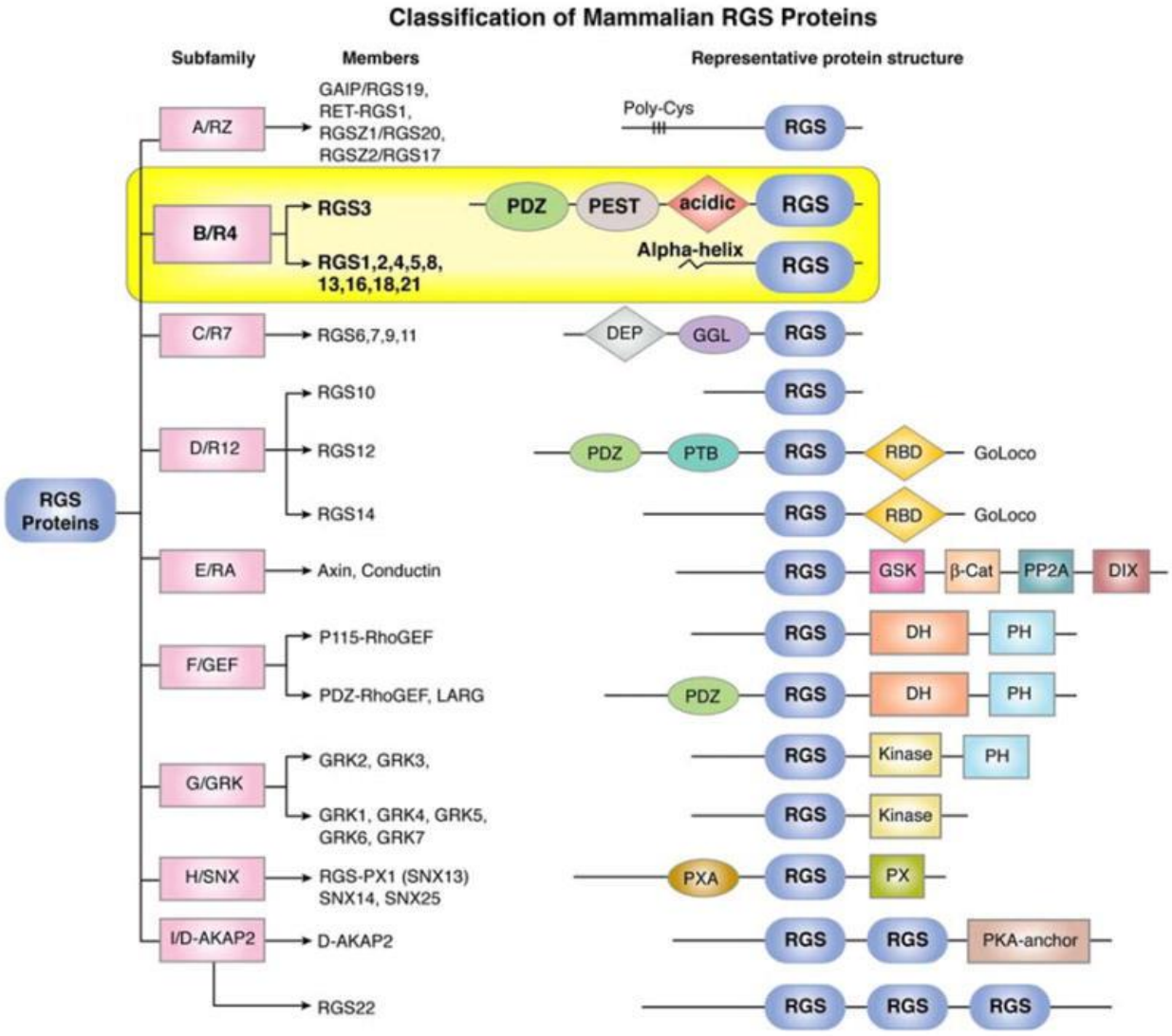

Figure4: RGS protein family and its subfamilies. From Bansal G, et al. 2007.

2.3 C/R7 Subfamily

This subfamily is made up of RGS6, RGS7, RGS9 and RGS11. The structural features of the R7 subfamily include the Disheveld Egl-10 Pleckstrin (DEP/DHEX)[24] and Gγ Like (GGL)[25] domains located on the N-terminal side of the RGS-box. The DEP/DHEX domain is responsible for binding the R7 Binding Protein (R7BP) or RGS9 Anchor Protein (R9AP). The GGL domain binds to Gβ5. Thus, this subfamily is behaving differently than others due to its ability to mimic a Gγ-G-protein subunit and to bind to the highly specialized Gβ5. Notably, the GGL domain of the R7 subfamily is the only gamma-type protein that Gβ5 is capable of binding. Ironically the reciprocal stability of the R7 subfamily members and Gβ5 requires this interaction[26]. For comparison, Gβγ requires prenylation of Gγ to promote plasma membrane binding whereas R7-Gβ5 does not have intrinsic lipidation and therefore requires binding to R7BP or R9AP (via the DEP/DHEX domain) to localize to the plasma membrane[27]. R7BP plasma membrane targeting is regulated by its palmitoylation status while R9AP is constitutively localized to the plasma membrane by its transmembrane domain[27;28]. R7 subfamily GAP activity is primarily toward Gαi, Gαo and Gαt[29]. These RGS proteins are highly expressed in the brain and retina, they are involved in sensory stimuli such as light, modulatory transmitters, psychotherapeutic agents, morphine and regulated motor coordination and locomotors response[30-32]. Similarly Gβ5 is detected in nervous tissue and cell of neuroendocrine origin. One of the most recognized function of an R7-RGS protein is the RGS9-1 retinal specific isoform that is inhibiting Gαt within the photo-transduction cascade (Figure5. Page23)[30]. Inactivation of the RGS9 gene leads to a greatly slowed inactivation of photon-induced signaling in both rod and cone photoreceptors. Preliminary data related to R7BP localization is presented in Appendix1.

2.4 D/R12 Subfamily

This subfamily contains three proteins: RGS10, RGS12 and RGS14. This is a heterogeneous family where RGS10 and RGS12 show respectively 173 and 1447 residues,

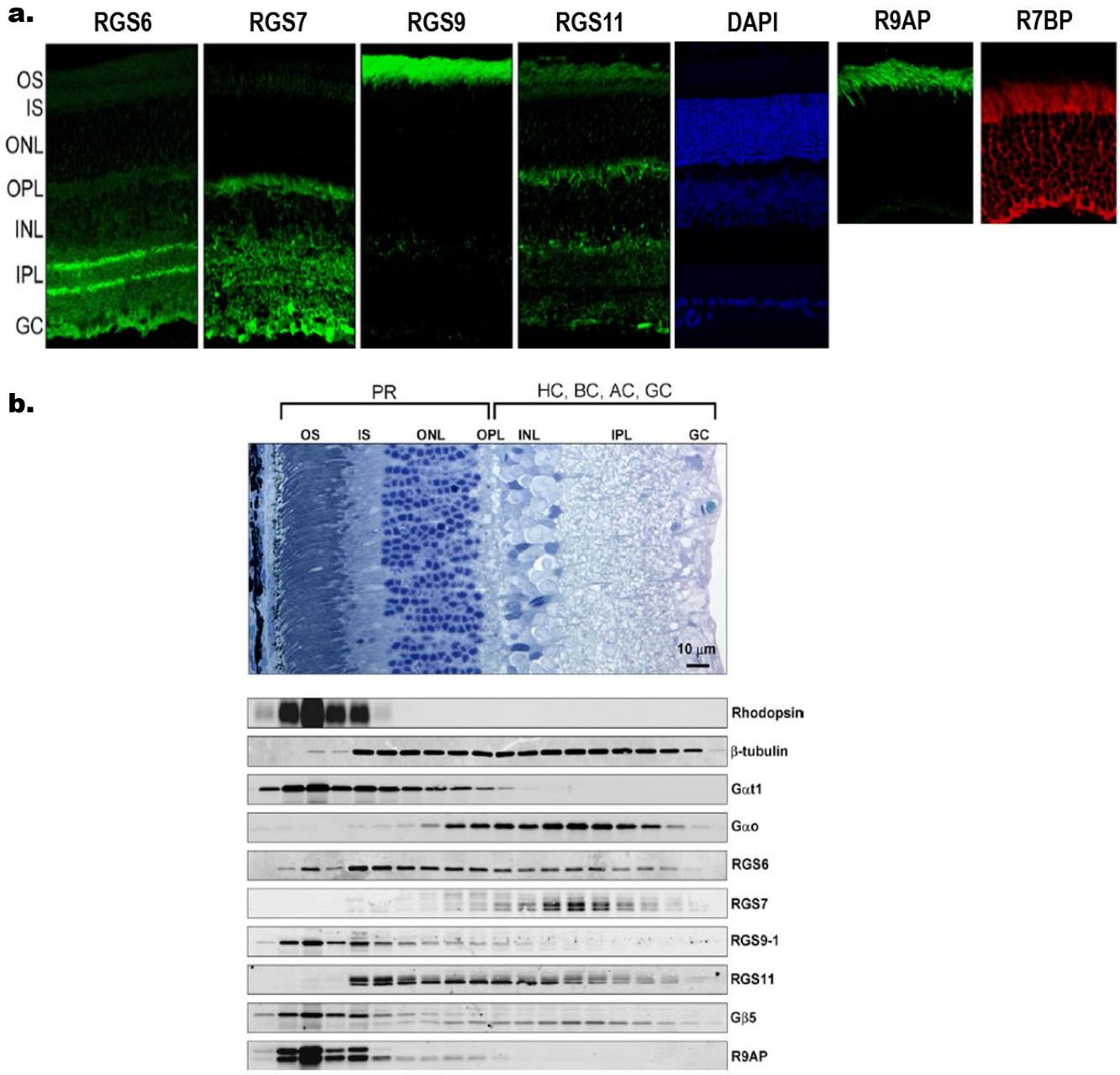

Figure5: Expression R7-RGS protein at the retina. a) GFP conjugated R7-RGS protein show their specific localization at the retina in side view. DAPI is a marker of nucleus. b) Western blot showing Gαt and o and R7-RGS protein expression corresponding to specific tissue of the retina showed above. OS: Outer Segment of Photoreceptors; IS: Inner Segments of Photoreceptors; ONL: Outer Nuclear Layer; OPL: Outer Plexiform; INL: Inner Nuclear Layer; Layer; IPL: Inner Plexiform Layer; GC: Ganlgion Cell Layer. From J. Song, et al. (2007).

only their RGS-box homology argue to group them together. RGS12 and RGS14 share more homology with a Ras- Binding Domain (RBD)[33] and a GoLoco motif[34]. Traver and colleagues have identified the small GTPases Rap1 and 2 as binding partner for the RBD region of RGS14. This interaction is dependent on the GTPases being in their GTP-bound/ "activated state", suggestive of a potential role for RGS14 as an effector for activated Rap protein. The GoLoco motifs of RGS12 and 14 interact selectively with GDP-bound Gαi-family and prevent guanine nucleotide dissociation. This gives these proteins guanine nucleotide dissociation inhibitor (GDI) function[33-35]. RGS12 contains also an N-terminal PDZ -PSD-95/Dlg/ZO-1- domain and a PTB -phosphotyrosine binding- domain. The PDZ domain have been shown *in vitro* to interact with GPCR C-termini of CXCR2 (interleukin-8 receptor)[36], CRF-R1 (corticotrophin-releasing factor receptor) and $GABA_B$- receptor coupling to calcium channel inhibition[37]. With the ability to bind phosphotyrosine- containing proteins, Gα subunits and Rap GTPases, RGS12 appears to represent a point of integration between receptor tyrosine kinase and heterotrimeric G-protein signaling[38].

2.5 G/GRK or G-protein-coupled- receptor kinases Subfamily

This family comprises GRK1, GRK2, GRK3, GRK4, GRK5, GRK6, and GRK7. This subfamily showing a conserved RGS-box is more often known for their second function which consists in phosphorylating activated GPCRs, thereby allowing the binding of arrestin proteins, functional uncoupling from G-protein and endocytosis of the phosphorylated receptor[39;40]. The N-terminal RGS-box can act to inhibit Gαq signaling; this phosphorylation-independent inhibitory activity of GRK2 is thought not to result from RGS-mediated GAP activity (which is barely detectable *in vitro*) but rather by sequestration of activated Gαq by the RGS-box[41].

3. RGS4

3.1 RGS4 function

The RGS-box is both necessary and sufficient for the Gα-GTP binding and GAP activity of RGS proteins. The first crystal structure for the RGS-box/Gα complex was for

RGS4 bound to Gαi1[42]. The RGS4 RGS-box can inhibit both Gαq and Gαi, and this bi-specificity provides suggests that it may inhibit a wide array of GPCR pathways[43;44]. Moreover, receptors that couple promiscuously to Gαq and Gαi may be expected to be potently regulated by RGS4, in the absence of any other RGS proteins.

Discovered fourteen years ago in yeast, RGS4 has been on the focus of human drug design by Neubig and Siderovski academic laboratories[45-49]. Its role as a potent inhibitor of Gαq and Gαi suggest that RGS4 may be a useful therapeutic target under pathophysiologic conditions where GPCRs signaling are abnormally high. Indeed, a large number of recently published studies have demonstrated the key role for RGS4 in maintaining physiologic homeostasis in a large number of cell and tissue types.

3.1.1 RGS4 in the Central nervous system

During embryonic development in mice, RGS4 is transiently expressed in several central nervous system cell types, such as sympathetic ganglia and cranial sensory and motor neurons[50]. Using a Bacterial Artificial Chromosome (BAC)-transgenic reporter construct model for studying RGS4 expression in the mouse brain, it was demonstrated that RGS4 expression occurs widespread in most cortical neuronal layers at all stages of development[51]. The same study revealed a strong correlation between location of RGS4 expression and acetylcholinesterase, which suggested a role of the RGS protein in muscarinic receptor signaling regulation. RGS4 has also been documented in several subcortical regions, most abundantly in the striatum and amygdala[52] (Figure6. Page26). While there have been varying reports of RGS4 involvement in opioid signaling in the brain [53;54], RGS4 has been implicated as a player in Parkinson's disease (PD). Depletion of dopamine in the striatum, as in PD, resulted in a variety of feedback responses, including an attenuation of M4 muscarinic receptor signaling attributed to upregulated RGS4 levels[55]. In addition to PD, RGS4 has also drawn consideration as a potential genetic factor in the development of schizophrenia. The RGS4 gene resides in the schizophrenia susceptibility locus, and RGS4 expression is decreased in several frontal cortex regions in schizophrenics [56;57]. However, functional studies have not sufficiently demonstrated a role for RGS4 in this neurological disorder. The only behavioral study conducted presented no abnormalities in

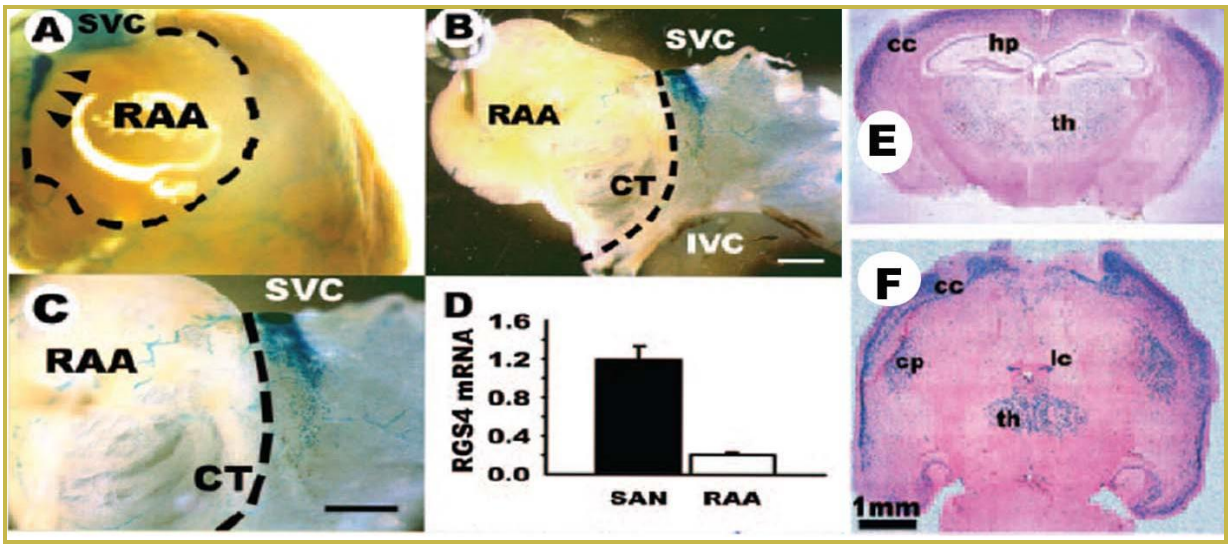

Figure6: Differential Mycocaridum and Brain expression of RGS4. RGS4-LacZ reporter expression is high within SAN myocytes. A, Whole-mount intact heart showing intense LacZ expression observed in a crescent-shaped pattern within the right atrium at the base of the SVC (arrowheads) extending along the crista terminalis into the right atrium. Dashed border shows outline of RAA. B, Wide-angle view of an atrial preparation showing the atrial septum and RAA from RGS4-null mice stained for LacZ expression. SVC indicates superior vena cava; IVC, inferior vena cava; CT, crista terminalis. C, High-magnification view of a stained atrial preparation shows RGS4-LacZ expression in the SAN. Scale bars_1 mm. Dashed border in B and C shows border of CT and atrial septum. D, Comparison of RGS4 mRNA expression in the SAN and RAA from wild-type (WT) mice was carried out by realtime RT-PCR as described above. E, Coronal (upper) and F,transverse (lower) cryosections of RGS4-null brains stained for LacZ show reporter gene expression in the cc: Cerebral Cortex; hp: HiPpocampus; th: Thalamus; cp: CaudoPutamen: lc: Locus Corealus. From Cifelli C. et al 2008.

RGS4-/- rodents that would suggest a schizophrenic phenotype[58]. At the mechanistic level, in examining the regulation of NMDA receptors- key players in cognition and emotion- by α1- and α2-adrenergic receptors in prefrontal cortex pyramidal neurons, Wenhua Liu and colleagues found that RGS4 was decreasing both of the α1- and α2- adrenergic respectively coupled to Gαq and Gαi receptors on NMDARs current amplitude[59]. Interestingly, RGS4 splice variants are expressed in the same region of schizophrenic and bipolar disorder patients, the splice variant more present in schizophrenic patients corresponds to a RGS4 protein N-terminal truncated[60]. In this document we are studying elements of N-terminal RGS4 protein that are influencing its functionality.

3.1.2 RGS4 tubulation and kidneys

RGS4 protein is expressed in kidneys, organs for which tabulation is crucial. "Lung Mv1Lu" epithelial cells were able to form tubule-like structures when cultured onto the synthetic basement membrane Matrigel. Using this model and condition the level of RGS4 mRNA was increasing by 8-fold when cells were tubulating[61]. Tubulation by epithelial and endothelial cells is coupled to their acquisition of polarity and to their proliferation, invasion, and migration toward the site of new tubule formation[62;63]. Angiogenesis-which is a similar process than tubulogenesis- is essential to many biological processes and uncoordinated or inappropriate angiogenesis is vital to the pathogenicity of many human diseases, such as arthritis, diabetic retinopathy, and cancer [62;64]. RGS4 expression was found to inhibit RNA synthesis of vascular endothelial growth factor (VEGF)-a cytokine induced tubulogenesis pathway- and extracellular signal-regulated kinase (ERK)1/ERK2 and p38 MAPK activation as well as ERK1/ERK2 activation stimulated by endothelin-1 and angiotensin II –agonists of Gαq receptors- . The study concluded that in inhibiting tubulation via VEGF, RGS4 was inhibiting Mv1Lu cell proliferation, migration, and invasion[61].

In mouse model, RGS4-/- developed rapidly fatal renal failure and reduced renal blood flow under cyclosporine A treatment - a Gαq mediating compound that can activate MAPK/ERK- and Calcineurin inhibitors (CNI) - a powerful immuno-modulatory agent used in 98% of kidney transplant that produces marked renal dysfunction due in part to

endothelin-1-mediated reductions in renal blood flow-[65;66]. The result of the study showed endothelin-1-mediated Gαq protein signaling plays a key role in the pathogenesis of vaso-constrictive renal injury and antagonizes the deleterious effects of excess endothelin receptor activation in the kidney[67]. Moreover, acute kidney injury in humans is often due to episodic hypotension, such as it occurs with septic, hypovolemic, or cardiogenic shock[68]. In shock, renal hypoperfusion is followed by reperfusion in surviving patients. These forms of kidney ischemia– reperfusion injury (IRI) often result in acute renal dysfunction due to acute tubular necrosis[69]. The concentration of ligands that bind to G protein-coupled receptors, including thromboxane A_2, angiotensin II, and endothelin-1, is increased in ischemic kidney injury. Endothelin-1 binds to endothelin-1A G protein-coupled receptors in vascular smooth muscle cells and activates the Gαq subunit which results in vasoconstriction[70;71]. The kidneys transplanted between knockout and RGS4WT mice had significantly reduced reperfusion blood flow and increased renal cell death. WT mice administered MG-132 -a proteasomal inhibitor of the N-end rule pathway responsible to RGS4 protein degradation- resulted in increased renal RGS4 protein level of expression and in inhibition of renal dysfunction after IRI in RGS4WT but not in knockout mice[72].

3.1.3 RGS4 and the intestine inflammation

Intestinal inflammation in humans and animals has been widely shown to be associated with changes in contractility[73;74]. There are two types of intestine smooth muscle contractility: initial contraction and sustained contraction respectively driven by Gαq/11 and Gαq12/13[75]. Il-1β signal is inhibiting the excitatory neurotransmitters -NeurokininA- contractile response of intestinal smooth muscle[76;77]. RGS4 –capable of inhibiting Gαq/11- is found expressed in rat ileal colonic smooth muscle and upregulated by Il-1β[75]. In fact it appears that RGS4 expression is upregulated through Il-1β, ERK1/2 and P38MAPK and downregulated by PI3K/Akt/GSK3β pathway[78]. Both pathways are upstream of activation or deactivation of IKK2/IK-Bα/p65/NF-KB pathway[78;79] which is known to influence gene expression. IL-1β induces NF-KB activation involving the phosphorylation of IKK2, degradation of IK-Bα and nuclear translocation of p65/p50, leading to the upregulation of RGS4mRNA expression while PI3K attenuates NF-KB activation at the level of IKK2 by inactivating GSK3β by increasing the phosphorylation of GSK3β via Akt[78]. Interestingly the

RNA-binding protein human antigen R (HuR)[80] has been demonstrated as another element influencing RGS4 level of expression in colonic intestine. This protein is binding the 3'-untranslated region UTR of RGS4mRNA and increase by two times its mRNA half-life[81]. Consistently with previous studies this has been investigated in colonic smooth muscle cells but in rabbit. Researchers who led the study showed that Il-1β was also inducing the HuR stabilization of RGS4mRNA[81].

These studies demonstrate signals that can interfere with RGS4 level of expression, interestingly some tissues show RGS4 expression being significantly decreased upon cancer development, it would be interesting to see how these demonstrated pathways are conserved and activated in cancer where RGS4 have been implicated.

3.1.4 RGS4 in Breast cancer and others

Often, cancer treatment is associated with targeting Receptors for Tyrosine Kinases (RTKs) for which knowledge of activation mechanisms and signaling pathways that regulate actin cytoskeleton dynamics have already allowed the development of target specific drugs and new therapies for cancer[82]. In contrast, knowledge of the GPCR-dependent signaling pathways involved in acquisition of migratory and invasive abilities by cancer cells lags far behind. Nonetheless, there is evidence from preclinical and clinical studies showing excessive activation of GPCRs in breast cancer due to overexpression of receptors[83] and/or abnormally elevated ligands for GPCRs [84;85]. Signals initiated by various activated GPCRs, including protease activated receptor 1 (PAR1) and CXC chemokine receptor 4 (CXCR4), drive breast cancer cells to migrate and invade through surrounding tissues and spread to target organs[83]. Thus, identifying molecules responsible for regulating signals initiated by many GPCRs could be an effective, alternative strategy for breast cancer treatment. RGS4 is expressed in normal breast epithelia and has been shown *in vitro* and *in murine* to inhibit breast cancer cell migration and invasion in a GAP-dependent manner[86]. By inhibiting Gαi, RGS4 may block CXC chemokine receptor 4 and PAR-1 dependent lamellopodia formation which is critical for cancer migration and invasion[87]. Moreover, RGS4 is down-regulated in human breast cancer: invasive carcinoma

cells were expressing only 50% of the nearby benign cells[86]. This down regulation in carcinoma tissue is due to proteasomal degradation and is causing the increase of cell migration and invasion[86].

In other cancers including gliomas, ovarian cancer, esophageal and pancreatic cancer, alterations in RGS4 gene transcription have been identified either due to microRNA, lacks of transcription and sometimes unidentified causes[88-91]. In all of these studies, reduction of RGS4 has been correlated to increased cancer susceptibility particularly as relates to increases in both invasion and migration. Thus understanding, characterizing or preventing RGS4 protein degradation pathways can help in the design of therapeutic strategies toward cancers.

3.1.5 RGS4 from pancreatic embryonic β-cell islet development till fatty acid and glucose homeostasis

RGS4-/- at 14.5-dpc Mouse and 24 hpf Zebrafish embryos failed to form single pancreatic islet; cells diverging trajectories were detected very early in the islet formation time-lapse sequence, supporting an early role of RGS4 in directional cell migration at the pancreatic embryogenesis formation stage[92]. Similar phenotypes were observed under Pertussis toxin -Gαi blocker- and S1P antagonist treatments. In mice, the transcription factor Neurogenin3 (Ngn3) is necessary and sufficient for the induction of the full spectrum of pancreas endocrine cell fates[93;94]. RGS4mRNA expression was significantly decreased when Ngn3 was knocked out[92].

While RGS4 affects endocrine pancreas morphogenesis in embryo, its presence in adult mice has been strongly linked with insulin resistance. In inhibiting the Muscarinic3-Gαq coupled receptor, RGS4-the main RGS protein expressed in pancreatic islet - is inhibiting the unique muscarinic receptor responsible for glucose-stimulated insulin secretion. A two- fold increase in insulin concentration is observed in the plasma of RGS4-/- mice[95;96], a condition known to promote the development of insulin resistance. Murine models have also consistently shown that absence of RGS4 results in loss of fatty acid

homeostasis. For example, acetylcholine stimulation of adrenal glands results in 4-fold more catecholamine secretion leading to increased plasma free fatty acid concentrations, liver steatosis and increases the risk of insulin resistance[97] . Insulin is known to decrease blood glucose concentration, by increasing the cytosol-plasma membrane translocation of glucose transport channels (GLUT receptors) GLUT4R translocation is mediated by Gαq and Gαi activation which are both inhibited by RGS4 in the heart and adipose tissues[98]. Notably, glucose intolerance in RGS4-/- mice was correlated with a decrease in insulin secretion in response to glucose load[98]. Overall RGS4 is inhibiting plasma glucose uptake, glucose-inducing insulin release while at the same time reducing free fatty acid concentrations and inhibiting catecholamine release. Thus RGS4 may be considered as a key element in the prevention of both insulin and glucose resistance.

3.1.6 RGS4 in the heart

RGS4 mRNA level was increased in hypertrophied cardiac tissues[99-101]. In cultured rat cardiomyocytes, Muslin and co-workers[102] demonstrated that RGS4 overexpression inhibited phenylephrine and endothelin mediated Gαq induced myofilament reorganization and cell growth related to hypertrophy[103;104]. Also, in atrial myocyte, RGS4 has been shown to associate with acetylcholine Muscarinic 2 coupled to Gαi Receptor (M2R) and GIRK channel. Its ability to act as a modulator for GIRK channel has been well described[105;106]. Potassium currents (I_{KAch}) are activated upon acetylcholine activation of M2R. GIRK channel activation provides an important hyperpolarizing current in response to parasympathetic signaling. Hence, due to its close association with this signaling pathway, RGS4 has been predicted to be a potential regulator of parasympathetic-linked dysrhythmias in atrial myocytes[107-109]. Recent work from our lab has strengthened this hypothesis. We have shown RGS4 to be much more highly expressed in sinoatrial node myocytes than in the myocardium[110](Figure6. P26). The RGS4 effect on M2-mediated parasympathetic signaling was shown at the *in vivo, ex vivo*, and *in vitro* levels. RGS4-/- mice showed increased bradycardic response to M2-mediated parasympathetic agonists and lowered baseline heart rates than wild type. Retrograde perfused RGS4-null hearts showed enhanced negative chronotropic response to carbachol. Finally, SAN myocytes

from RGS4-/- mice demonstrated greater sensitivity to M2-mediated reduction in action potential firing, decreased GIRK channel desensitization to parasympathetic stimulus, and altered I_{KACh} kinetics[111]. Moreover, in mice where diabetes type1 has been triggered by injection of streptozotocin, RGS4 was shown to prevent severe bradycardia induced by overexpression of Gαq involving calcium signals[112]. The function of RGS4 regulating the parasympathetic signaling is multiplied by the fact that RGS4 is also an inhibitor of catecholamines[97] release which naturally increase heart rate via cardiac adrenergic receptors.

3.2 Opening

RGS4 presents interesting regulation of many processes in the human/animal body. One potential strategy for targeting RGS4 function is to target the endogenous cellular pathways that influence its functionality. For example, since most of RGS4's function is thought to occur at the plasma membrane, then defining the determinants of RGS4 plasma membrane targeting may provide an interesting opportunity for its regulation. Of particular relevance to the work in this thesis are post translational modifications and sub-cellular trafficking routes as potential points of RGS4 regulation. The next part will list already stated RGS4 post-translational modifications showed to affect its function.

3.2.1 N-terminal α-amphipathic helix

This secondary structure has been modeled based on the data from yeast by Chen C. *et al.*[113] (Figure7. P34). RGS4 amphipathic helix was initially modeled between amino acids 1 till 32 based on 3.4 aa per helix turn. The amphipathic nature was demonstrated by the concentration of hydrophilic and hydrophobic/aliphatic residues on adjacent sides. RGS4 helix hydrophilic face is mostly positively charged which helps its binding to negatively charged phosphatidylserine on the inner leaflet of the plasma membrane. The hydrophobic face contains a core of aliphatic residues whose side chain length is capable of interacting with the hydrophobic core of the plasma membrane lipid bilayer. It has been demonstrated that RGS4 N- terminal α amphipathic helix remains disordered until it interacts with a

negatively charged phospholipids bilayer. This secondary structure has been shown to be necessary and sufficient for RGS4 plasma membrane binding[114]. However several studies have shown that posttranslational modifications in close proximity to the amphipathic helix domain may also be important for optimal plasma membrane targeting in mammalian cells[115;116].

3.2.2 Cysteine2 and 12 palmitoylation sites

Cysteine2 and 12 have been shown previously to be palmitoylated in autologous expression systems[117]. In mammalian cells, several laboratories highlighted the potential importance of cyteine2 as a site of RGS4 stabilization since it is an important substrate residue for oxidation and targeting by the N-end rule pathway of proteasomal degradation[118-120]. Upon its palmitoylation by palmitoyl CoA-transferases (DHHC3 and 7) enzymes, RGS4 is protected from N-end rule pathway degradation so that its steady state protein expression may rise by up to ten times[120]. This mechanism is apparently deregulated in breast cancer, leading to altered RGS4 stability and allowed cell migration/invasion[86].

Until now, no studies have examined a specific role for Cysteine12. Thus in this work we have examined the distinct functions of both Cysteine 2 and 12 palmitoylation and their relationship to the nearby amphipathic helix domain.

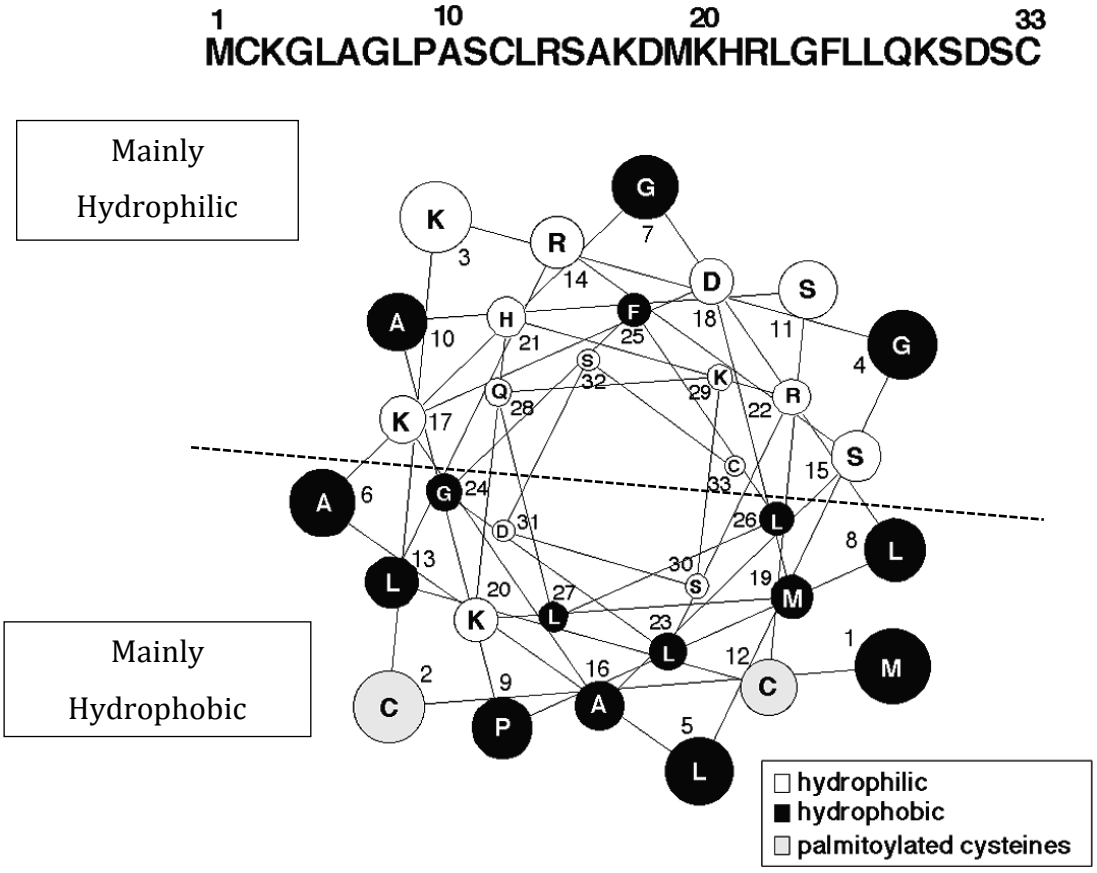

Figure7: α-Helical wheel model for the N-terminal 33-amino acid domain of RGS4. The hydrophobic residues (*black*) may interact with phospholipid tails inside the membrane bilayer. Basic residues (white) along the top of the helix may electrostatically interact with anionic phospholipid head groups on the membrane surface. Palmitoylated cysteines (*gray*) reside on the hydrophobic face. From Leah S. Bernstein et al. 2000[114].

3.2.3 Phosphatidic acid binding site

Ying-Shi Ouyang *et al*. (2002) tested the possibility that the plasma membrane binding activity of RGS4 required specific interaction with phospholipids components of the bilayer including such as phosphatidylserine, phosphatidylglycerol and phosphatidic acid. Notably, RGS4 showed a very high affinity for anionic phosphatidic acid vesicles[121]. This group also showed that this interaction was inducing a change of conformation of the RGS domain such that its GAP activity as measured by single turnover assay was decreased by 90% and 70% for Gαi and Gαq respectively[121]. They determined that deleting the first 57 amino-acid eliminated the RGS4/phosphatidic acid interaction. They further showed that a mutation in RGS4 (K20E) was partly interfering with the phosphatidic acid induced change in conformation and decrease of GAP activity, despite the fact that RGS4 was still capable of interacting with phosphatidic acid-containing vesicles[122].

3.2.4 Phosphorylation by PKA and PKG on Serine52

In smooth muscle cells from the gut, RGS4 has been shown to translocate to the plasma membrane after activation of PKA or PKG with cell fractionation techniques. PKA and PKG activation enhanced acetylcholine-stimulated association of RGS4 and Gαq-GTP and intrinsic Gαq-GTPase activity, which leads to less activation of PLCβ1 and therefore decreased smooth muscle cells contractions. When Jiean Huang *et al*. did this study, they show that mutation of RGS4 S52 in alanine was blocking the susceptibility of RGS4 to respond to PKA and PKG activation[123]. They proposed this serine as the PKG phosphorylation site, however, future studies will be required to determine whether it is a direct target of PKG/PKA phosphorylation or an interaction site for these kinases and/or their effectors.

3.2.5 Cysteine 95 palmitoylation site

This cysteine palmitoylation site is well conserved among members of the RGS protein superfamilly. Studies often mention RGS10 and RGS16 together with RGS4 as model to characterize the functional role of palmitoylation on this residue[124]. This posttranslational modification is located in the RGS domain and consequently may directly regulate its conformation and activity. In this model Cys95 palmitoylation acts as a GAP activator[124;125].

3.2.6 PIP3 and Ca2+-Calmodulin

Multiple studies described competitive binding of PIP3 and CaM to the RGS domain of RGS4[126-128]. PIP3 and CaM are predicted to bind the dilysine motif (KK99-100) where PIP3 would decrease RGS4 activity and Ca2+-CaM would act as a competitive inhibitor of PIP3 inhibition[127]. One interesting point of this discovery is that G-protein pathways normally inhibited by RGS4 may be expected more potently inhibited upon increase in intracellular Ca2+-CaM. This study also showed that KK99-100 PIP3/CaM binding motif (Figure8. Page38) may be conserved in many different RGS proteins[127].

3.2.7 Homer2 protein interactor

Homer proteins are scaffolding proteins that bind G protein–coupled receptors, IP3 and IP3 receptors. Dong Min Shin and colleagues demonstrated that Homer proteins function to increasing the GAP activities of both PLCβ and RGS4 by 140 and 90% respectively. While it was already assumed that Homer proteins were acting as scaffolding proteins to assemble Ca2+-signaling complexes in cellular microdomains, this discovery have shown the major importance of Homer2 protein which is presumably allowing all the components of the calcium machinery to be confined to a minimal space, thus maximizing their time-space interactions[129].

3.2.8 RGS domain - RGS box

The RGS protein fold is a conserved stable protein domain of 9 α-helices that is comprised of approximately 130 amino acids. This domain binds preferentially to GTP-bound Gα subunits and acts by stabilizing the transition state of Gα-mediated GTP hydrolysis[42]. In some cases, the RGS domain can inhibit effector signaling pathways by interfering with Gαq-PLCβ interaction. The RGS domain of RGS4 is situated near its carboxyl-terminus. , Previous work has demonstrated that this domain loses its ability to regulate Gαi function when residues EN87/88 are mutated[130] (Figure8. Page38).

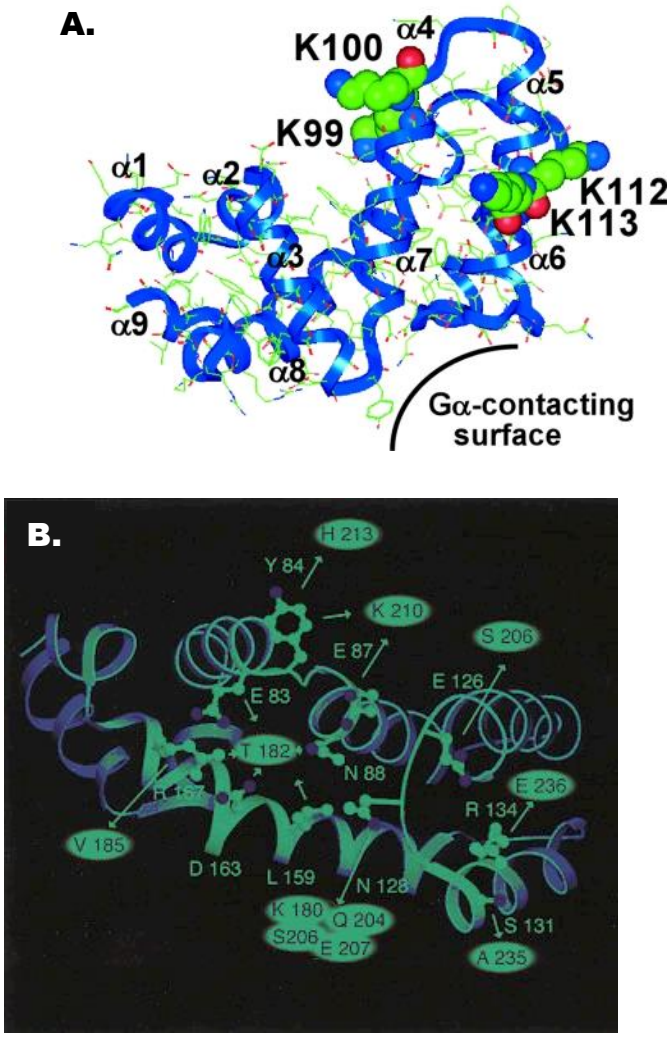

Figure8: A, Crystal structure of the RGS4 RGS domain (PDB no. 1AGR, [23]). The blue ribbon represents the core structure. Carbon, nitrogen and oxygen atoms are denoted by green, blue and red balls respectively. Positively charged residues are highlighted by a Corey–Pouling–Keltun space-filling model. From Masaru ISHII et al. 2005. B, The Gαi1-binding surface of RGS4 is shown. The view of the footprint in corresponds to a 1808 rotation around the vertical axis from the view in. Oxygen, nitrogen, and carbon atoms are colored red, blue, and green, respectively. Contacts with specific residues in Gαi1 are indicated by arrows, and the name of the contacted residue is highlighted in yellow. From John J.G. Tesmer et al. 2000.

PartII

4. Palmitoylation

Palmitoylation is a post translationnal modification occurring on cysteine or glycine residues. Palmitoylation of glycine may occur following cleavage of the N-terminal methionine and addition of a palmitoyl-CoA on the glycine -NH2 moiety. This modification, usually called "N-palmitoylation", is binding to the glycine via an amide bound and is stable and irreversible[131]. By contrast, palmitoylation occurring on cysteine results from the addition of a palmitoyl-CoA on -SH moiety via a thioester linkage is called "S-palmitoylation" and is regulated by palmitoylating and depalmitoylating enzymes[132] that will be detailed further below. The main distinction between these two types of palmitoylation modifications relates to the irreversibility of the N-palmitoylation linkage. Notably, it is possible to distinguish these two types of palmitoylation events using hydroxylamine, treatment with which specifically hydrolyzes the thioester bond on S-palmitoylated residues[133]. Unless otherwise stated, I will be using the general term: "palmitoylation" for "S-palmitoylation" in the whole document.

4.1 Palmitoylation Roles

In the last decade, great strides have been made in defining the role of palmitoylation in different biological fields. Indeed the family of more than 20 mammalian palmitoylating enzymes has been characterized only recently[134]. Palmitoylation is known to occur on a number of physiologic regulators of cell function including H- and N-Ras[135], endothelial-Nitric Oxide Synthase (e-NOS)[136], Gα-subunits[14;137;138] , GPCRs[139], Postsynaptic Density Protein 95(PSD-95)[140], Major

Histocompatibility Complex MHC classII[141], some Src kinases[142], Soluble N-tehylmaleimide-sensitive factor Attachment protein REceptor (SNAREs)[143], transferrin receptor[144;145] (Figure9. Page 43). Palmitoylation has been proposed to have a wide array of functions including: protecting protein from degradation[120;146], plasma membrane targeting[147;148], endosome targeting[149], protein-protein interaction[150], gating channels[151], driving recycling of protein[152], changing the hydrophobicity and stearic hindrance of domains thus their conformation and or activity[124]. The very fact that S-palmitoylation is reversible thus creates the interesting opportunity to regulate a wide number of intracellular functions[145].

4.2 Palmitoylating Enzymes and History

Palmitoylating enzymes have been firstly identified in 1999 by Deschene[153] and Linder[154] in S. *cerevisiae*. They reported the activity of Ras2 as palmitoylation- dependent. Since Ras2 is essential for maintaining cell's life, these investigators used a survival assay to screen for yeast genes and responsible for Ras2 palmitoylation[155]. Subsequently, using bioinformatics tools were used to identify 6 others proteins that contained a similar domain to the Erf proteins identified above, the so called "ZDHHC" (Zinc finger – Asp-His-His-Cys) motif. Recently, Dr. M. Fukata cloned and characterized the superfamily 23 human palmitoylating enzymes[134]. This new clone library has prompted a recent flurry of experiments in the DHHC/palmitoyl CoA transferase field to identify the function of the different DHHCs and their substrates [145;156].

4.3 Palmitoylating Enzymes Structures and Specificities

All known palmitoylating enzymes containing the ZDHHC domain is responsible for permitting the addition of a palmitic acid to their substrate. "ZDHHC" are usually called palmitoylating enzymes, as we will for the rest of the document. The structure of the ZDHHC mimics a zinc-finger structural motif and contains numerous cysteine residues[157]. Each palmitoylating enzyme ZDHHC motif is surrounded by the CRD -Cysteine Rich Domain-. A ClustalX alignment of the yeast and human DHHC proteins was performed,

accordingly, a consensus sequence for the DHHC was proposed by Mitchell and co-workers[157;158].

C x_2 **C** x_3 (R/K) P x R x_2 H **C** x_2 **C** x_2 **C** x_4 **D H H C** x W (V/I) x N **C** (I/V) G x_2 N x_3 F

The ZDHHC proteins are all integral membrane proteins with the number of transmembrane domains varying between 4 and 6[159] (Figure9. Page43). They are found within most intracellular membrane compartments including: endosomes, Golgi, plasma membrane and ER with a large number of DHHC proteins showing some steady state localization at the Golgi[160]. Indeed, some investigators have suggested the Golgi may be the primary site of protein palmitoylation in the cell[136;159]. Notably, the ZDHHC catalytic site is always oriented toward the cytosol rather than the lumen of the Golgi and any other membrane compartments[159].

Bioinformaticists and biologists have attempted to identify consensus sites for cysteine palmitoylation by different DHHCs. Indeed, specific palmitoylation motifs have yet been established. Nevertheless some on-line software such as "CSS-Palm"[161;162] have been developed and can predict palmitoylation sites, but as you may understand, this only predict palmitoylation site without proposing ZDHHC enzymes.

4.4 DHHC palmitoylating enzymes for G-proteins and RGS4

Dr. M. Fukata's group recently published a study examining the palmitoylation status of Gαq[163]. This work showed Gαq was a substrate of both ZDHHC 3 and 7. Specifically, inhibiting ZDHHC3 and 7 activities was shown to regulate Gαq plasma membrane targeting and resulted in mislocalization of Gαq to the Golgi compartment. Wang and colleagues showed that ZDHHC3 and 7 were also capable of palmitoylating RGS4 but have not examined the effects of these enzymes on RGS4 localization. Instead they

focused on the role of ZDHHC3 for palmitoylating Cysteine2 on RGS4 and promoting its protein stability [120].

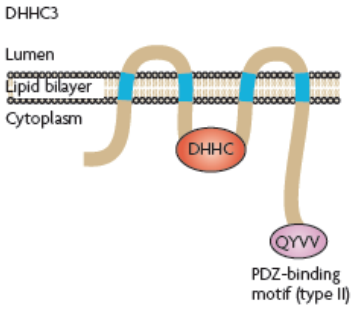

DHHC	Domain structure	Substrates	Related diseases
2		PSD95, GAP43, eNOS, CKAP4, CD9, CD151 and $G\alpha_{12}$	Colorectal cancer, hepatocellular carcinoma and non-small-cell lung cancer
15		PSD95, GAP43, CSP and sortilin	X-linked mental retardation
3		PSD95, PSD93, GAP43, $G\alpha_q$, $G\alpha_s$, SNAP25, CSP, $GABA_AR\gamma$, NCAM, eNOS, CaMK1G, GluR1 and GluR2	ND
7		PSD95, PSD93, GAP43, $G\alpha_q$, $G\alpha_s$, SNAP25, CSP, $GABA_AR\gamma$, NCAM and eNOS	ND
6		ND	ND
8		Paralemmin	Schizophrenia
9		HRAS and NRAS	X-linked mental retardation and colorectal cancer
17		SNAP25, CSP and huntingtin	Huntington's disease
21		eNOS, LCK, FYN and $G\alpha_{12}$	ND

Figure9: **a.** DHHC3, a representative DHHC (Asp-His-His-Cys) protein, has four transmembrane domains and a conserved cysteine-rich domain (CRD) containing a DHHC motif in the cytoplasmic loop. The DHHC sequence is essential for palmitoylating activity. DHHC3 also has a PDZ-binding motif at its carboxy-terminus.From Yuko Fukata. 2010. **b.** Domain structures and identified DHHC enzyme–substrate pairs. Besides a DHHC core domain, each DHHC protein has individual protein–protein-interacting domains such as a PDZ-binding motif, an SH3 domain and ankyrin repeats. Blue and green backgrounds show the DHHC2/15 and DHHC3/7 subfamilies, respectively. DHHC proteins have distinct but overlapping substrate specificity, and several DHHC proteins are associated with human diseases. In the amino-acid sequence of the consensus DHHC-CRD, letters shown in red and green represent conserved sequences of the DHHC motif and CRD, respectively; X represents any amino acid. CaMK1G, Ca_{2+}–calmodulin-dependent protein kinase type 1G (also known as CLICK-III); CKAP4, cytoskeleton-associated protein 4 (also known as p63); CSP, cysteine string protein; eNOS, endothelial nitric oxide synthase; $GABA_AR\gamma$, γ-aminobutyric acid receptor type A γ subunit; GluR, glutamate receptor; NCAM, neuronal cell adhesion molecule; ND, not determined; PSD, postsynaptic density protein; SNAP25, synaptosomal-associated protein 25. From Yuko Fukata. 2010.

PartIII

5. Protein Trafficking

Mammalian cells are composed of multiple compartments; each of them proposed to have specific roles and protein composition. Each compartment may be considered as one element of a more complete infrastructure. Compartmentalization allows cells to segregate environmentally incompatible reactions (i.e. different pH environments), allowing sequential modifications or processes, and a diversity of intracellular environments. A simple analogy likens cellular compartments to organs of the human bodies; perhaps providing an explanation for the term "organelle" to describe them.

Protein trafficking has been widely studied since the 1960s, pioneered by the study of plasma membrane receptor desensitization. Specifically, investigators noticed intracellular internalization of GPCRs following agonist treatment and proposed that these events may prevent internal cell signaling mechanisms from being overwhelmed. Since those early days it has been determined that mammalian cells are composed of a wide array of membrane-bound compartments which are able to undergo dynamic remodeling[164;165]. These compartments are usually called "endosomes", and their homeostasis is maintained by complex intracellular sorting mechanisms involving small GTPase such as Arf and Rab proteins[166;167]. Endosome lipid bilayer composition may be highly regulated by active enzymatic processes including PI kinases and PI phosphatases[168]. Compartmental communication and trafficking of cargo proteins between endosomes implies a role for tethering and fusion proteins such as Golgin[169], Family Interacting Proteins/Rab-Coupling Protein (Fip/RCP)[170], and SNAREs[171] in addition to dynamic microtubule[172] and actin fiber networks[173].

The complexity and diversity of different endosomal compartments have pushed scientists to define markers in order to distinguish them. In this purpose they used key

proteins for which sub-cellular trafficking have been well defined - TGN38, Transferrin receptor, Furin, Mannose-6-phosphate receptor, Lamp1-[174;175]. They also characterized some resident protein of key endosome compartments – Rab5, 4, 11, 7, 9- [176].

5.1 Endosome Compartments Markers

5.1.1 Rab proteins

Rab proteins belong to the Ras superfamily. They are approximatly 60 small GTPase of about 25kDa. Their activity is regulated at multiple levels: enzymatic C-terminal lipid addition is required for proper endosomal membrane binding (i.e. prenylation, geranylation, geranylgeranylation) which is mediated by GGT-I or II[177]and REP protein[178] (Figure10. Page 46). REP proteins are also involved delivering lipidated Rab protein to endosomal membranes[178]. Rab-bound GDP is exchanged for GTP with the help of specific GEFs[179]. Rab proteins are active only in the GTP-bound state, and like the G-protein α subunit, there exist specific GAPs for Rabs that inactivate them and therefore regulating the lifetime of their activity [179;180]. The potential importance of proper Rab protein regulation is highlighted by the proposition that multiple disease processes may be caused by a defect in specific Rab GEFs TRAPPC9: non syndromic autosomal recessive mental retardation, intellectual disability and postnatal microcephaly[181]; GGTα: Hermansky-Pudlak and albinism syndromes[182]; Rab3 GAP: Warburg Micro and Martsolf syndromes[183] and REP-1: Choroideremia-retinal pigment defect[184].

5.1.2 Rab proteins, endosomal markers

Some Rabs are found to reside in specific endosomal compartments. Rab5 has been very well characterized by Marino Zerial and is in partly responsible for the clathrin dependent vesicle budding out from the plasma membrane, homotypic membrane fusion and association with actin fibers to promote early endosome migration where Rab5 is considered as a marker[185]. (Figure11. Page49). Other endocytic pathways such as caveolae and Arf6 dependent endocytosis are found to merge with Rab5 early endosome after endocytosis[186].

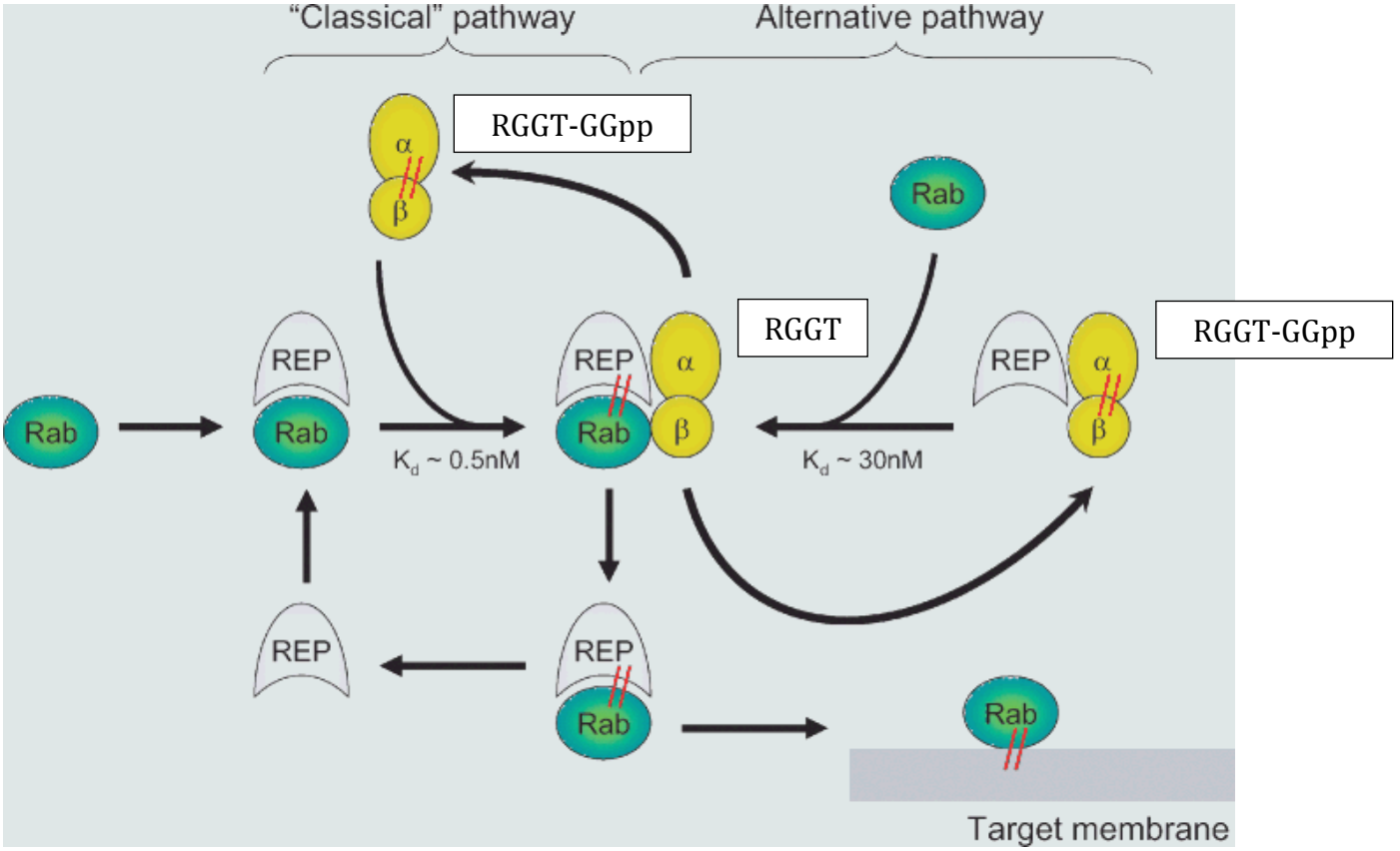

Figure10: Cartoon showing the two possible pathways for Rab protein prenylation. In the classical pathway, newly translated Rabs bind REP and the complex is recognized by GGpp-bound Rab geranylgeranyl transferase (RGGT). RGGT catalyzes the transfer of geranylgeranyl groups to C-terminal cysteines of the Rab protein. After prenylation, RGGT dissociates from REP, which remains bound to the prenylated Rab protein and delivers it to target membranes. REP is then released into the cytosol to take part in a new cycle of prenylation. In the alternative pathway, REP forms a complex with RGGT in the presence of GGpp under conditions in which these constituents are at higher concentrations relative to the Rab protein. The REP:RGGT:GGpp complex then binds newly translated Rab protein and the geranylgeranylation reaction takes place. RGGT dissociates as before, whereas REP escorts the prenylated Rab to membranes as in the classical pathway. K_d values of the Rab:REP:RGGT:GGpp complex for each pathway are indicated. From Ka Fai Leung et al. 2006.

Rab5 will be replaced by Rab7 during early endosome maturation to late endosome or lysosome- organelle responsible for protein or else degradation (XX), Rab9 mediates the recycling of proteins from late endosomes to the TGN[187;188].(Figure12. Page50). From Rab5 early endosome, Rab4 is responsible for fast recycling of proteins to the plasma membrane, a process that takes seconds to a few minutes[189].(Figure11. Page49). The slower retrograde trafficking that occurs minutes to hours involves maturation from Rab5 early endosome compartments to Rab11 positive recycling endosome requiring a sequential switch of Rab5 with Rab4 and then with Rab11[189]. Rab11 participates in the retrograde trafficking from recycling endosomes to TGN[190] as well as exocytic trafficking from recycling endosomes to the plasma membrane[189].(Figure13. Page51).

5.1.3 TGN38

Trans Golgi Network 38 is a transmembrane protein which is constitutively trafficking between the TGN and the plasma membrane via endosomal compartments. TGN38 partially colocolized with recycling endosome[190]. TGN38 is found at high steady state levels in the trans Golgi network but due to its well-described shuttling between the plasma membrane and Golgi it has been widely used to colocalize protein with different endosomal compartments[174]. (Figure14. Page 52).

5.1.4 Transferrin Receptor

Transferrin receptor is responsible for internalizing transferrin, to bring Fe3+ ions toward the inner cellular environment. The Fe3+ ions will be released in the inner cellular environment, but transferrin will stay bound to its receptor until it is recycled back to the plasma membrane[191]. The intracellular trafficking pathway of the transferrin receptor has been well established. (Figure14. Page52). It is a marker of endocytosis, its internalization is mediated by Rab5 clathrin-dependent internalization[192], and it is recycled back to the plasma membrane via Rab11 compartment[191;193]. Some lysosomal localization can also be observed for receptors that are targeted for degradation[194]. Traditionally researchers use transferrin conjugated to a fluorophore such as Texas Red(TR). Transferrin-TR binding to

its receptor is internalized and its trafficking can be followed by fluorescence microscopy. As the transfferin receptor is known to pass through Rab5 and Rab11 compartments, then any protein found to colocalize with transferrin might be present in either of these two endosomal compartments.

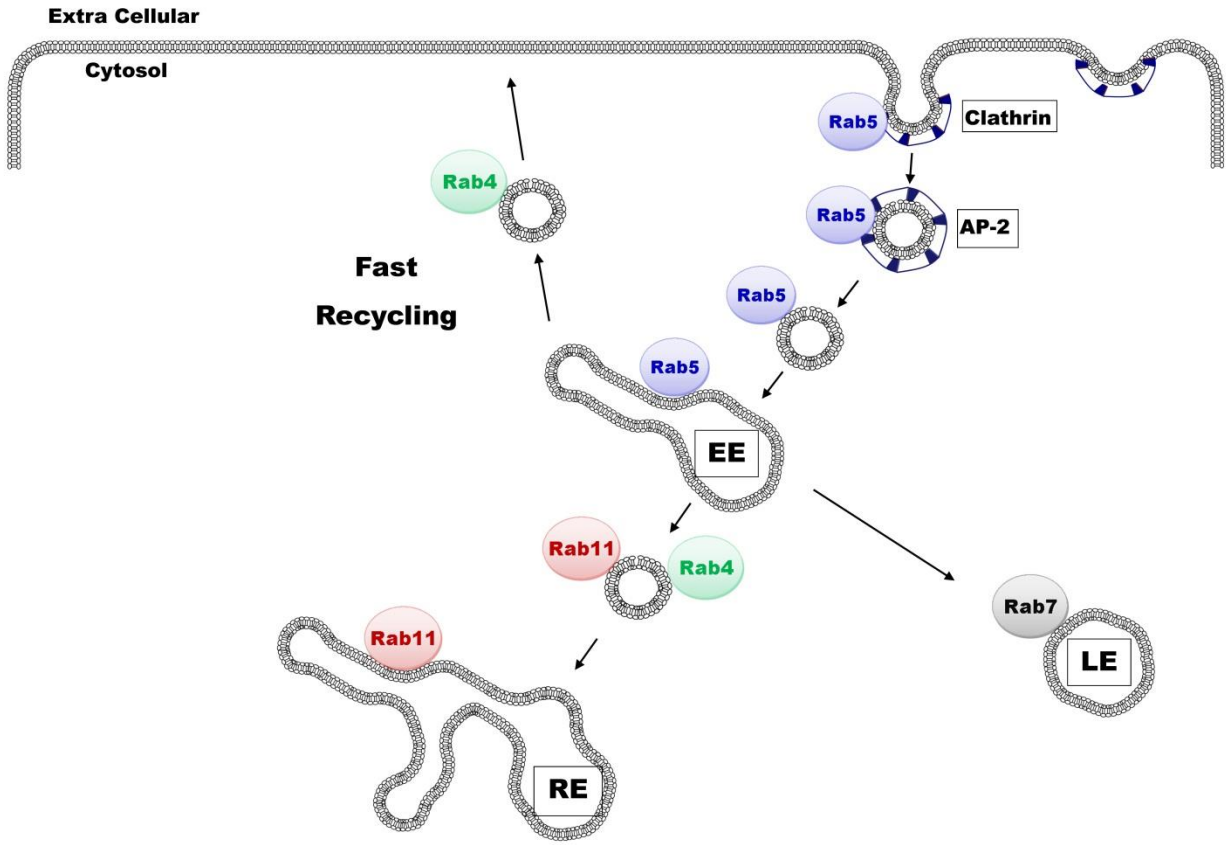

Figure11: Rab5 mediated clathrin dependent endocytosis from the plasma membrane to Early Endosome. Rab5 compartment is intimately linked to Rab7/late endosome; Rab11/slow recycling endosome and Rab4/fast recycling endosomes. AP-2: Adaptator protein -2; EE: Early/Sorting Endosomes; LE: Late Endosome; RE: Recycling Endosome; TGN: TransGolgi Network. By G.Bastin

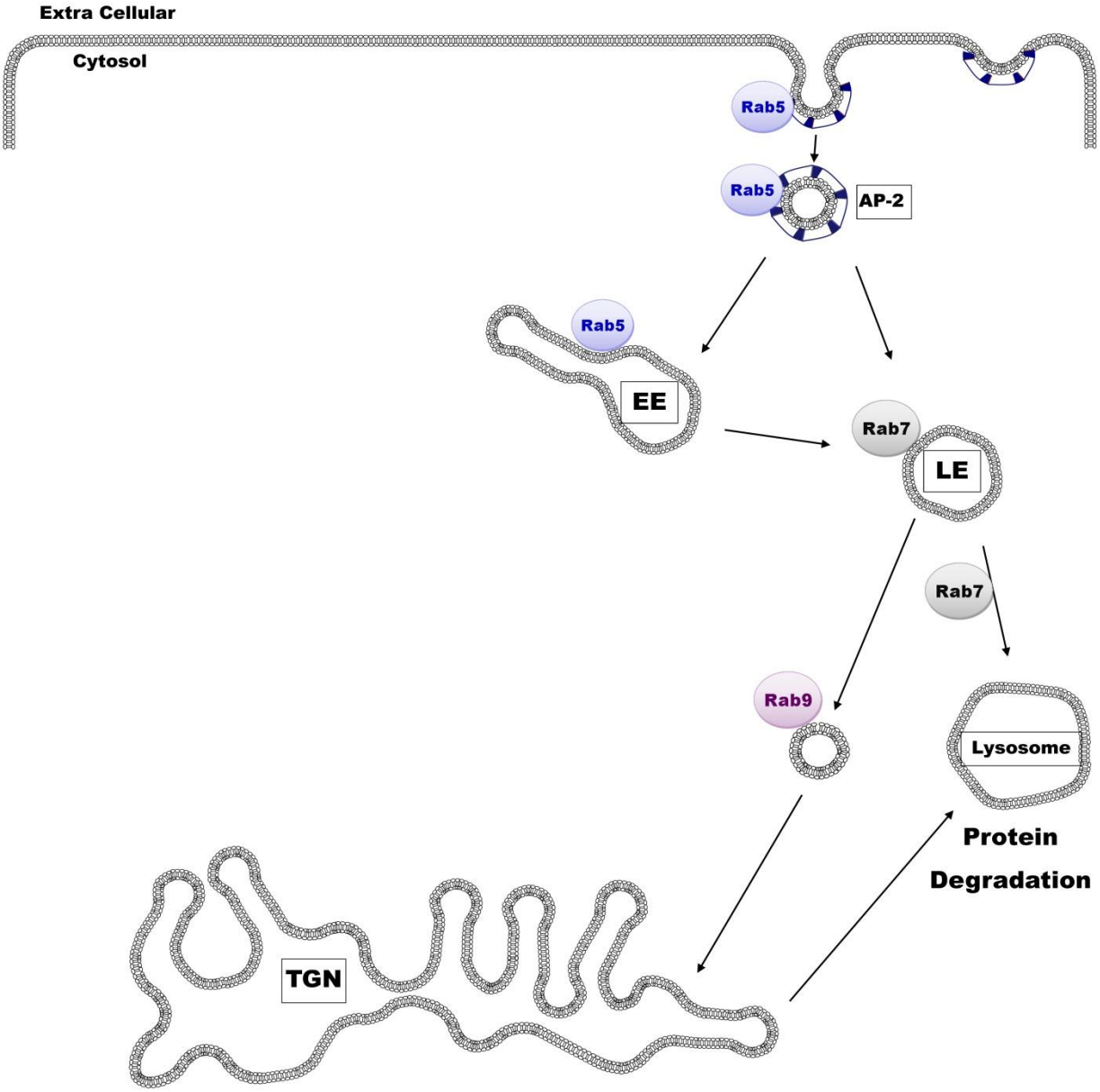

Figure12: Endosomal Protein Degradation pathways. Rab5 will be replaced by Rab7 during early endosome maturation to late endosome or lysosome- organelle responsible for protein or else degradation. Rab9 mediates the recycling of proteins from late endosomes to the TGN. AP-2: Adaptator protein -2; EE: Early/Sorting Endosomes; LE: Late Endosome; TGN: TransGolgi Network. By G.Bastin

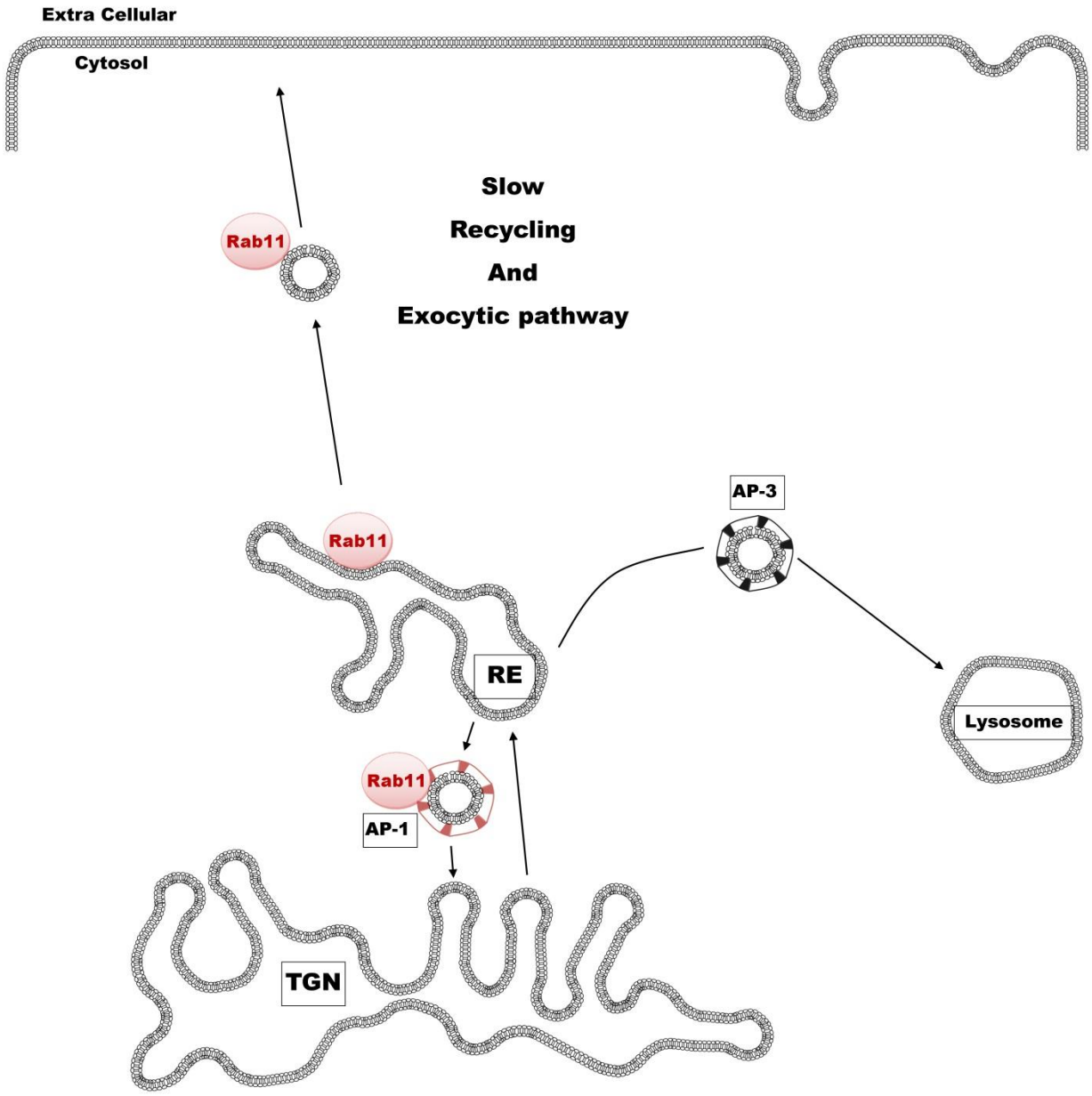

Figure13: Rab11 Recycling endosome. Rab11 participates in retrograde trafficking from recycling endosomes to TGN as well as slow exocytic trafficking from recycling endosomes to the plasma membrane. RE: Recycling Endosomal Center; AP-1: Adaptor protein1; AP-3: Adaptor Protein3; TGN TransGolgi Network. By G.Bastin

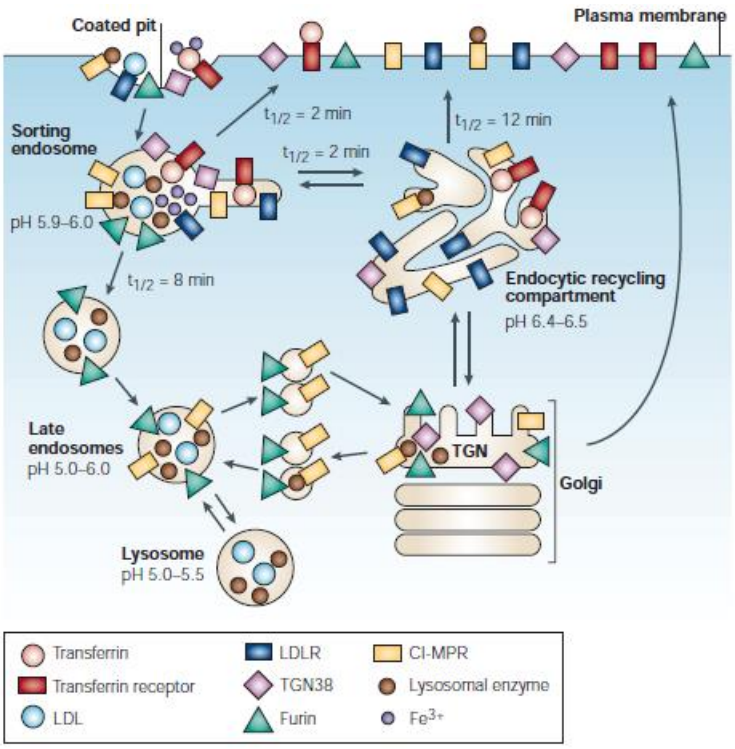

Figure14. **Endocytic recycling pathways.** The model shows the post-endocytic itineraries of several molecules. The transferrin receptor binds its ligand, diferric transferrin; the low-densitylipoprotein receptor (LDLR) binds low-density lipoprotein (LDL); and the cation-independent mannose-6-phosphate receptor (CI-MPR) binds lysosomal enzymes. All of these membrane proteins concentrate into clathrin-coated pits, and their initial delivery site is sorting/early endosomes. The transmembrane proteins furin and *trans*-Golgi network TGN38 also enter through clathrin coated pits. Most membrane proteins rapidly exit sorting endosomes and are either returned directly to the plasma membrane or are transported to the endocytic recycling compartment (ERC). Furin is retained in the sorting endosome as the sorting endosome begins to mature into a late endosome, and furin is delivered to the Golgi from late endosomes. From the ERC, essentially all of the LDLRs and transferrin receptors recycle to the cell surface. Transferrin, unlike most other ligands (for example, LDL), is not released from its receptor in the acidic environment of sorting endosomes. The two irons (Fe_{3+}) are released from diferric transferrin at the acidic pH and transported into the cytoplasm, but iron-free transferrin remains bound to its receptor until it is returned to the cell surface. At the neutral extracellular pH, iron-free transferrin is released from the receptor. About 80% of the internalized TGN38 and CI-MPR also returns to the cell surface, and the rest is delivered to the TGN. The CI-MPR can go from the TGN to late endosomes, where any ligand that is still bound can dissociate as a result of exposure to low pH. From the late endosomes, furin and free CI-MPR can move to the TGN, and molecules in the TGN can be delivered back to the cell surface . It is uncertain whether CI-MPR and furin are transported in the same or different vesicles between the TGN and late endosomes. The $t_{1/2}$ values are approximate and cell-type dependent. They are based on the papers that are cited in the text. From Frederick R.Maxfield and Timothy E.McGraw.2004

Rationale/ Introduction

As described previously, RGS4 is a member of the R4 subfamily that is able to inhibit both Gq and Gi. While the carboxyl terminus is made up primarily of the RGS domain, the relatively small amino terminus contains a number of interesting regulatory sequences. Cysteine2 and 12 are putative palmitoylation sites conserved in RGS4, 5 and 16. Although much previous work has shown the importance of palmitoylation of amino terminal cysteines as regulators of RGS protein function [195;116;118-120] no study has specifically examined the relative contribution of Cys2 and Cys12 to RGS4 plasma membrane targeting, intracellular trafficking, and function. Our lab has published studies showing that the length of hydrophobic surface of the amino terminal α-amphipathic helix is an important determinant plasma membrane targeting[196]. Alignment of the sequences for the RGS amphipathic helix domains revealed a close proximity of the Cys12 residue to the hydrophobic interface of the RGS4 helix. Lastly palmitoylation is often found as a key element in signaling protein trafficking where palmitoylation and de-palmitoylation are responsible for directing their movement between different intracellular compartments[132;145;149]. Therefore we hypothesized that Cys2 and Cys12 palmitoylation would be important for its intracellular localization, trafficking and function.

Here we followed RGS4 localization in living cells using confocal microscopy. Our strategy consisted of transiently transfecting HEK293cells with fluorescently-tagged RGS4 wild type and point mutants of Cys2 and 12. This approach allowed us to examine the importance of Cys2 and Cys12 palmitoylation on RGS4 trafficking and function. Cys12 palmitoylation appeared to promote RGS4 plasma membrane targeting, while Cys2 palmitoylation was required for directing RGS4 into the intracellular endosome pool. We also examined potentially novel roles for DHHC3 and 7 palmitoylating enzymes. We used genetic strategies to reduce the activity of DHHC3 and 7 and examined their importance for RGS4 plasma membrane targeting and function. Indeed, DHHC3 and 7 appear to both

participate in RGS4 endosomal targeting. Mutation of Cys2 abrogated the effect of DHHC3 and 7 on RGS4 endosome targeting. Lastly we compared RGS4 localization with that of a number of known intracellular trafficking markers including TGN38, Rab11 and transferrin receptor. Overall the results suggested a model whereby palmitoylation of Cys2 occurred on Rab11-containing endosomes and palmitoylation of cys12 was required for RGS4 to exit the endosomal pool, and traffic to the plasma membrane. Indeed, co-expressing Rab5 or Rab11 dominant negative highlighted the key roles for Rab5 and 11 as mediators for RGS4 intracellular trafficking on endosomes.

Material And Methods

Materials- The pEYFP-C1 plasmid, Clontech/ BD Biosciences, Mississauga, ON, Canada and pQE Trisystem1, Qiagen, Mississauga, ON, Canada, expression vectors were used for expression of all RGS protein constructs. HA-tagged Gq-R183C was generously provided by P. Waedegartner, Thomas Jefferson University, Philadelphia, PA,USA. Fluorescent-tagged versions of the Trans Golgi Network marker protein TGN38 were a kind gift from J. Lippincott-Schwartz, National Institutes of Health, Bethesda, MD, USA. GFP and CFP Rab5, 4, 11 have been provided by M. Zerial from Max Planck Institute, Germany. RFP-Rab7 is a kind gift from Dr. Grinstein, Sick kids hospital, Toronto, ON, Canada. Gαq/11-CFP has been forwarded by Joachim Goedhart - Amsterdam Univeristy, Netherland- but was originally made from Cathy Berlot -USA-. Transferrin-Texas Red and Azide Alexa-488 have been purchased from Invitrogen, Burlington, ON, Canada. 17-ODYA was bought at Cayman chemicals. The monoclonal anti-His tag antibody was from Clontech (# 631212), anti-HA antibody was from Roche Scientific, Mississauga, ON, Canada(# 11666606001) and the anti- mouse secondary antibody was from GE Healthcare, Mississauga, ON, Canada (# NXA931). All tissue culture media and transfection reagents were from Invitrogen, Burlington, ON, Canada and Roche Scientific respectively. HEK293 cells (tsA-201 derivative) were a kind gift from Z-P. Feng, University of Toronto, Toronto, ON, Canada. Unless otherwise stated all other reagents and chemicals were from Sigma, Oakville, ON, Canada.

Cell culture – HEK293 cells were grown in Dulbecco's modified Eagle's medium (DMEM): Ham's F12 medium (1:1), supplemented with 10% (v/v) heat-inactivated fetal bovine serum, 2 mM glutamine, 10 µg/ml streptomycin, 100 units/ml penicillin) at 37 °C in a humidified atmosphere with 5% CO_2.

RGS4 expression constructs – For subcellular localization studies RGS4-YFP expression plasmids were generated in the pEYFP-C1 vector by cloning the human RGS4 cDNA into the NheI/AgeI sites to generate a carboxyl terminal YFP fusion. Robust expression was ensured by inclusion of an optimized translation initiation signal in the context of the first methionine codon (GCCACCATGGCG). For functional studies RGS4-His expression constructs were generated in the pQE Trisystem1 vector by cloning RGS4 coding sequences into the NcoI/BamHI polylinker sites. Cysteine point mutations were introduced by site-directed mutagenesis and primer sequences will be made available upon request. All plasmid constructs were purified using the Endofree Maxi kit (Qiagen) and verified by sequencing of the complete protein-coding region. The expression of the pQE trysistem clones were analyzed by Western blotting using anti-His-tag antibody and ECL detection.

Assays of Gq-dependent Phosphoinositide Hydrolysis—HEK293 cells (2.0 x10^6 in 6-well plates) were transfected in triplicate using of Fugene 6™ transfection reagent according to the manufacturer's specifications. DNA amounts used in transfection were determined empirically to ensure similar expression levels of all RGS4 constructs tested. Specifically we used 0.5 μg of Gq(R183C); 3 μg of RGS4WT-His, 0.5 μg of RGS4C2A-His, 3 μg of RGS4C12A-His, 0.5 μg of RGS4C2AC12A-His, 1 μg of RGS4L23D-His and an appropriate amount of empty HisStrep vector to ensure 4.0 μg of total plasmid DNA/well. After 24h cells were trypsinized, pooled and replated in 6-well plates for analysis of inositol phosphate production (n= 3 wells /construct) and corresponding protein expression determination by Western blotting.. Inositol phosphate production was measured 48 h after transfection as described previously (14). Briefly, 5h after plating cells were washed with phosphate buffered saline and labeled in complete Dulbecco's modified Eagle's medium (without inositol) containing 10 mM LiCl and 1.4 μCi/mL myo-[^{3}H]-inositol (Perkin Elmer, Vaughan, ON) for exactly 15h. Then cells were washed with phosphate buffered saline and the inositol phosphate production was stopped with 750 μL of ice-cold 20 mM formic acid. The entire contents of the wells were collected and spun at 13,000 x g for 15 min in a microcentrifuge at 4°C. The supernatant fraction (700μL) was neutralized with 214 μL of

0.7M NH_4OH before proceeding to the ion exchange chromatography steps. For each well to be measured, a 3-mL Dowex resin (AG 1-X8, 200-400-mesh, formate form) column was separated. The entire sample was added to the column, and unbound ^3H-labeled material consisting of the total inositol-containing fraction was collected, after, the phosphate inositol-containing fraction was eluted into collection tubes with 5mL of 1.2M ammonium formate. 0.5mL of each sample from total inositol-containing and inositol phosphate-containing fractions was added to 10mL of scintillation fluid and counted. Inositol phosphate levels were expressed as the fraction of the total soluble ^3H-labeled inositol material (inositol phosphate total inositol-containing fraction) for each sample.

Calcium signaling- For DHHC study, M2-stably expressing-HEK cells were seeded onto Poly-L-Lysine coated #1 glass coverslips in 12-well dishes 48 hours prior to assay. For dominant negative DHHC studies, cells were transfected with 1µg YFP-tagged RGS4 plasmid and 1µg DHHS plasmid as indicated. For DHHC knockdown studies, cells were transfected with 1µg YFP-tagged RGS4 and 1µg Gqi9 plasmid; 6 hours later, media was removed and fresh media replaced, and cells were transfected with 12pmols of indicated DHHC siRNA (final concentration 10nM). 24 hours following transfection (18 hours following siRNA knockdown).

For studying the influence of Rab5a and Rab11SN, M1-stably expressing-HEK cells were seeded onto poly-L-Lysine coated #1 glass coverslips in 12-well dishes 24h hour prior to assay. Cells were transfected with 1.5ug of YFP-tagged RGS4 and 1.5ug of CFP-tagged Rab plasmid as indicated. For all studies: coverslips were washed and incubated in calcium imaging buffer (11 mM glucose, 130 mM NaCl, 4.8 mM KCl, 1.2 mM MgCl2, 17 mM HEPES, and 1 mM CaCl2, pH 7.3) containing 5 µM Fura- 2/AM ratiometric dye (Invitrogen) and 0.05% pluronic acid for 40 min at 37 °C. Fura-2-loaded cells were washed again and incubated for at least 5 min in calcium imaging buffer to allow hydrolysis of the acetoxymethyl ester. Coverslips were mounted in a modified Leyden chamber and imaged on an Olympus BX51WI upright microscope using a 40x water-dipping objective. Excitation light was provided by a DeltaRam V monochrometer (PTI, Lawrenceville, NJ). Fluorescence

imaging was performed with ImageMaster imaging software (PTI). Images were acquired with a Photometrics Cascade 512B cooled charge-coupled device camera (Roper Scientific, Tucson, AZ). YFP-expressing cells were identified using 510 ± 3nm excitation light in conjunction with a YFP filter set (Chroma Technology Corp., Brattleboro, VT) and selected as regions of interest within the ImageMaster software. For Fura-2 imaging, alternating excitation wavelengths (340 ± 5nm/380 ± 5 nm) were provided at ~1 excitation pair/s in conjunction with a 495-nm dichroic mirror and a 510 ± 20-nm emission filter (Chroma Technology Corp.), and paired images were collected after a 600-ms exposure. Fluorescent ratio (FR) values for the image pairs were determined for regions of interest previously selected on the basis of their YFP expression. Baseline FRs (BFRs) (340nm/380nm) of nonstimulated cells (both transfected and non-transfected) were collected for 30 frames prior to the addition of 200 μM carbachol. Only cells with a baseline FR of less than 0.6 where selected for analysis. The fold-increase from BFR levels to the stimulated peak FR (PFR) was calculated only for cells with a relative YFP fluorescence of 4000 to 30,000. Identical excitation/emission conditions and data collection parameters were maintained for all individual experiments performed in this study.

Confocal microscopy- For most experiments HEK293 cells were plated at 50% in tissue culture-treated microsopy dishes (Ibidi, #81156) and transfected with 1 μg of each construct to be tested using Fugene6 transfection reagent as describe above. For localization of RGS4 during phosphoinositol hydrolysis experiements, constructs were transfected in the identical ratios that were used for functional analysis (outlined above). Following 20h incubation dishes were sent for confocal microscopy to determine their plasma membrane/cytosol localization ratio containing transfected cells. Confocal microscopy was performed on ~70% confluence live cells at 37°C using an Olympus FluoView™ 1000 laser-scanning confocal microscope. Images represent single equatorial plane on the basal side of the cell obtained with a 60x oil objective, 1.4 numerical aperture. Confocal images were processed with Microsoft Office 2010. Quantification of plasma and endo-membrane localization was performed in a blinded manner, with membrane/cytosol

ratios measured using the Image J software package and Pearson Correlation Coefficient (PCC) for each endosome was calculated by the Fluo-View™ software.

Immunostaining- HEK293 cells were plated in BD-Falcon(ref: 354108). Cells were grown in 45%DMEM, 45% F12,10%FBS. 24h after Fugene6 (Roche) transfection with 0.5ug of DNA per well, cells were fixed with 4%PFA in PBS (no Mg and Ca), pH7 for 15mn at room temperature. Permeabilized with 0.2%Triton X-100 in PBS (no Mg no Ca) for 10mn at room temperature. Samples were blocked overnight at 4C, with 5%BSA, 0.1% Triton X-100 in PBS (no Mg no Ca). Primary antibody (anti-HA from Roche 11 666 606 001) at 1:1000 was incubated overnight at 4C in 1%BSA, 0.1% triton X-100, rinsed 4-6 time by slow pipetting with PBS (no Mg no Ca). Secondary antibody was A21049 Invitrogen 350, diluted at 1:500 in 1%BSA, 0.1% triton X-100 and PBS (no Mg no Ca) for 30mn. rinsed 4-6 times. Prolong gold antifade from Invitrogen (ref P36930) was used. Samples were observed according to Invitrogen instruction by confocal microscopy using 60x water objective.

Clic Chemistry- We used 10x 10cm dishes of HEK293 cells for each RGS4 clones. Each plate was transfected with 6uL of X-tremegene HP (Roche). We used 6ug and 2ug for RGS4WT and C2AC12A respectively per 10cm dish. Each RGS4 clone was conjugated to a StreptavidinBindingPeptide (SBP) allowing us to purify the proteins of with Streptavidin Sepharose High Performace beads (GE Healthcare). 12h post tranfection we switched medium from 45%DMEM, 45%F12, 10%FBS to 50%DMEM, 45%F12, 5%charcoal treated serum-no fatty acid. After 24h we starved the cells for 1h in 55%DMEM, 45%F12. Cells were then incubated for 8 hours in palmitic acid labeling medium 89.6%DMEM, 10% charcoal treated serum, 0.4% of 25 mM alkyl-17-ODYA- palmitate analogue. Cells were collected and lysed at 4C, using lysis buffer 20 mM HEPES, 150 mM NaCl, 3 mM $MgCl_2$, 1% Triton-X, pH7.4. We briefly sonicated the samples. Lysates were incubated with Streptavidin Sepharose High Performace beads, overnight at 4C. Beads were washed five times with lysis buffer, and an additional wash using acidic lysis buffer (pH 4) was performed. For clic chemistry, beads were continuously mixed with lysis buffer and 1 mM

$CuSO_4$, 1 mM TCEP, 100 μM TBTA, and 20 μM Alexa-488 azide (Invitrogen) at room temperature for 1.5 hours. Following the click reaction, the beads were washed three times with lysis buffer, and RGS4 was eluted with SDS PAGE loading buffer. After SDS PAGE, the resulting 12%polyacrylamide gels were placed in a fixing solution (40% methanol, 10% acetic acid), and in-gel azide Alexa-488- fluorescence was detected using Invitrogen instruction on a Typhoon scanner (access provided courtesy the Terrance Donnelly Centre, University of Toronto). Sample fractions at lysate, washes and elution were saved and analysed by western blot to ensure yields of transfection, expression and purification for each clones.

Western Blot- Proteins were transferred from 12%polyacrylamide gel to nitrocellulose membrane with 100 V, 70 mn, 4 °C. Blots were blocked in 0.1%tween and 5%BSA for 1h. Primary antibodies were incubated overnight at 4C. Concentrations of antibodies were used accordingly to companies' instructions in 5%BSA solution. After 3-5 washes in blocking solutions, we added HRP linked-secondary mouse or rabbit antibody for 2h in 5%BSA. We 3-5 times wash the excess of secondary antibody and detect HRP signals with chemoluminescent substrate -SuperSignal West Pico Chemiluminscent Substrate, Thermo Scientific.

Statistical Analysis – Statistics One-way ANOVA with a Tukey's HSD post hoc test was used to determine statistical significance between the groups. *$P<0.05$.

Results

Wild type RGS4-YFP shows a high degree of localization to the plasma membrane and endosome compartment in HEK293 cells as demonstrated by confocal imaging (Figure 15A). Mutation of L23 within the amphipathic helix domain (L23D) resulted in complete redistribution of RGS4 from the plasma membrane and endosomes to the cytosol. Compared to nontransfected controls, expression of Gq(R183C) markedly increased the production of inositol phosphates in HEK293 cells. As expected co-expression of wild type RGS4 with Gq(R183C) resulted in a reduction (~ 80%)of inositol phosphate production. Consistent with the notion that proper plasma membrane targeting is required for RGS4 function, the mislocalized L23D mutant was unable to inhibit Gq(R183C)-mediated inositol phosphate production compared to wild type RGS4 (Figure 15B). The L23D mutant was used hereafter as a nonfunctional negative control construct.

We next asked whether palmitoylation of the amino terminus was an important determinant of its plasma membrane localization and function in mammalian cells. Indeed, inhibition of endogenous palmitoyl-CoA transferases with 2-bromopalmitate (2-BP) resulted in marked redistribution of RGS4 from the plasma membrane to the cytosol (Figure 16A). The mislocalization effect of 2-BP may reflect reduced Cys2- and Cys-12 palmitoylation since the double-mutant C2A; C12A shows a dramatic decrease in its palmitoylation status and is likewise mislocalized to plasma membrane (Figures 16B and17). Indeed, the extent of mislocalization of the combined mutant approached that of the L23D clone. To determine the relative contribution of Cys2- and Cys12-palmitoylation to the membrane localization of RGS4, we also studied the localization of individual C2A or C12A mutants of RGS4. Surprisingly, mutation of Cys12 alone (C12A), but not Cys2 (C2A) was sufficient to disrupt the plasma membrane targeting of RGS4. Notably, the relative membrane localization potential of the wild type and cysteine mutants was similar in the absence (Figure 16) and the presence (Figure 18) of coexpressed GqR183C. Together, these

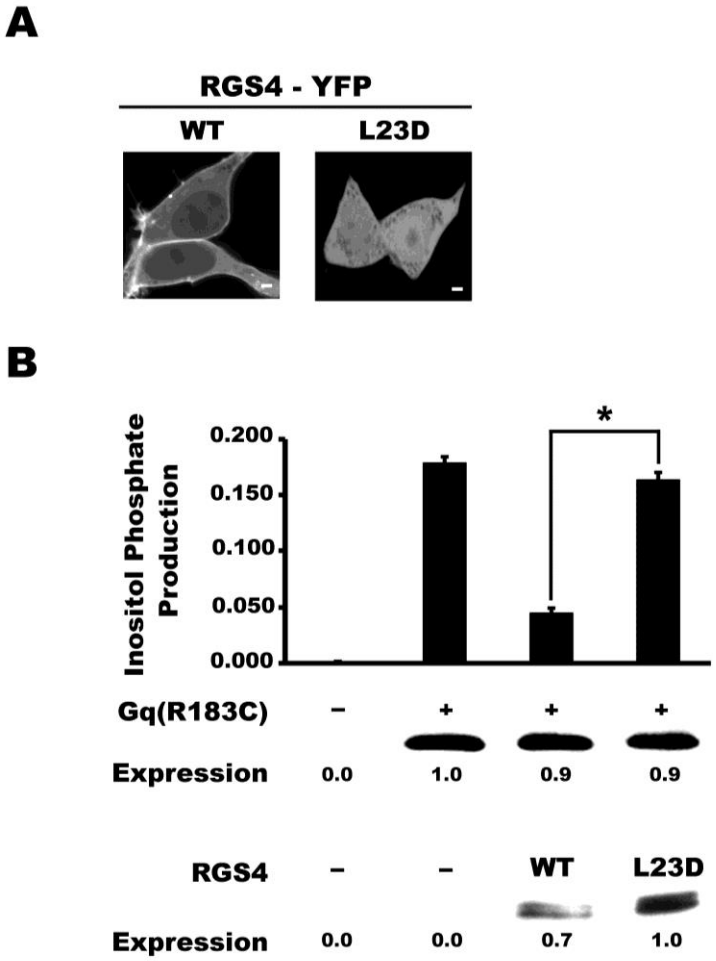

Figure 15: Disruption of RGS4 plasma membrane targeting domain abrogates its Gq inhibitory function in HEK293 cells. *A*. Localization of YFP fusion constructs was examined by transient transfection and confocal microscopy in live HEK293 cells. Shown are YFP fluorescence images of the basal side (relative to the nuclear equator) of the cells with low to intermediated fluorescence. Images are representative of at least 80 cells examined in each of 3 independent experiments. *Scale bars* represent 1 μm. *B*. Inositol phosphate production was measured using ^{3}H-myoinositol labeling of transfected cultures. HEK293 cells were co-transfected with vector control or constitutively active Gq(R183C) and the indicated HisStrep-tagged RGS4 construct. Relative expression levels of RGS4-HisStrep proteins and Gq(R183C) were determined by immunoblotting (*inset*). Following overnight labeling, inositol phosphate production was measured as described in the "Experimental Procedures". Values indicate absolute inositol phosphate/total soluble inositol ratios and are the mean of 5 independent experiments each performed in triplicate. S.E. are indicated by *error bars*. One-way ANOVA with a Tukey's HSD post hoc test was used to determine differences between groups (*$p < 0.001$).

data suggest that interaction of the carboxyl terminal RGS box domain with activated Gq is not an important determinant of its plasma membrane targeting.

Functional studies for the RGS4 cysteine mutant series roughly paralleled the plasma membrane localization data. Specifically, compared to the wild type protein the mislocalized C12A and C2A;C12A proteins showed virtually no Gq-inhibitory function whereas the C2A protein retained some Gq inhibitory function (Figure 19). In an attempt to explain the differential importance of Cys2 and Cys12 with respect to RGS4 localization and function we used a helical net projection to map the positions of Cys2 and Cys12 relative to the stretch of amino acids in RGS4 containing its amphipathic helix domain (amino acid residues 12-30) (Figure 20). Based on the relative proximity of Cys12 to this helix domain and its position immediately adjacent to the putative membrane-binding surface, it seems likely that palmitoylation of Cys12 would have a greater impact on the length of the hydrophobic interface of the helix than would palmitoylation of Cys2. Previous work on the RGS2 protein showed that the length of the aliphatic interface in the amphipathic helix domain can have a profound effect on its plasma membrane localization and Gq-inhibitory function[196].

Considering the importance of N-terminal palmitoylation of RGS4 for plasma membrane targeting and Gq inhibition, we asked which palmitoylating enzymes may be responsible for Cys2 and Cys12 palmitoylation. Previously DHHC3 and 7 have been demonstrated palmitoylating Gαq[163] - protein known to be inhibited by RGS4 and is therefore thought to be in similar cellular environment-. Accordingly, after testing the potential action of DHHC3, 5, 7 and 21 on RGS4, only DHHC3 and 7 showed the capacity to alter the localization of RGS4-YFP from plasma membrane to perinuclear intracellular structures (Figure21). It appeared that RGS4-YFP localization in the presence of DHHC3 and 7 was well overlapping with TGN38-CFP (Figure22) - a trans-Golgi compartment marker known to traffic constitutively between the Golgi and plasma membrane[197]- indicating that RGS4 could, under some circumstances traffic through the TGN compartment. In HEK cells, HA-tagged-DHHC3 and 7 localization corresponded to a well

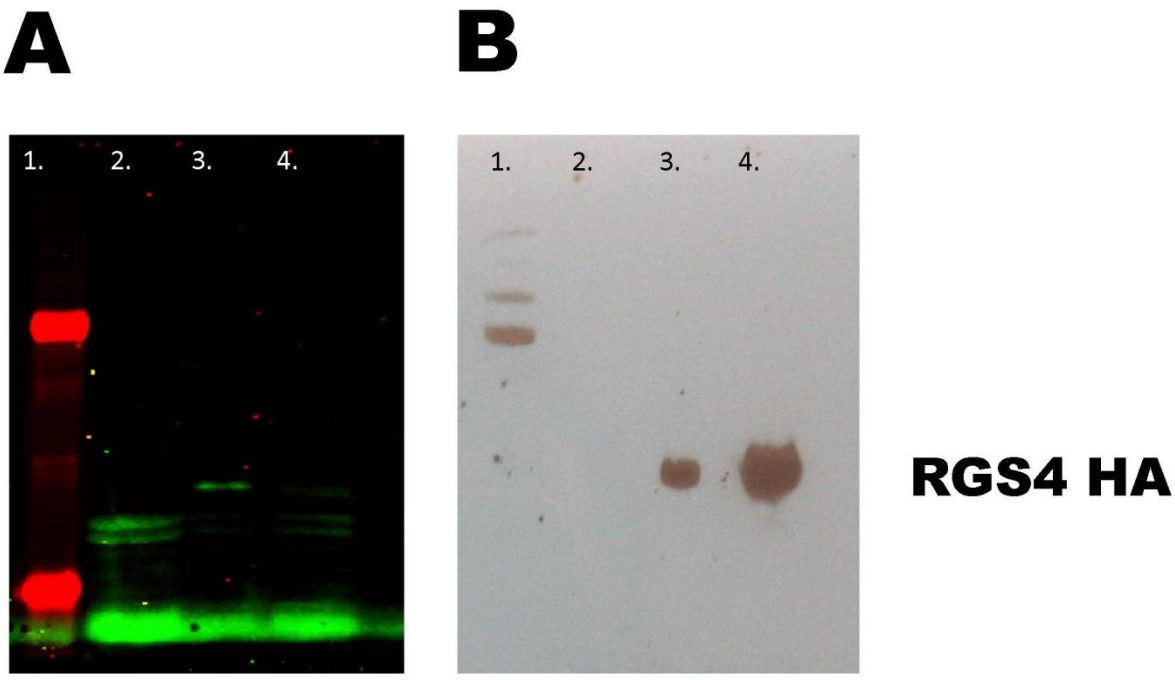

Figure16: Mutation of Cys2 and cys12 significantly decreases RGS4 palmitoylation status. Compare to RGS4WT, RGS4C2AC12A show significant lower palmitoylation status despite higher protein level of expression. A. Green fluorescence signal indicates the palmitoylation status of RGS4WT and C2AC12A. B. RGS4-HA protein expression detected by western blot. 1. Ladder;2. Untransfected control; 3. RGS4WT; 4. RGS4C2AC12A

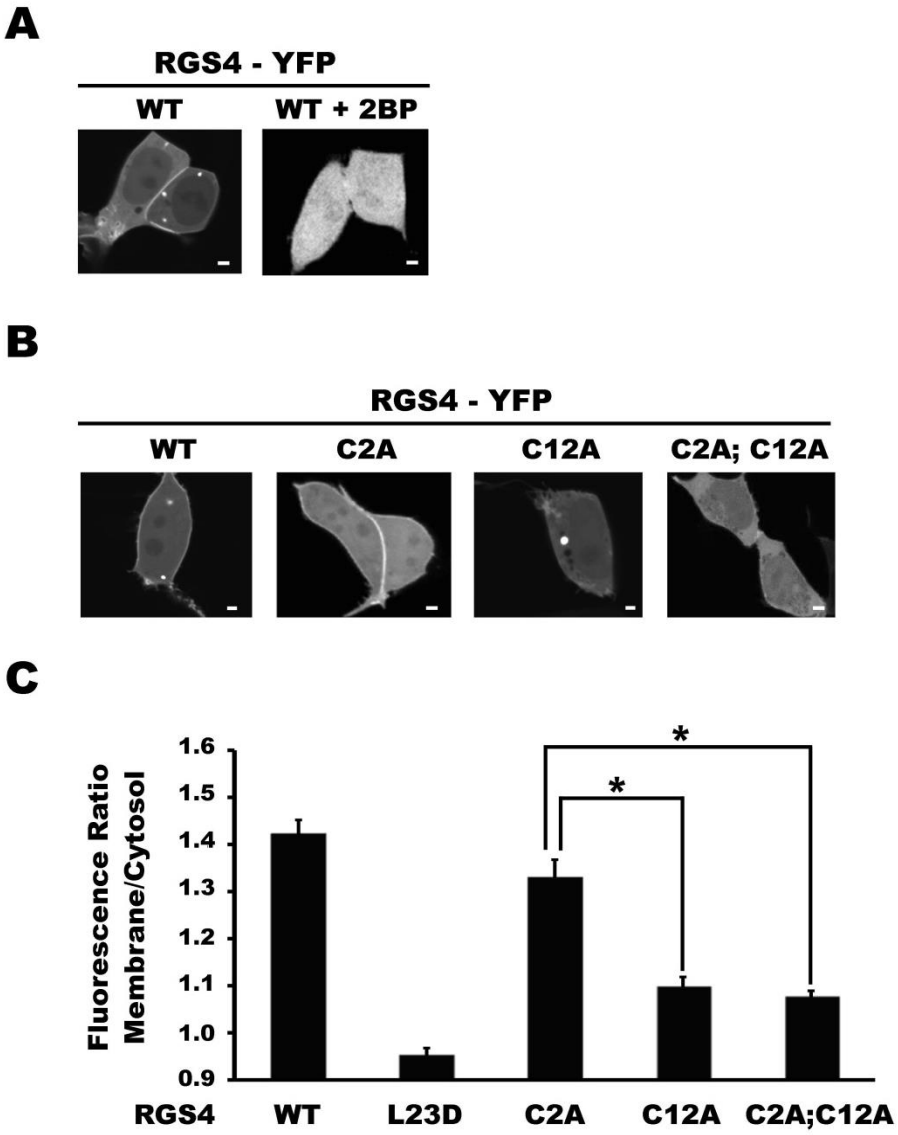

Figure 17: Defining the effect of palmitoylation and N-terminal cysteine residues mutation on the plasma membrane targeting of RGS4. *A*. Localization of the wild type RGS4-YFP construct in the presence and absence of the palmitoyl-CoA transferase inhibitor 2-bromopalmitate (2-BP) was examined by confocal microscopy as described above. *B*. Localization of different YFP-tagged cysteine mutants of RGS4 fusion constructs in HEK293 cells. *Scale bars* represent 1 μm. *C.* The ratio of the RGS4-YFP signal between the cytosol and plasma membrane was analyzed by densitometry using ImageJ software. Shown are means ratio of n >80 cells. S.E. are indicated by *error bars.* One-way ANOVA with a Tukey's HSD post hoc test was used to determine differences between groups (*$p < 0.01$).

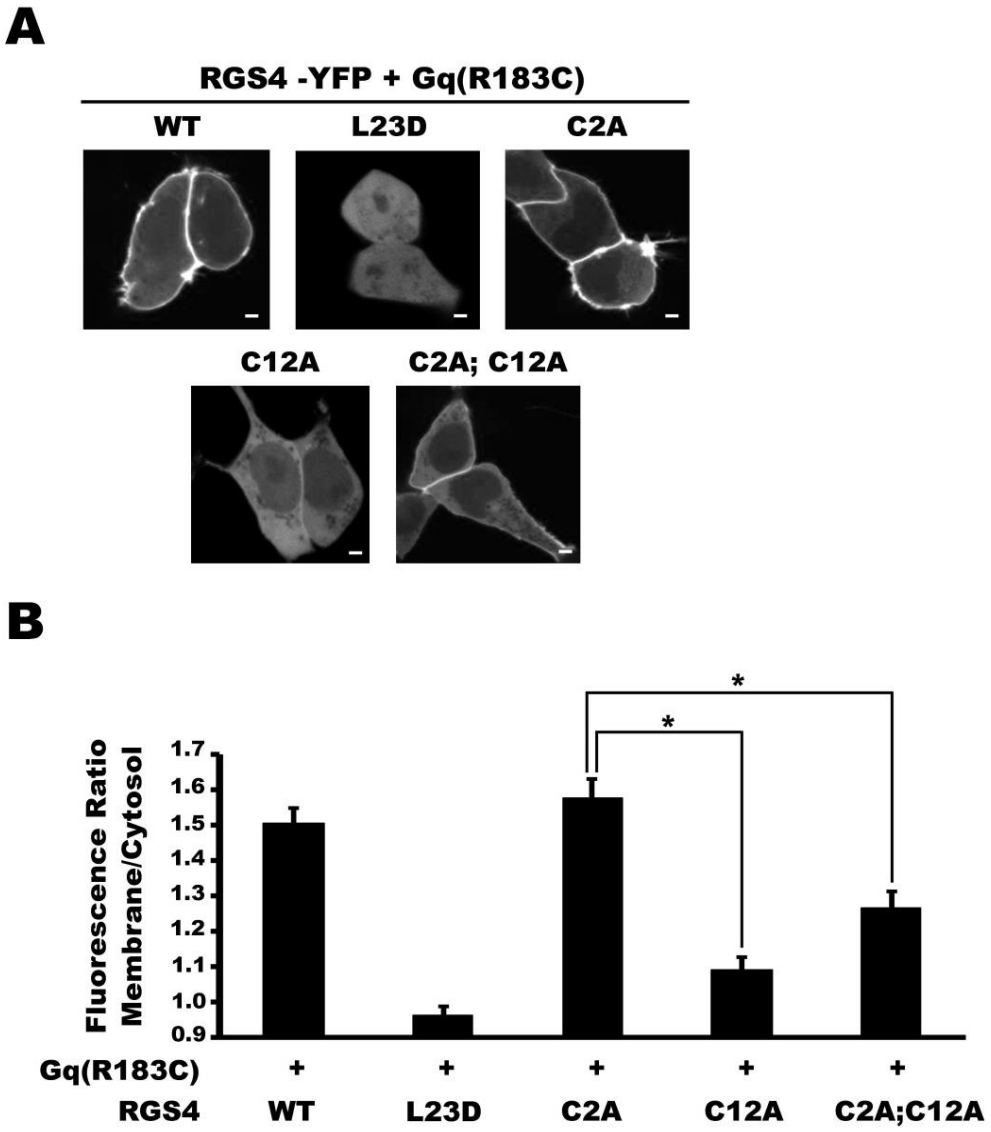

Figure 18: Localization of RGS4 wild type and mutant constructs is relatively unaffected by Gq(R183C). *A.* Localization of different YFP-tagged cysteine mutants of RGS4 fusion constructs in HEK293 cells in the presence of co-expressed Gq(R183C) was examined by confocal microscopy as described above. *Scale bars* represent 1 μm. *B.* The ratio of the RGS4-YFP signal between the cytosol and plasma membrane was analyzed as above (n >30). One-way ANOVA with a Tukey's HSD post hoc test was used to determine differences between groups S.E are indicated by *arrow bars* (*$p < 0.05$).

delimitated but large peinuclear pattern, presumably associated with the Golgi region as previously suggested (Figure21;22).

With the aim of defining the role of RGS4 N-terminal palmitoylation and their potential addition by DHHC3 and 7, we investigated the hypothetical effects of knocking down DHHC3 and 7 on RGS4 plasma membrane targeting and capacity to inhibit Gαq. Indeed, it appeared that RGS4-YFP plasma membrane/cytosol fluorescence intensity ratio significantly decreased when DHHC3 and 7 were knocked down. The ratio with scrambled SiRNA was 1.35 and went down to 1.2 and 1.15 with SiRNA DHHC3 and 7 respectively (Figure23). Supporting the importance of RGS4 targeting the plasma membrane in order to inhibit Gαq signaling, preventing palmitoylation addition on RGS4 by knocking down DHHC3 and 7 was significantly decreasing RGS4 capability to inhibit intracellular calcium release induced by carbachol stimulation (Figure23). In this experiment a chimeric Gαqi9 construct was used in place of the classical Gαq to eliminate potential confounding effects of altered DHHC 3 and 7 activities on Gq, an established palmitoylatable substrate of these two enzymes. The chimeric Gαqi9 contained a transmembrane domain for constitutive plasma membrane expression and the 9 C-terminal amino acids of Gαi allowing to couple effectively to Gαi-coupled receptors such as the M2 muscarinic receptor. With acetylcholine stimulation of M2 receptors, Gαqi9 was able to couple to its classic effector pathways including PLCβ and intracellular calcium. Since the N-terminal palmitoylation sites of Gαqi9 were replaced by its transmembrane domain, we could study the effect of knocking down DHHC3 or 7 on RGS4 function without interfering with Gαq function. Notably, M2 muscarinic receptor coupled to Gαqi9 provided similar intracellular calcium response to 200uM carbachol as did the M1muscarinic receptor coupled to Gαq/11 in HEK cells[198]. RGS4 was capable of inhibiting M2/Gαqi9-mediated stimulation of intracellular calcium release; whereas knock downs of DHHC3 and 7 both decreased the potency of RGS4 for this effect. (Figure23). Together these data expose the importance of DHHC3 and 7 in the regulation of RGS4 localization and its capability to inhibit Gαq mediated signaling.

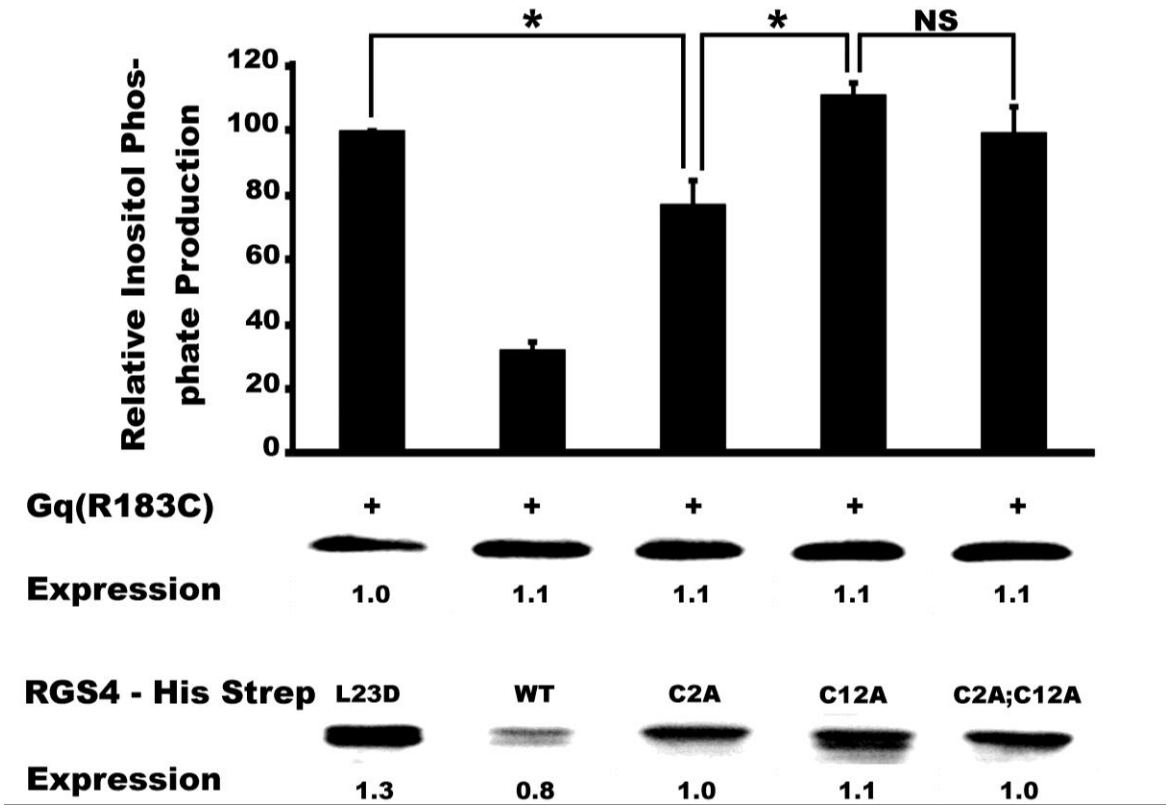

Figure 19: Mutation of Cys2 and Cys12 exert differential effects on RGS4 Gq inhibitory activity. Inositol phosphate production was measured using ^{3}H-myoinositol labeling from triplicate wells for each transfection condition. Briefly, HEK293 cells were co-transfected with constitutively active Gq(R183C) and the indicated HisStrep-tagged RGS4 construct. Relative expression levels of RGS4-HisStrep proteins and Gq(R183C) were determined by immunoblotting (*inset*). Following overnight labeling, inositol phosphate production was measured as described in the "Experimental Procedures". Values indicate the mean inositol phosphate/total soluble inositol ratio relative to that for the internal RGS4-inactive control (L23D) and are the mean of 5 independent experiments performed on separate days. S.E. are indicated by *error bars*. One-way ANOVA with a Tukey's HSD post hoc test was used to determine differences between groups ($*p < 0.05$).

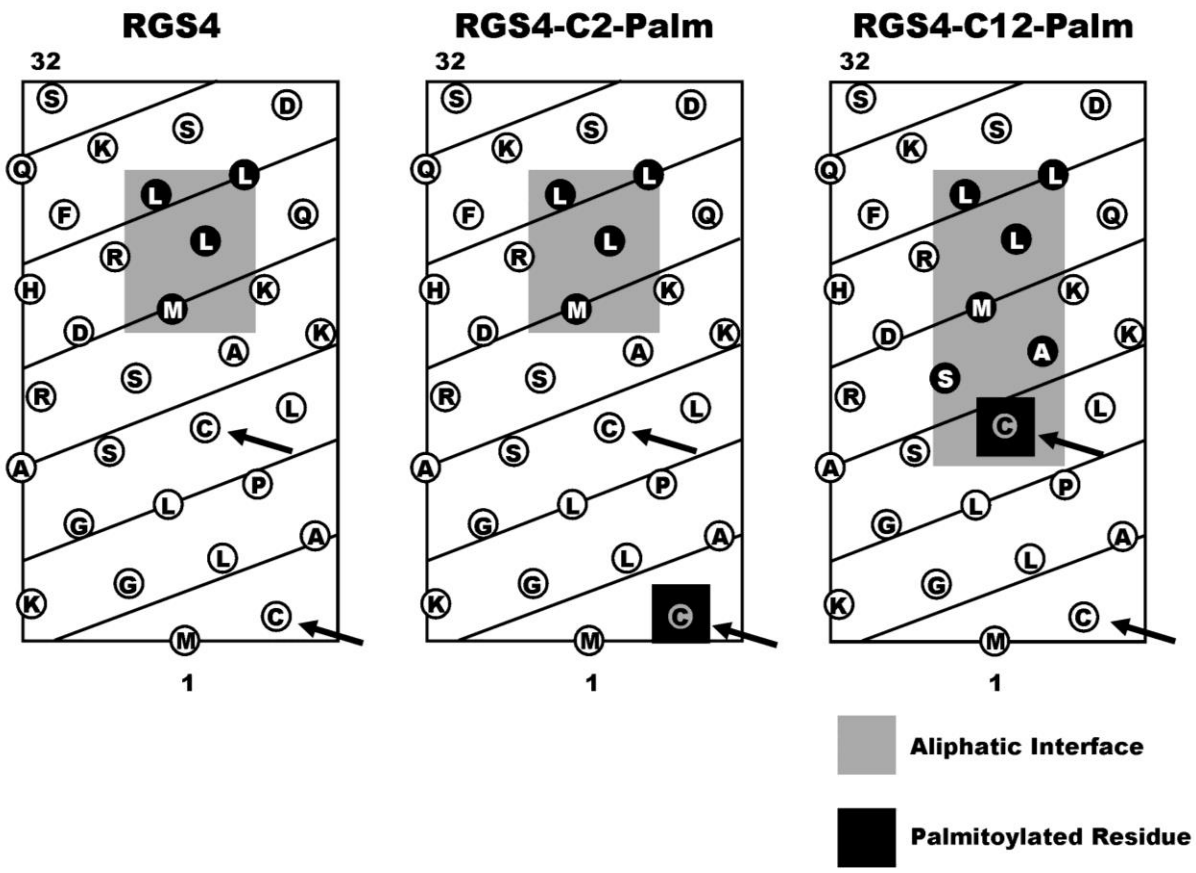

Figure 20: Helical net modeling of the hydrophobic surface on the RGS4 amphipathic helix in non-palmitoylated (left) and mono-palmitoylated states. Shown is a 2D schematic representation of the alpha helical RGS4 membrane association domain. Arrows denote putative palmitoylation sites (Cys2 and Cys12) in the RGS4 amino terminus. *Shading* indicates the length of the hydrophobic surface on the amphipathic α-helix of RGS4. Aliphatic and nonpolar aromatic residues are shown as *black*, polar residues in *white* and palmitoylated cysteine residues in *yellow*. Note how Cys12 palmitoylation may be predicted to increase the length of the hydrophobic surface by at least one turn of the helix.

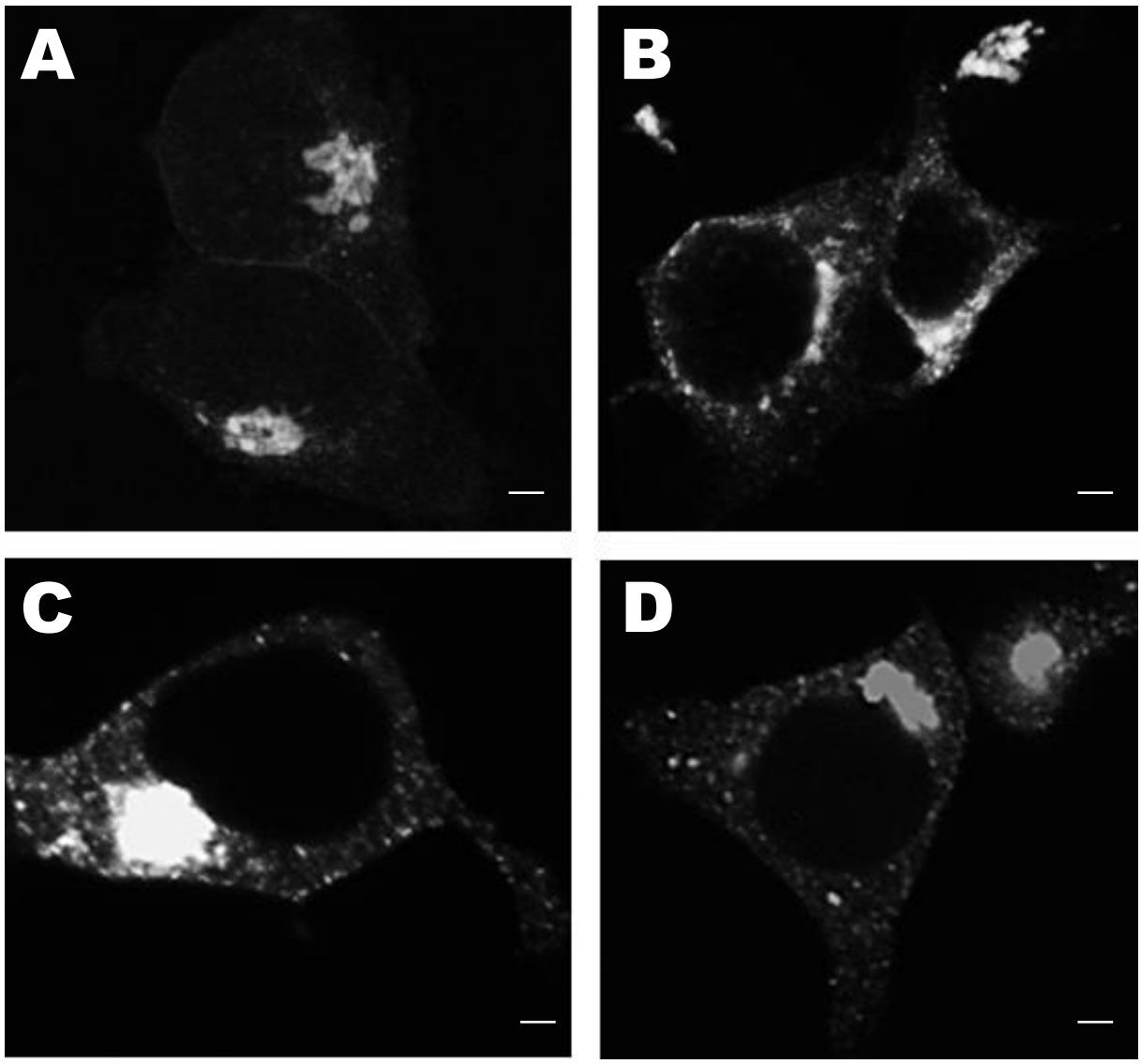

Figure21: RGS4 localizes to perinuclear region Golgi related and endosomes when co-expressed with DHHC3 and 7. Immunostaining in HEK293 cells of A. DHHC3-HA and B. DHHC7 reveal their localization to large perinuclear region Golgi related and endosomes. Living cell imaging of RGS4-YFP co-transfected with C. DHHC3-HA and D. DHHC7 show an impaired localization of RGS4 to large perinuclear region Golgi related and endosomes throughout the cytosol. White bars are scale representative of 1um.

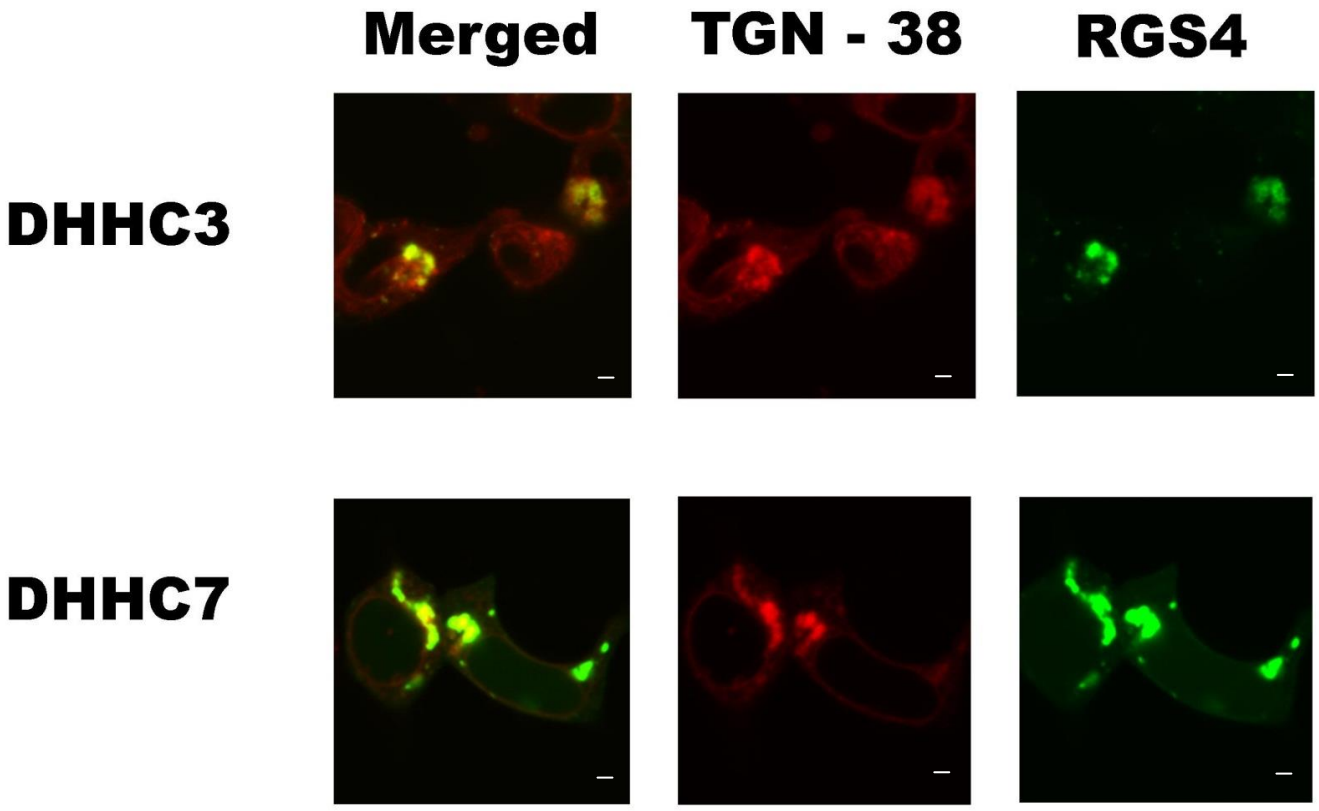

Figure22: RGS4 perinulcear localization is overlapping TGN38 when coexpressed with DHHC3 and 7. We observed RGS4-YFP (right panel) localizing to perinuclear regions colocalizing with TGN38-CFP (in red; center panel) when co-expressed with DHHC3 (top) and DHHC7 (bottom). White bares are scales representatives for 1um.

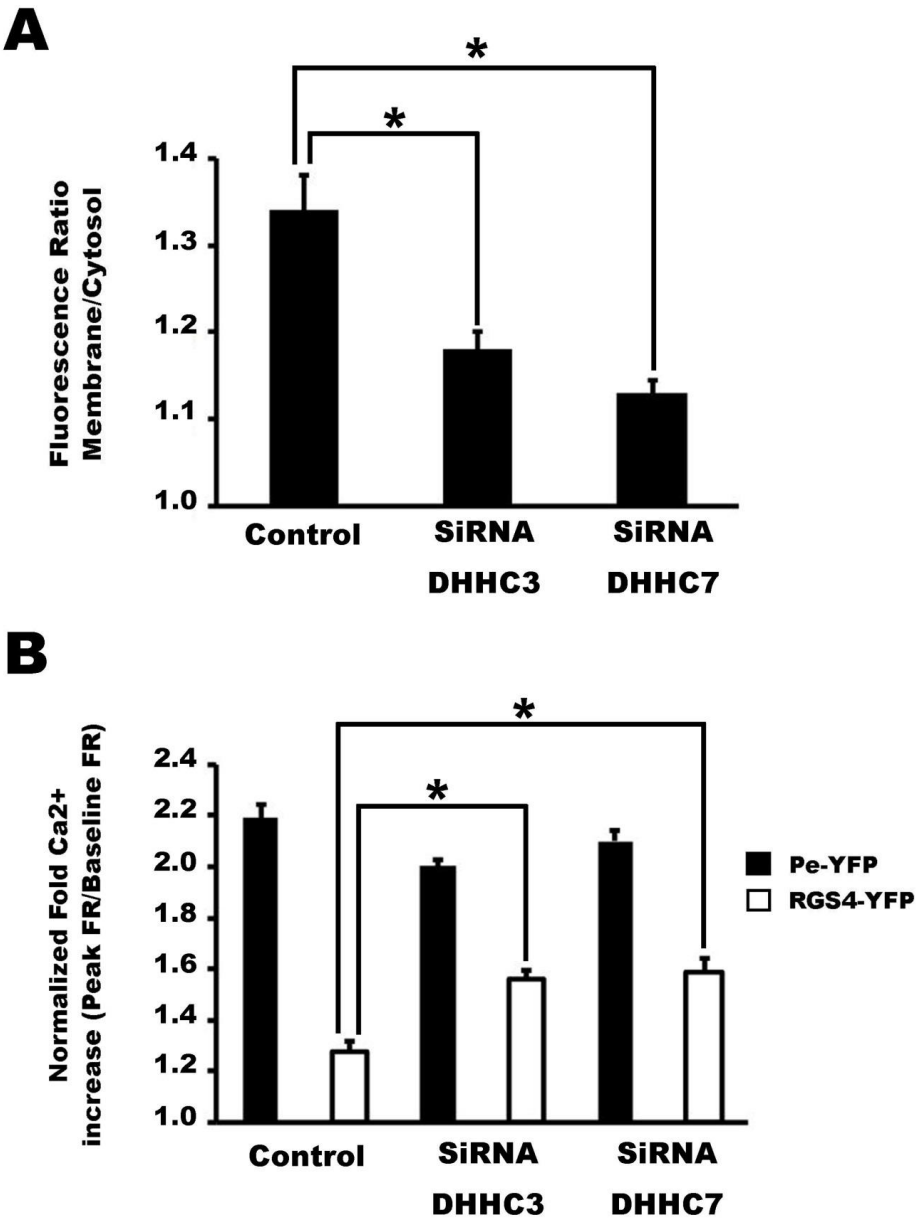

Figure23: DHHC3 and 7 regulate RGS4 plasma membrane targeting and inhibition of Gq mediated signaling. *A*. Knock down of DHHC3 and 7 decrease RGS4-YFP plasma membrane targeting in HEK293 cells. Results from living cell imaging. Picture taken by Olympus Fluoview-1000, oil objective 60x, 1.4NA and analysed by ImageJ software. One-way ANOVA with a Tukey's HSD post hoc test was used to determine differences between groups (*$p < 0.05$). *B*. Knock down of DHHC3 and 7 decreased inhibition of Gqi9 mediated intracellular calcium release under200uM carbachol stimulation. fold of Fura-2 340/380nm fluorescence were analyzed to determined intracellular calcium release under carbachol stimulation. One-way ANOVA with a Tukey's HSD post hoc test was used to determine differences between groups (*$p < 0.05$).

Next we asked whether DHHC3 and 7 show any specificity toward amino terminal RGS4 cysteines. HA-DHHC7 interaction wasn't affected by any single mutation on Cys2- and Cys12- whereas mutation of Cys2- significantly altered HA-DHHC3 interaction (Figure24). Overall, these results indicate that DHHC3 interacts primarily with Cys2 whereas DHHC7 interact with any Cys2 and Cys12 of RGS4-YFP. However, neither DHHC3 nor 7 were able to promote perinuclear clustering of RGS4 when both Cys2;Cys12 were mutated suggesting that phenotypes observed by knocking down DHHC3 and 7 on the localization and function of RGS4 may be independent of its Cysteine 95 palmitoylation site.

Since palmitoylation regulates intracellular trafficking of multiple components of the GPCR signaling pathways including G-protein α subunits[163], RGS proteins[199], and some RGS protein-binding proteins[200] we examined whether palmitoylation on Cys2 or Cys12 affects the intracellular trafficking of RGS4. First we determined the extent to which wild type RGS4 expression was localized to endosomal compartments. As illustrated in Figure 25, RGS4-YFP could be observed in discreet intracellular compartments in ~40% of the cells examined (Figure25). Addition of 2-BP prevented observation of RGS4 to the endosome compartment in ~ 99% of cells. Notably, Cys2 and Cys12 seem to contribute differentially to the distribution of RGS4 within the intracellular pool. Mutation of Cys12 reduced the percentage of cells showing endosomes to ~15% while mutation of Cys2 nearly completely disrupted RGS4 localization to endosomal structures (Figure25).

G-protein alpha subunits cycle between the plasma membrane and the Golgi compartment. Palmitoylation at the level of the Golgi is a key step in this process[163]. We wondered whether the Cys2 and Cys12 palmitoylation sites on RGS4 may likewise be a component of its cycling between the PM and Golgi. Indeed RGS4 was reported to be associated with both the PM and Golgi compartments[201]. We thus examined the potential for RGS4 to colocalize with TGN38. In cells expressing TGN38-CFP, it is localized primarily to the trans-Golgi region as expected, but its expression was also observed in endosomal structures proximal to the Golgi. Although strong trans-Golgi colocalization was not

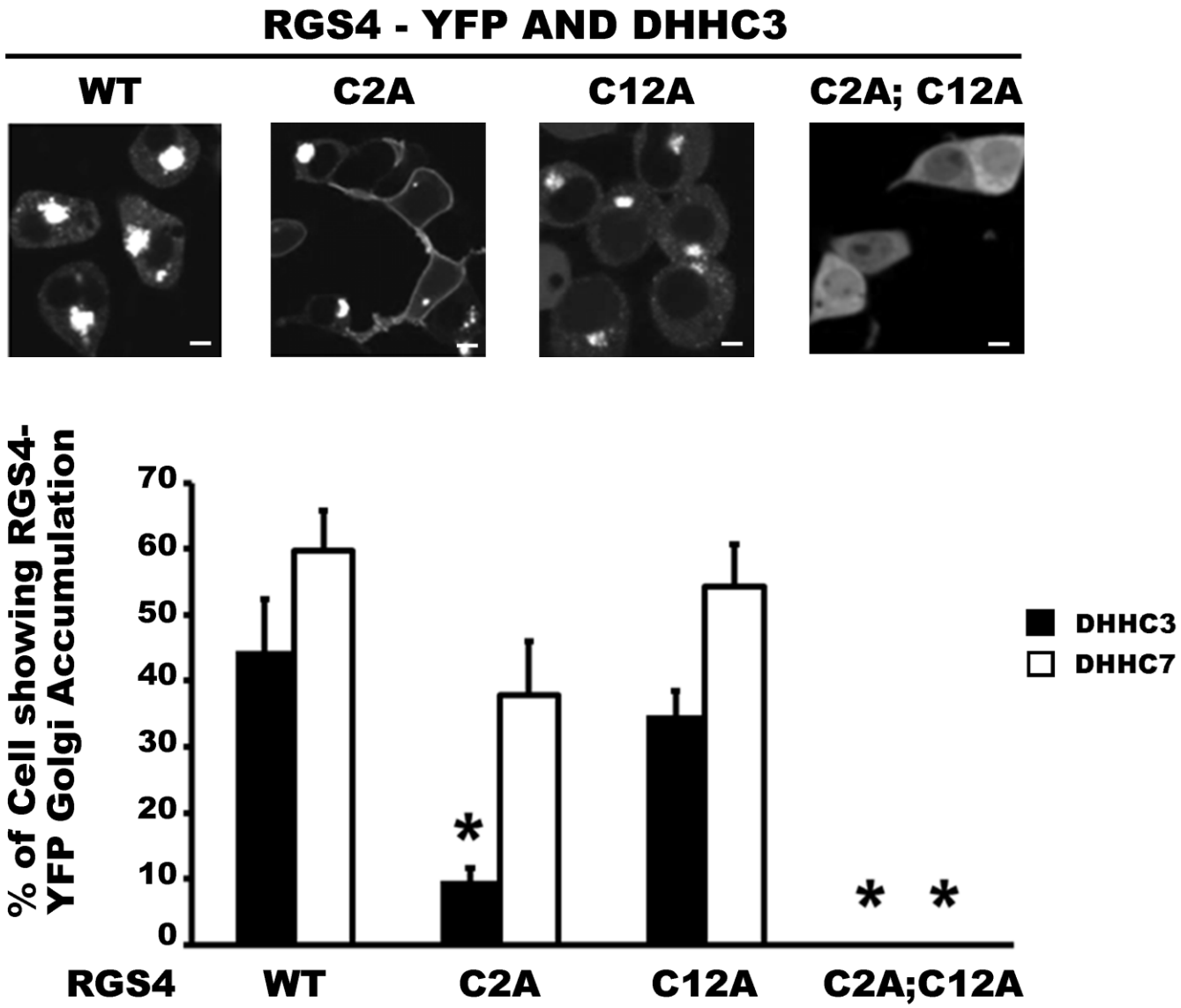

Figure24: DHHC3 and 7 interact with RGS4cys2 and cys12. Mutation of Cys2 altered DHHC3-HA capacity to localize RGS4-YFP at perinuclear Golgi related region. Both mutation C2AC12A completely disrupted DHHC3 and 7 capacity to localize RGS4 to perinuclear Golgi related region. One-way ANOVA with a Tukey's HSD post hoc test was used to determine differences between groups *$p < 0.01$ for C2A and DHHC3; *$p < 0.0001$ for C2AC12A and DHHC3-7. White bars are scale representative of 1um.

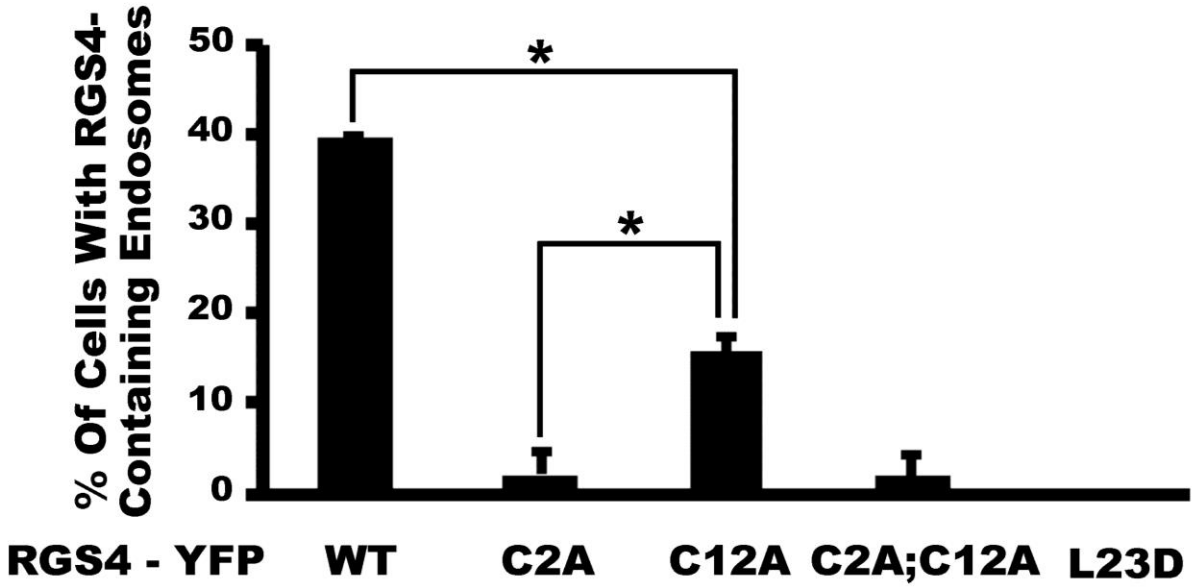

Figure 25: RGS4 requires the N-terminal amphipathic α-helix and amino-terminal cysteine residues for endosome localization. The indicated RGS4-YFP fusion constructs were examined for the presence of RGS4-containing endosomes. For each construct, cells with low to intermediate fluorescence intensity were scored for the presence or absence of endosome structures. Shown are the mean of the percentage of cells with RGS4-containing endosomes determined during 4 independent experiments (n > 40 cells/experiment, n > 180 total cells/construct). One-way ANOVA with a Tukey's HSD post hoc test was used to determine differences between groups (*$p < 0.01$). S.E. are indicated by *error bars.*

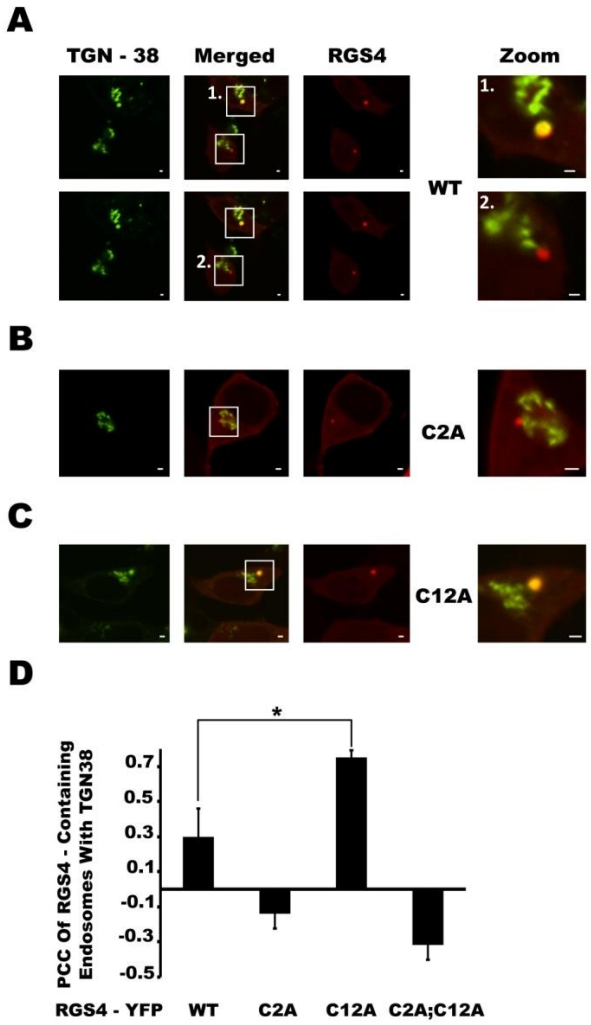

Figure 26: Colocalization of RGS4–containing endosomes with TGN38 is differentially affected by Cys2 and Cys12. Localization of RGS4-containing endosomal structures with the trans-Golgi-endosome marker TGN38 (TGN38-CFP) was examined by co-transfection in HEK293 cells followed by fluorescent microscopy of live cells. *A*. WT (*upper* and *lower panels* highlight the existence of both strongly (cell #1) and poorly (cell #2) colocalized endosomes in different cells), *B*. C2A (show typically poorly colocalized endosomes), *C*. C12A (show typically well-colocalized endosomes). Using the excitation and emission discrimination capabilities of the Olympus FV1000 confocal microscope, RGS4 (*red pseudocolor*) and TGN38 (*green pseudocolor*) images were collected from the same confocal plane. Merged images indicate areas of potential colocalization (shown in yellow). *Scale bars* represent 1µm. *D.* Pearson correlation coefficients (PCCs) for RGS4-containing endosomes with TGN38 expression were determined using Olympus Fluo-View™ software. Shown are mean PCC values (n >3 cells/experiment for C2A and C2AC12A; n >15 cells/experiment for WT and C12A) from 4 independent experiments. One-way ANOVA with a Tukey's HSD post hoc test was used to determine differences between groups (*$p < 0.05$). S.E. are indicated by *error bars.*

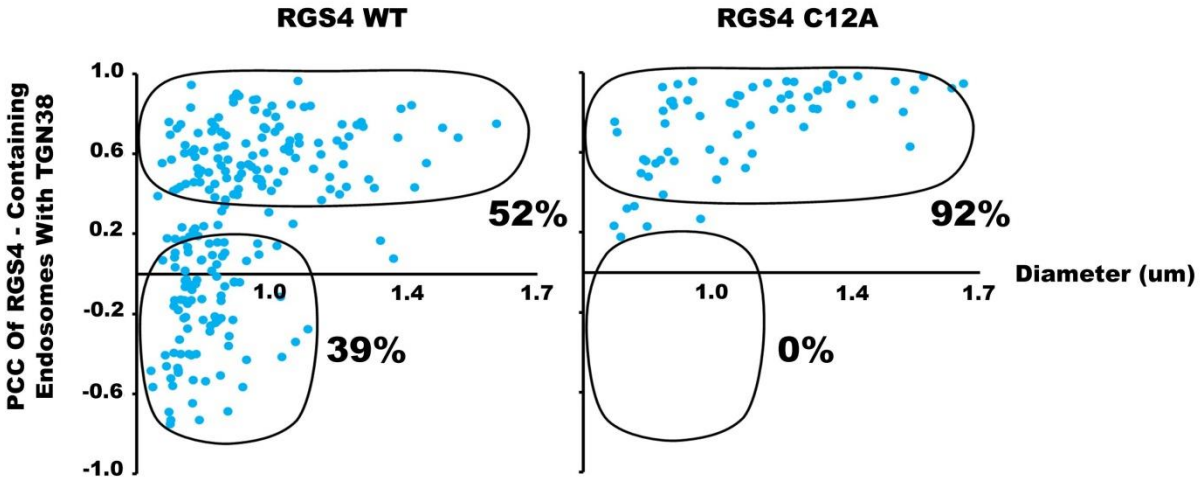

Figure 27: Distribution of RGS4-containing endosomes by endosome size and TGN38 colocalization coefficient. Scatter plot for RGS4-containing endosomes comparing diameter and extent of colocalization with TGN38 colocalization (PCC). Plotted data were only available for WT and C12A as C2A and C2AC12A constructs localized very poorly to the endosome pool. Each data point represents a single endosome collected over 4 independent experiments. RGS4-containing endosomes were arbitrarily sorted into strongly (PCC > 0.4) and weakly (PCC < 0.2) TGN38-colocalized pools. Pool distribution profiles of RGS4-containing endosomes varied greatly between the WT and C12A constructs.

observed for wild type RGS4-YFP, the fluorescent endosomes containing RGS4 frequently coincided with vesicles containing TGN38-CFP (Figure26A). Indeed, when the entire RGS4-YFP endosome population was examined for its colocalization with TGN38-CFP, a Pearson correlation coefficient (PCC) of 0.3 was obtained. Consistent with a differential role for Cys2 and Cys12 in the intracellular trafficking of RGS4, endosomes containing the C12A mutant showed a high extent of colocalization with TGN38-CFP (PCC = 0.75) whereas the rare endosomes containing C2A or the double mutant C2A:C12A were poorly colocalized with the TGN38 pool (PCC values of -0.1 and -0.3 respectively) (Figure26B). Together, these data suggest that putative palmitoylation of Cys2 or Cys12 differentially affects the trafficking of RGS4 along endosome recycling circuits that normally allow the traffic of RGS4 and other similarly recycled proteins such as TGN38 between the plasma membrane and Golgi.

The difference in TGN38 colocalization between wild type RGS4- and C12A-containing endosomes was examined in Figure 27. When scatter plots of endosome colocalization coefficient versus diameter were examined, two interesting patterns emerged. First, the wild type protein has a vastly different endosome size distribution profile compared to C12A. In particular, the wild type protein is observed much more commonly in small sized (< 1 μm) endosomes than is the C12A protein (73% versus 35% of total endosomes respectively). Secondly, when the size distribution of endosomes with high and low TGN38 colocalization coefficients is compared we observe that for the wild type clone there is a large (39% of total endosomes) unique pool of small sized endosomes that does not colocalize with TGN38. The mutation of Cys12 seems to prevent the localization of RGS4 to this small sized TGN38-refractory pool since most Cys12 containing endosomes contain TGN38 irrespective of their size (Figure 27). Taken together, these data are consistent with a model where palmitoylation at either Cys2 or Cys12 can differentially regulate the intracellular trafficking of RGS4. Mutation at Cys2 almost completely eliminates its endosomal localization whereas mutation at Cys12 impairs its localization to TGN-38-refractory endosomes without affecting its targeting to a TGN38 containing endosomal compartment.

Because Cysteine2 palmitoylation site mutation and RGS4WT treatment with 2-BP nearly completely abrogated RGS4 endosomal localization, we hypothesized that co-expression with DHHS3 or 7 - dominant negative form of DHHC incapable of palmitoylating substrates- would abrogate RGS4 endosomal localization. However, surprisingly, the occurrence of cells showing RGS4 at endosomal pool increased from 55% in RGS4WT single to 97% and 96% when co-expressed with DHHS3 and 7 respectively(Figure28). These results correspond to numerous studies showing that palmitoylation-dependent plasma membrane targeting proteins are trapped at intracellular compartments when appropriate palmitoylation is lacking[149;156;163]. But interestingly the occurrence of cells showing RGS4 endosomes went down from 55% to 39% when we knocked down any DHHC3 and 7 (Figure28). The fact that RGS4 Cys2 mutant is not present at endosomes (Figure25) suggested cysteine2 to be candidate in RGS4 and DHHC3 and 7 interactions leading to RGS4-YFP endosomal localization. Indeed, co-expression of DHHS7 significantly increased both RGS4 WT and C12A but not C2A presence at intracellular compartments (Figure28). Together, these data show that DHHC3 and 7 are interacting with RGS4 cysteine2 in a DHHC motif- independent and palmitoylation -dependent manner to target RGS4 to endosomal pool.

In the aim of identifying new targets for therapeutic design, we decided to precise RGS4 subcellular trafficking. As studies reported TGN38 trafficking through Rab proteins endosomal compartment[202], we examined whether RGS4WT colocalizes with Rab proteins. Rabs proteins are known to be endosomal compartment markers. Rab11 is localized to recycling endosomes and is participating to both exocytotic trafficking to the plasma membrane and retrograde trafficking from recycling endosomes to TGN[190;191]. In our hands, Rab11-CFP typically localized to a stable irregular-shaped organelle deep in the cytosol from which smaller fast moving endosomes were observed to arrive and depart. RGS4WT-YFP showed extensive overlap with Rab11-CFP, since almost 100% of RGS4 endosomes colocalized with Rab11 (Figure29). When DHHS3 and 7 were co-expressed, RGS4WT-YFP was still very well co-localizing with Rab11-CFP (not shown).

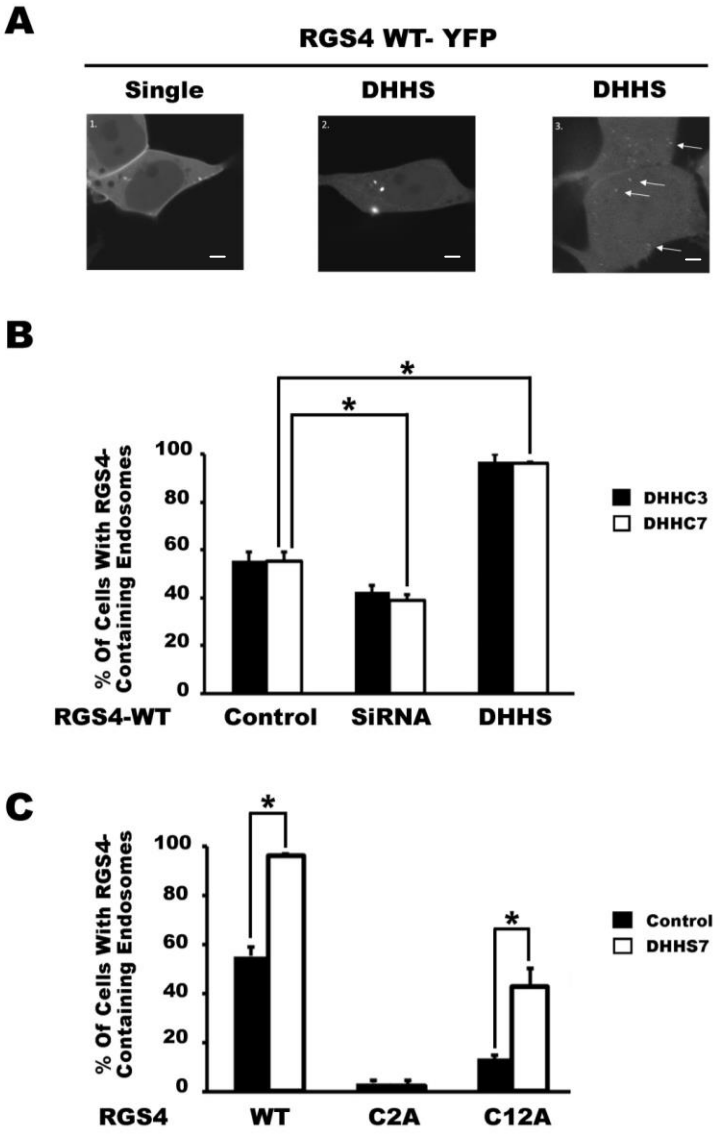

Figure28: Knock downs of DHHC3 and 7decreased RGS4 endosomal targeting whereas DHHS3 and 7 interacted with cys2 to significantly increase RGS4 endosomal targeting. A. DHHS3-7 increase RGS4-YFP endosomal population. We can observe a high diversity in the endosomal population as there are large, slow movers and round endosomes (central picture) and punctates, very tiny and fast movers (right). White bars are scale representative of 1um B. SiRNADHHC3 and 7 decrease the number of cell showing RGS4-YFP at endosomes whereas DHHS3 and 7 dramatically increase RGS4 endosomal population. Cells were observed under Fluoview1000-Olympus confocal microscopy with oil objective, 60x, 1.4NA. One-way ANOVA with a Tukey's HSD post hoc test was used to determine differences between groups *$p < 0.05$ between control and SiRNA and $p<0.001$ between control and DHHS. S.E. are indicated by *error bars* C. DHHS increased both RGS4WT and C12A but not C2A endosomal targeting. One-way ANOVA with a Tukey's HSD post hoc test was used to determine differences between groups *$p<0.01$ C12A and C12A+DHHS7. $P<0.001$ between WT and WT+DHHS7. . S.E. are indicated by *error bars.*

Over-expressing proteins may lead to false positive colocalization. Since RGS4WT – YFP endosomes show close to 100% colocalization with Rab11-CFP, it was important to demonstrate that RGS4WT colocalization with Rab11 endosomes in the absence of Rab11 overexpression. For this purpose, we used TR-labelled transferrin which is known to internalize from the plasma membrane via Rab5 clathrin dependent endocytosis and to recycle back to the cell surface in trafficking through Rab11 compartments[194]. RGS4WT-YFP did show some colocalization with transferrin-texas red (Figure30) indicating that RGS4 is indeed present in Rab11 positive endosomal pool.

RGS4 is present in Rab11-exocytic/endosomal pool, therefore we asked whether its trafficking through that compartment was important for its targeting to the plasma membrane where it functions as an inhibitor of G-protein signaling. Indeed, when co-transfected with Rab11SN, a dominant negative Rab11 construct incapable of binding GTP, RGS4 showed reduced plasma membrane targeting (Figure31). Consistent with the fact that RGS4 would traffic to the plasma membrane from Rab11 endosomal pool we observed that the percentage of RGS4-YFP transfected cells showing endosomes increased from 40% to 70% (Figure31). Rab11 endosomal compartments are well connected with other endosomal compartments, for example Rab5-mediated clathrin-containing endosomes can evolve toward Rab11 endosomal pool. Proteins such as transferrin receptor[194] and β1-adrenergic receptor[203] undergo endocytosis through Rab5 compartments and reach Rab11 pools to recycle back to the plasma membrane. We thus wondered whether RGS4 likewise underwent Rab5a mediated endocytosis. Indeed, RGS4-YFP was less present at the plasma membrane and the percentage of cells showing endosome increased from 40% to 80% when co-expressed with Rab5a(Figure31). Inversely, dominant negative Rab5SN prevented RGS4 endocytosis via clathrin-mediated mechanism and promoted increased plasma membrane accumulation and decreased RGS4 endosomal targeting (Figure31). These changes of RGS4 cellular localization directly regulated its capacity to inhibit M1 muscarinic receptor mediated signaling when co-expressed with Rab11SN and Rab5a (Figure33). Together, these data define a number of previously unknown aspects

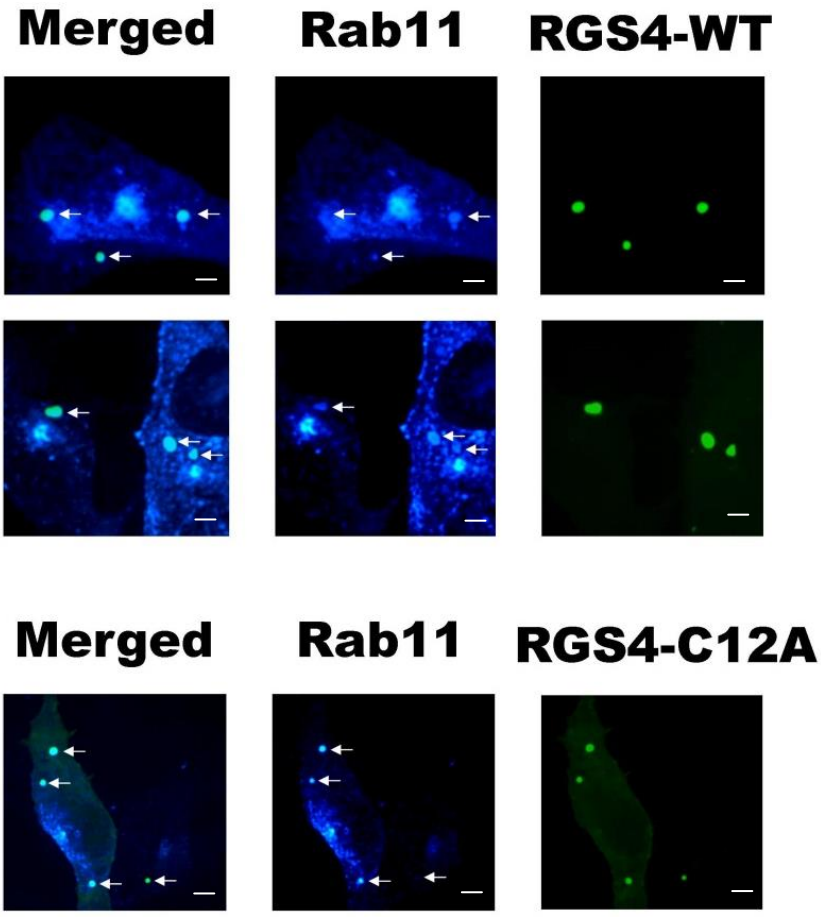

Figure29: RGS4WT and C12A-YFP endosomes very well colocalizes with Rab11-CFP. Pictures taken with spinning disc confocal microscope of RGS4-YFP clones (right panel) and Rab11-CFP (center panel). Objective 60x oil. 1.4NA. white bars are scales representatives of 1um.

of RGS4 trafficking through intracellular endosomal compartments and highlight their potential for the regulation RGS4 function as an inhibitor M1 muscarinic receptor mediated signaling.

Lastly, we wondered whether RGS4 G-protein binding capabilities would influence its localization and trafficking. We thus used the G-protein binding deficient RGS4 mutation EN-87/88th. Notably, the EN-AA mutation did not affect RGS4 intracellular cellular trafficking. Specifically, Rab5a, Rab5SN and Rab11SN coexpression with RGS4EN-AA looked very similar to the plasma membrane distribution profile for RGS4WT, (Figure31-32). RGS4EN-AA also overlapped the pattern of endosomal localization than RGS4WT under similar conditions (Figure31-32). Only RGS4-ENAA with no co-transfected Rabs didn't reproduce the result obtain with RGS4WT, but this may be due to an experimental abnormality as this was not reproduced yet.

We used RGS4EN-AA- G-protein binding mutant- to control whether Rab5 and 11 affected M1-muscarinic receptor signaling. Interestingly, M1 muscarinic receptor signaling showed very similar responses to carbachol independently to Rab5 or Rab11SN expression (Figure33). These data suggest that all components among the calcium signaling pathway (Figure34) such as M1 muscarinic receptor, Gαq/11, PLCβ, calcium storage and IP3-receptor calcium channel are not altered by Rab11 or Rab5a activity in this particular assay. To our knowledge, no publications have connected the activity of any of these proteins to their endosomal trafficking mediated by Rab5a or Rab11. Overall, these data show that Rab5a and Rab11 regulated RGS4 selectively and independently to the M1 mediated calcium machinery. Thus, modulating Rab5a and Rab11 compartment function may provide a novel approach for regulating RGS4 function without affecting parental signaling pathways such as M1 muscarinic receptor-dependent activation of intracellular calcium signaling (Figure34).

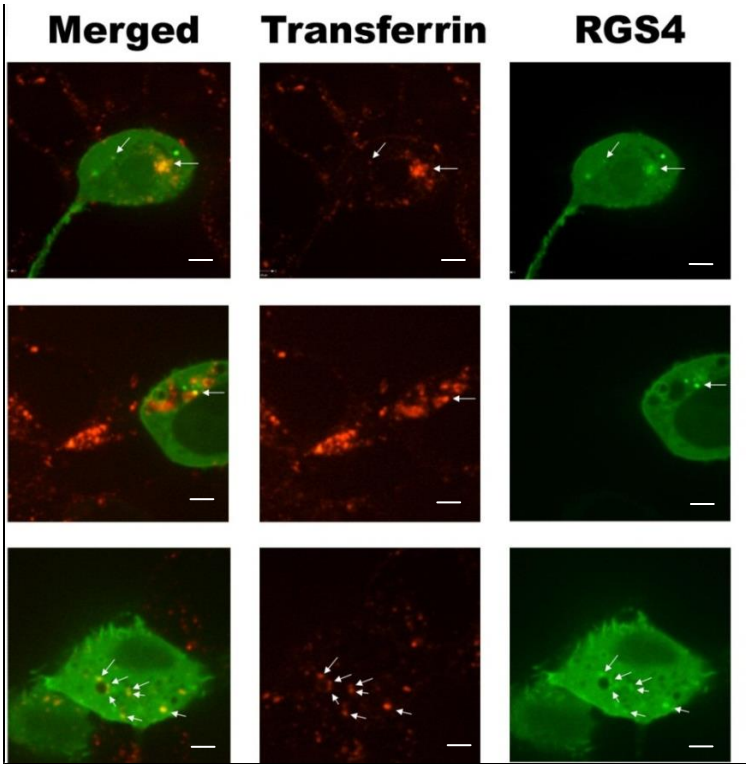

Figure30: RGS4-YFP is colocalizing with Transferrin texas red. Pictures taken by spinning disc confocal microscopy with oil objective 60x. 1.4NA. RGS4-YFP (right panel) is showing some colocalization with internalized transferrin –texas red (center). White bars are scales representatives of 1um.

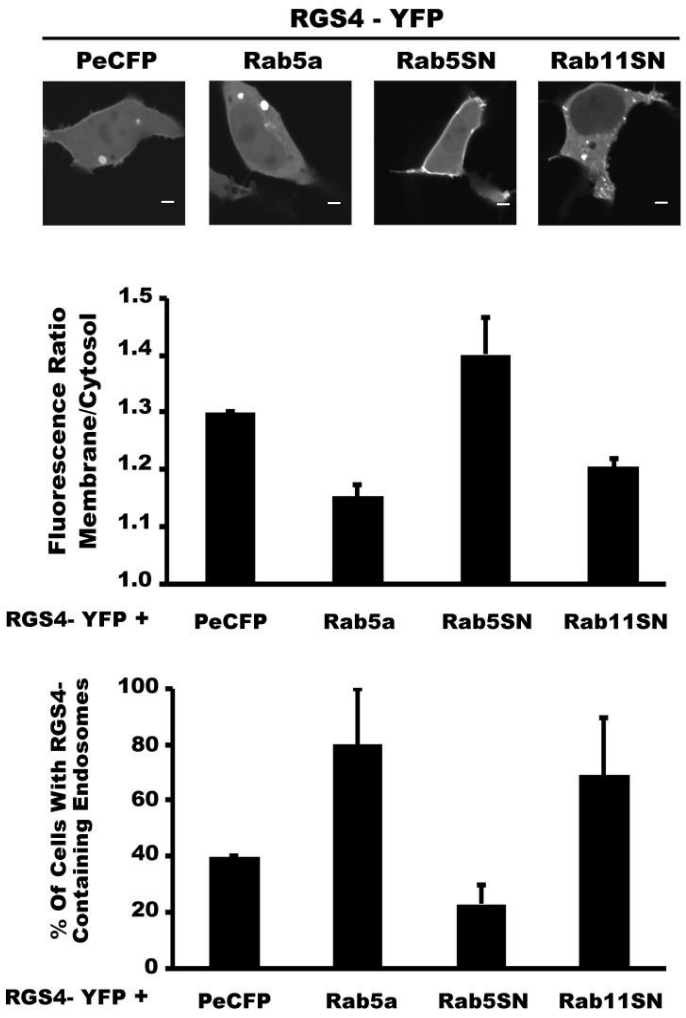

Figure31: RGS4 traffics through Rab11 exocytic pathway and Rab5 clathrin mediated endocytosis. *A*. Localization of RGS4WT-YFP with different CFP-tagged Rab constructs in HEK293 cells. *Scales bars* represent 1 μm. *B.* The ratio of the RGS4-YFP signal between the cytosol and plasma membrane was analyzed by densitometry using ImageJ software. Shown are means ratio of n >70 cells per condition. S.E. are indicated by *error bars. C*. RGS4-YFP fusion constructs were examined for the presence of RGS4-containing endosomes with different Rab proteins. For each condition, cells with low to intermediate fluorescence intensity were scored for the presence or absence of endosome structures. Shown are the mean of the percentage of cells with RGS4-containing endosomes determined during 2 independent experiments (n > 35 cells/experiment, n > 70 total cells/condition).

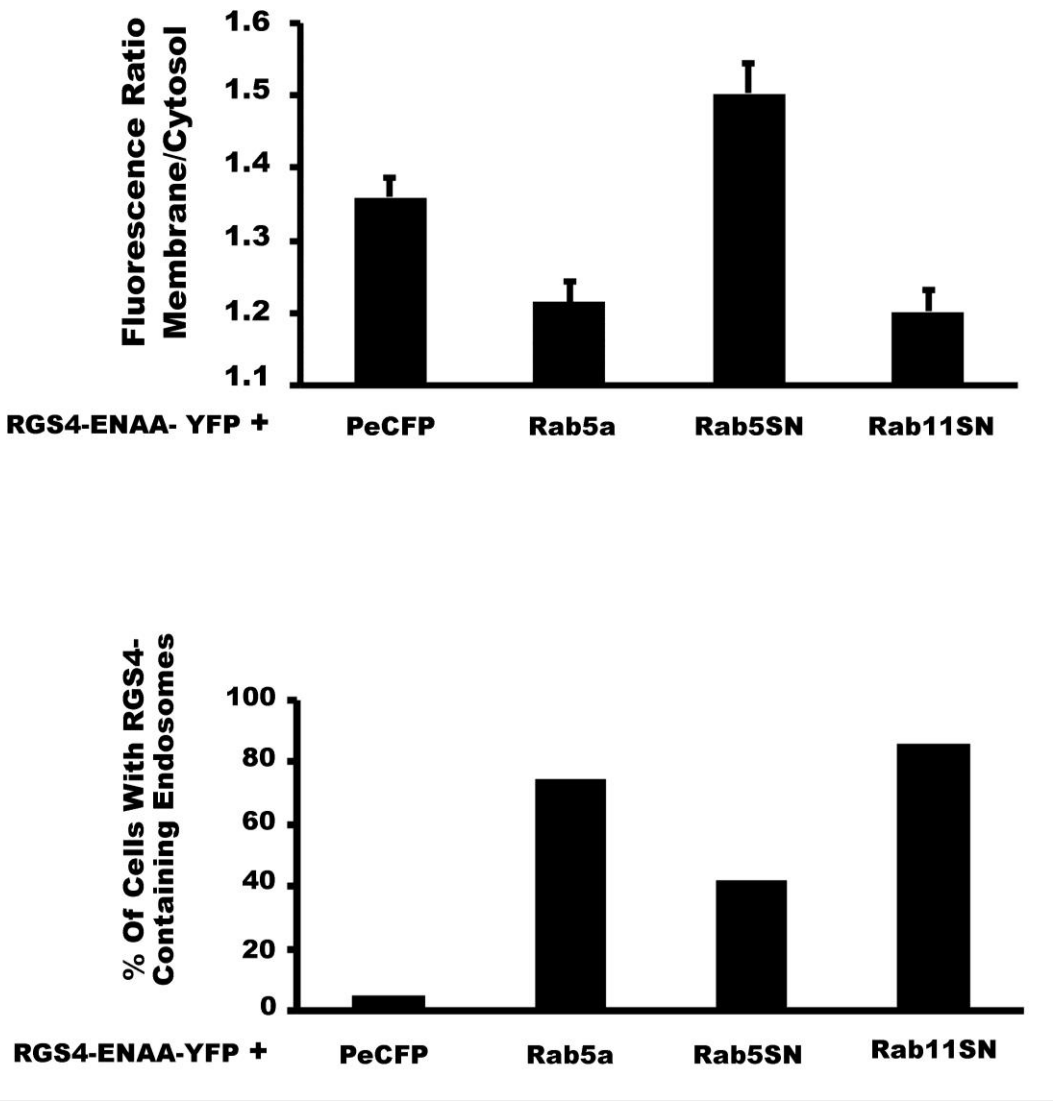

Figure32: RGS4 G-protein binding does not affect its trafficking through Rab11 exocytic pathway and Rab5 clathrin mediated endocytosis. *A.* The ratio of the RGS4-YFP signal between the cytosol and plasma membrane was analyzed by densitometry using ImageJ software. Shown are means ratio of n >35 cells per condition. S.E. are indicated by *error bars. B*. RGS4-YFP fusion constructs were examined for the presence of RGS4-containing endosomes with different Rab proteins. For each condition, cells with low to intermediate fluorescence intensity were scored for the presence or absence of endosome structures. Shown are the mean of the percentage of cells with RGS4-containing endosomes determined during 1 independent experiments (n > 35 cells/condition)

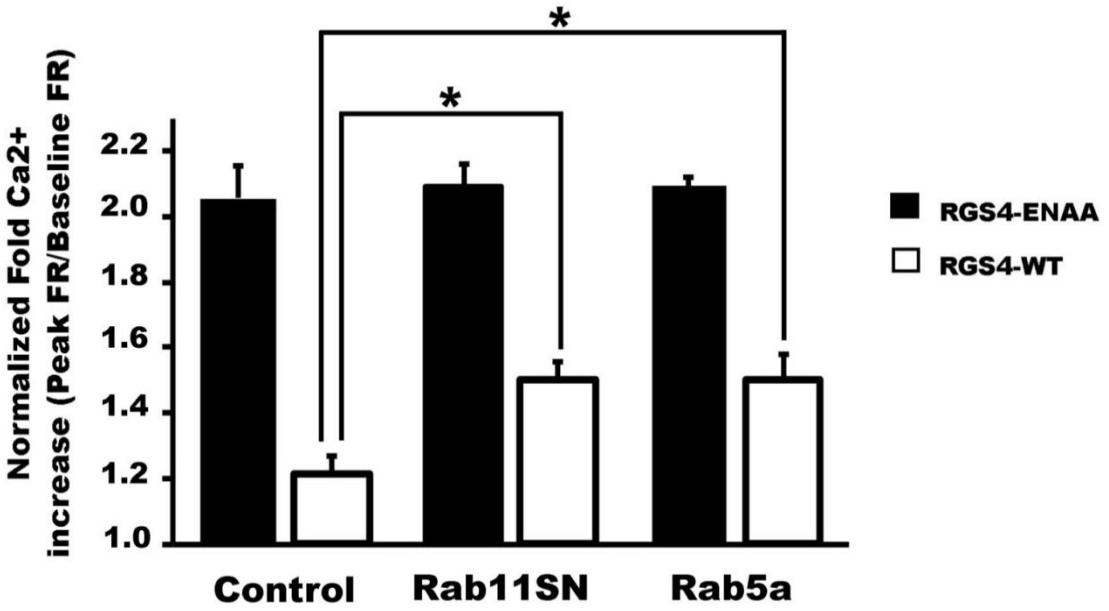

Figure33: Rab5 and 11SN do not affect M1 Mediated intracellular calcium release whereas both decrease RGS4 inhibition of Gq signaling. Intracellular calcium release was stimulated by200uM carbachol stimulation. fold of Fura-2 340/380nm fluorescence were analyzed to determined intracellular calcium release under carbachol stimulation. One-way ANOVA with a Tukey's HSD post hoc test was used to determine differences between groups (*$p < 0.01$). S.E. are indicated by *error bars and are representative of 10 transfected cells/ normalized on at least 10untransfected cells per monoplicate/ condition/day. These experiments have been made in triplicate in 3independent days.*

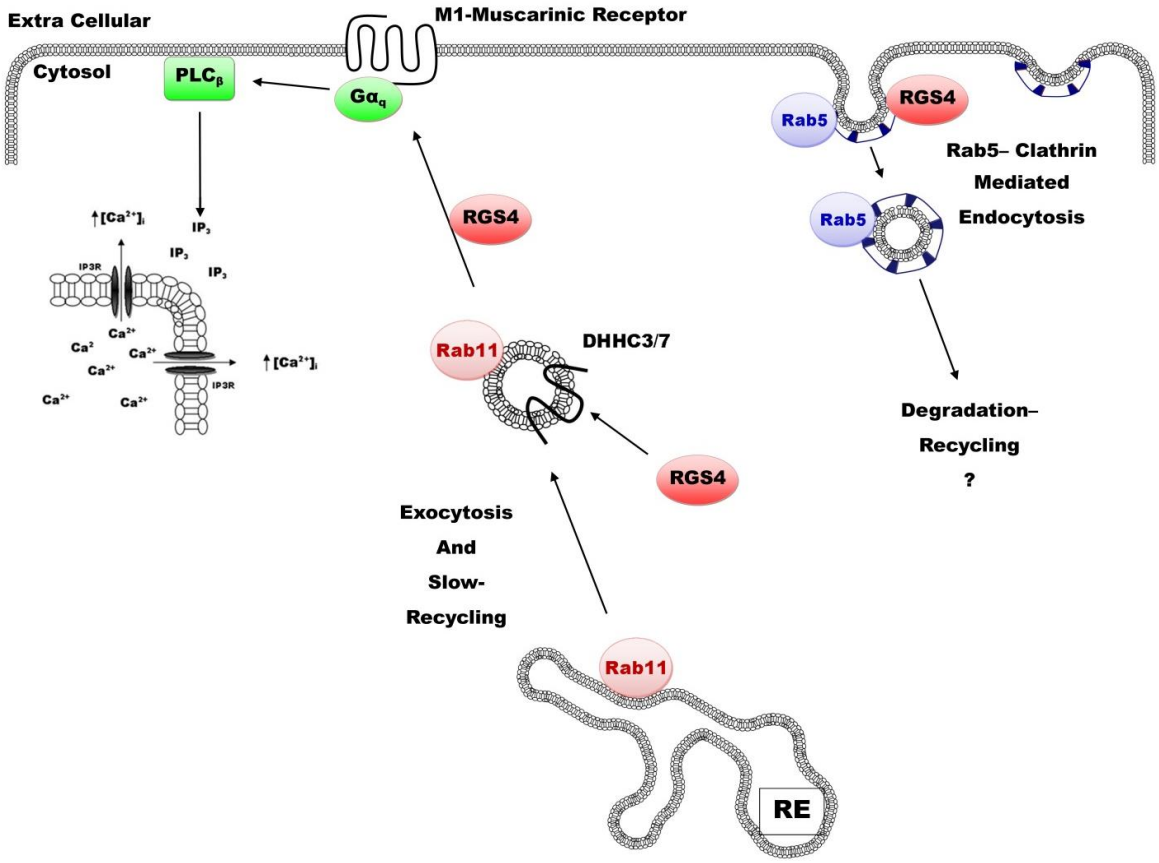

Figure34: Model of RGS4 trafficking. DHHC3and 7 regulate RGS4 trafficking in helping its binding to Rab11 compartments from where Rab11 will mediate RGS4 trafficking to the plasma membrane where RGS4 function to inhibit G-protein signaling is elicited. RGS4 is leaving the plasma membrane with Rab5 clathrin mediated endocytosis.

Discussion

Over the last decade, palmitoylation has been shown to be a key regulator of signaling protein localization and function. Specifically, this reversible post-translational modification of cysteine residues has been reported to regulate the intracellular trafficking of proteins such as Ras, Gαi, Gαq and Src-family kinases[142;201]. Potential sites of palmitoylation are often clustered together within protein domains and in many cases they are believed to work in concert to promote proper intracellular targeting. Such is believed to be the case for the tyrosine kinases Fyn, Yes[142] and Lck[204] that undergo palmitoylation at cysteine residues 3 and 6 in their amino terminal targeting domain[115;205]. It has been similarly suggested that a pair of closely spaced cysteines (Cys 2 and Cys 12) found in the amino terminal domains of RGS4, RGS5, and RGS16 may work in concert to promote their proper localization and G-protein inhibitory function[115]. We here show the surprising result however, that Cys2 and Cys12 appear to act independently to modulate plasma membrane targeting, intracellular trafficking and function of RGS4 in mammalian cells.

We set out to characterize the relative contribution of determinants within RGS4 that are necessary for its plasma membrane targeting and function in mammalian cells. Consistent with previous studies that showed the relative importance of the amphipathic helical domain[114;114]; the L23D mutant remained completely cytosolic with no detectable membrane localization. It was interesting to observe that inhibition of RGS4 palmitoylation by 2-bromoplamitate also results in a complete disruption of plasma membrane targeting. Thus, the amphipathic helix domain and cysteine palmitoylation both appear necessary but not sufficient for optimal plasma membrane targeting of human RGS4 in human cells. Together these data indicate that the G-protein binding domain (RGS box) with its previously reported palmitoylation site at Cys95 may not be a primary determinant of RGS4 plasma membrane localization. However, the observation that C2A:C12A shows low,

but appreciable levels of tonic membrane localization compared to L23D and WT following 2-BP addition suggests that Cys95 may contribute a minor component of RGS4's membrane targeting capacity.

The data herein show that Cys12, the palmitoylatable residue adjacent to the amphipathic helix domain, is the most important cysteine residue for plasma membrane targeting of RGS4. By contrast, Cys2 residue appears to be dispensable for membrane localization of RGS4. The simplest explanation for these data is that palmitoylation of Cys12 increases the length of hydrophobic surface of the amphipathic alpha helix to promote greater steady-state association with the inner leaflet of the plasma membrane. In an analogous situation, an extended hydrophobic surface of the RGS2 amphipathic helix was shown to be critical for its strong localization to the cell membrane[196]. Circular dichroism studies have shown that peptides containing the amphipathic helical domain of RGS4 maintain a disordered (random coil) structure until presented with lipid vesicles whose phospholipid composition resembles the anionic plasma membrane inner leaflet[114]. Whereas Cys12 palmitoylation may be able to cooperate with the adjacent hydrophobic amino acids to promote formation of an extended helix domain (one additional turn), it may be that Cys2 palmitoylation is located at too great a distance from the core helix to promote extended helix formation. It is prudent, however, to consider the alternative possibility that Cys12, in its palmitoylated or non-palmitoylated state, is working independently from the amphipathic helix to promote association with an unknown plasma membrane protein or protein complex. Consistent with the notion that membrane targeting is necessary for RGS4 function, mutation of Cys12 in the context of both the C12A and C2A; C12A reduced RGS4 Gq inhibitory function to a level similar to that of the L23D mutation.

Many palmitoylated proteins shuttle continuously between the plasma membrane and other intracellular compartments[142;145;163]. Since 2-BP treatment of RGS4-transfected cells completely prevented its localization to the endosomal compartment, we asked

whether Cys2 and Cys12 may contribute to endosomal trafficking and localization of RGS4. The C2A mutant showed dramatically impaired localization to the endosomes population consistent with the idea that endosome localization is dependent on Cys2 palmitoylation. If endosome localization is required for a posttranslational modification or protein interaction that serves to increase RGS4 function, then its impaired localization to the endosome pool could explain its impaired inhibition of Gq signalling. By contrast, the C12A mutation had a quite distinct effect on endosomal localization. Although this mutant targeted TGN38-containing endosomes with a similar efficiency as the wild type protein, it was completely absent from the TGN38-deficient pool of small-sized endosomes that is normally populated by the wild type protein. To the extent that trafficking of RGS4 through endosome compartments that do not contain TGN38 may be important for its G-protein function, this observation might further serve to explain the lack of inhibitory activity that we observed for the C12A mutants.

The fact that the L23D amphipathic α-helix mutant did not populate either endosomal compartment is consistent with the possibility that these previously unreported structures are bounded by lipid bilayers. The nature of the compartment that is populated by both wild type and C12A mutant proteins is of much interest. Its high TGN38 expression and localization deep within the cytosol suggest that it is an intracellular sorting compartment related to the trans-Golgi network. To our knowledge no such compartments have been previously described for fluorescently tagged TGN38 constructs. Clearly, Cys12 is not required for localization to this endosomal structure. Taken together these data are consistent with a model whereby sequential palmitoylation of Cys2 and Cys12 may be required to promote proper trafficking of RGS4 between the plasma membrane, Golgi related endosomal compartments. Specifically, Cys2 palmitoylation would allow access to the endosomal TGN38 containing pool and Cys12 palmitoylation presumably occurring within that compartment would be required for exiting that TGN38 containing pool. The precedent for this type of sequential trafficking model are proteins such as H- or N-Ras where palmitoylation was shown to be required for them to migrate out of the Golgi[150;206;207].

Functional data for the C2A mutant, however, suggest that membrane localization alone may not be sufficient for optimal RGS4 activity. Specifically, despite the strong membrane localization of the C2A, this clone also showed a measurable decrease in its Gq inhibitory function suggesting that Cys2 may contribute to an additional previously uncharacterized functional activity to RGS4. It is important to note that this novel activity appears to be independent from the known protein-stabilizing effects of Cys2 palmitoylation[118;119] since protein expression levels were normalized at the transfection stage for these experiments. Instead it appears that Cys2 is required for DHHC3 and 7 mediated RGS4 endosomal targeting. RGS4 Cys2A impaired localization to the endosome pool could explain its impaired inhibition of Gq signalling. It will be of future interest to determine whether RGS4 activity promoting modifications such as PKG/PKA-dependent phosphorylation[123], Ca2+/calmodulin-binding[126-128], spinophilin[59] and/or Homer2 interaction[129] require recycling of RGS4 through an endosomal compartment.

Palmitoylation induced by palmitoylating enzymes have been previously shown to participate in proteins such as R7BP and H; N-Ras shuttling between the plasma membrane and intracellular compartments[150;206;207]. Among palmitoylating enzyme family, DHHC3 and 7 are the two proteins for which activities have been related to a maximum of protein substrates, for example many famous proteins such as SNAP25, e-NOS, Gαq, Gαi, PSD-95, GABAa and GluR1 have been shown to be palmitoylated by DHHC3 and 7[159]. Consistent with the work of Wang *et al.*[120] , we here add RGS4 to the list of proposed protein substrates of DHHC3 and 7 since cotransfection with DHHC3 and 7 SiRNA impaired RGS4 plasma membrane targeting and inhibition of Gαqi9 mediated signaling. Mutations of Cys2 and Cys12 abolished interaction between DHHC3- 7 and RGS4, leaving open the question as to which DHHC may be regulating Cys95. We also show that Cys2 is the primary substrate on RGS4 for DHHC3, confirming recent work[120]. These data may aid in the future determination of targeting sequence specificity and substrate recognition by DHHC3, 7 and other DHHC family members. Interestingly, the difference in RGS4 endosomal targeting

efficiency whether DHHC3-7 are dominant negatively expressed or knocked down highlighted that palmitoylating enzymes 3 and 7 would interact with RGS4 independently of the "DHHC" motif. Among the palmitoylating enzymes, only one non-CRD sequence: PaCCT[208] has been shown to play a role in DHHC protein-substrate recognition. But this domain is missing in DHHC3 and 7. And, despite being well conserved, the CRD domains of DHHCs are not interchangeable between DHHCs[208] indicating a role in substrate recognition. As the CRD contains the DHHC motif, it is possible that cysteines in the CRD domain of DHHS3 and 7 are be capable of interacting with RGS4 cys2. Further investigation helping at defining the region of interaction of DHHC3 and 7 with RGS4 is of interest as it appears to be capable of recruiting RGS4 into the endosomal compartment, a newly discovered pathway for maximizing RGS4 function as a Gq inhibitor.

The first evidence that RGS4 may undergo intracellular trafficking came from Kirk Druey et al. who co-immunoprecipitated RGS4 and β-cop[201], a coatamer protein for vesicle trafficking between the ER and Golgi. Other publications reported RGS4 in intracellular compartments by electronic microscopy[209]. However, none of these previous studies investigated the biological importance of these observations. We here for the first time show that RGS4 traffics through several endosomal compartments. As RGS4 endosomal pool very well colocalized Rab11 and that Rab11SN prevented both RGS4 plasma membrane targeting and to properly inhibit M1-mediated Gq signaling pathway, thus RGS4 likewise traffics via rab11 exocytic pathway to reach the plasma membrane where it is capable of inhibiting Gq signaling pathway. Inversely, Gq signaling pathway was less inhibited by RGS4 when Rab5 was promoting its trafficking from the plasma membrane to intracellular compartments. However, interestingly, no colocalization was observed between Rab5a and RGS4, suggesting that RGS4 was absent from or very transiently localized to the early endosome pool before being either released into the cytosol or recycled via the Rab11 pool. Since RGS4 contains a known PIP3 binding domain[126-128] -an important lipid component regulating Rab5- and clathrin- mediated endocytosis[168;210;211] it is tempting to speculate that RGS4 may interact, albeit transiently with this pool. Indeed other proteins such as EEA1, an important protein localizing to Rab5 clathrin coated

vesicle, requires its PIP3 binding domain in order to bind Rab5 clathrin-coated vesicles [210;211]. Shortly after endocytosis PIP3 in these vesicles is hydrolysed by phosphoinositide phosphatases[168] which changes the lipid composition of Rab5-containing vesicles. It is therefore possible that once internalized via Rab5a- and clathrin-dependent mechanisms, RGS4 is released into cytosolic fraction. Another possibility is that RGS4 directly traffics from the plasma membrane to Rab11 recycling endosome pool, a hypothesis that would be supported by the dramatic increase in the percentage of cells showing endosomes when RGS4 is co-expressed with Rab5a. It will be of interest to identify whether one or both of these models are sufficient to explain the observed trafficking patterns for RGS4.

The characterization of protein trafficking routes for RGS4 requires defining the contribution of various known pathways to the regulation of its localization and function. Understanding these processes may allow us to influence in vivo signalling models via external stimuli such as drug treatments. M1 muscarinic receptor mediate calcium signaling[212], M1 muscarinic receptor also link to prominent signaling pathways, including the ERK[213] and PI3K[214]. M1 muscarinic receptors are involved in fragile X syndrome[215], glaucoma[216], brain and schizophrenia- cognitive symptoms[217;218]. In using the inactive RGS4 isoform EN-AA, we here show that M1 muscarinic receptor-mediated calcium signaling in HEK cells is dependent on neither Rab11 nor Rab5a endosomal trafficking routes. Thus all the compounds of M1 mediated calcium machinery such as M1 muscarinic receptor itself, Gαq/11, PLCβ, calcium storage and IP3-receptor calcium channel functioned independently of Rab11 and Rab5a activities. Few studies reported trafficking of these proteins: Gαq seems to interact with ARNO[219]- a GTPase related to Arf6 which mediates clathrin independent endocytosis, and, M1 muscarinic receptor has been reported to be the least sensitive of the five different muscarinic receptor to Rab5 mediated endocytosis[220] whereas PLCβ trafficking by Rabs proteins has not been reported. It is prudent, however, to consider the possibility that some of these proteins may be trafficking through Rab11 and Rab5a compartments but the signalling model wouldn't be sensitive enough to detect small changes in calcium regulation. In either case, such regulation must

be considered minor relative to the phenotype observed when RGS4 function is altered by changing Rab5a or Rab11 function.

Taken together these data suggest that an endogenous inhibitor of muscarinic 1 calcium signalling such as RGS4 can be regulated independently of its effectors by external stimuli that may regulate Rab11 or Rab5a endosomal compartment activity. Since numerous studies have linked disregulation of GPCR signalling in pathophysiology[101;221-223], activating Rab11 or inhibiting Rab5a endosomal compartments activity may be a novel solution for enhancing RGS4 function and inhibition of pathophysiology. Further studies of RGS4 regulated signaling pathways trafficking may uncover external stimuli possibilities aiming at modulating Rab11 and Rab5 and may lead to determine drug therapies.

I have here studied the effect of palmitoylation on two independent RGS4 N-terminal cysteine residues at positions 2 and 12, which appear to differentially affect key elements of RGS4 function including plasma membrane targeting, endosomal trafficking and Gq inhibition. I here propose the novel model that Cysteine12 elongates the hydrophobic core of RGS4 amphipathic helix. By characterizing the impact of DHHC3 and 7 palmitoyl CoA transferases on RGS4 trafficking, I confirmed their ability to modulate RGS4 function as an inhibitor of M2 muscarinic receptor-mediated Gqi9 calcium signaling. Continued investigation into the mechanisms of RGS4 trafficking showed DHHC3 and 7 may be involved in a DHHC motif independent manner to promote RGS4 association with the Rab11 compartment via palmitoylation of cysteine2. Cysteine2 appears necessary for RGS4 to access the endosomal pool and Cysteine12 appears to be required for its exiting endosomes and binding the plasma membrane. I also demonstrated that the M1 mediated calcium machinery was unaffected by Rab11 and Rab5 endosomal activity. Conversely RGS4 regulation of M1 mediated calcium machinery is targeting the plasma membrane and function in Rab11 and Rab5a clathrin dependent manner. Finding external stimuli increasing DHHC3 or 7 activity aiming at increasing RGS4 palmitoylation status, helping its accession to Rab11 pool, targeting the plasma membrane or deactivating/activating Rab5a

and Rab11 compartment respectively may be key steps for putting RGS4 on focus for pharmaceutical company investigating drug therapeutic design toward diseases where RGS4 have been involved in considering schizophrenia, cardiomyopathy, bradycardia, insulin resistance, glucose intolerance, liver steatosis, increases in catecholamine, pancreatic, ovarian, oesophageal and breast cancer.

Limitation and Future Directions

While our studies used molecular and genetic tools to identify novel mechanisms of RGS4 protein regulation, we acknowledge that there are limitations to both our study design as well as general strategies. Perhaps the largest limitation that is applicable to all of my studies is the use of overexpression as a tool for studying RGS4 localization and function. First overexpression of protein can drive them into subcellular compartments that they normally wouldn't be found in. Therefore, it is possible that the tonic plasma membrane and strong endosomal localization is the result of overexpressing RGS4. This would also affect the function of these proteins as aggregated RGS proteins are presumably not functional. This however, is unlikely as these cases would result in protein being directed into aggregates in the cytosol for degradation. None-the-less, our studies, particularly the intracellular calcium measurements, allows us to select cells based on their RGS protein expression through measuring YFP fluorescence. We therefore, are able to carefully select cells based on their expression under controlled conditions. This allows us to not only avoid cells with too much RGS protein but also with cells that contain too little expression.

Finally, our entire study is carried out in HEK cells instead of tissues where RGS4 was endogenously expressed. This strategy has several advantages as well as disadvantages. First, the use of HEK is extremely easy and cost effective. These cells are already available and we can passage them for prolonged periods of time. They are easily transfectable using standard liposome techniques including Fugene6 (Roche) and Lipofectamine (Invitrogen). Using these techniques we are able to easily visualize and analyze the function of RGS4 efficiently. The most obvious disadvantage is that these cells are not ex vivo tissues and may display different isoforms of proteins which can impact our experiments. For example Splice variants of RGS4 are expressed in prefrontal tissues in schizophrenic patients. Nonetheless, palmitoylation occurs in every type of tissue and rab5 and 11 are both ubiquitously expressed throughout the human body. So presumably our studies in HEK cells will be reproducible in all tissues where RGS4 protein is expressed.

In the near future, our goal is to identify treatment strategies for pathologies that result from changes in RGS4 activity. Our study represents the starting point for this purpose. Our next work will be to identify cellular endogenous stimuli that lead to an increase in RGS4 plasma membrane targeting and therefore increased inhibition of G-protein signaling pathways. To carry out these studies we plan to use a number of methods and tools developed herein. Previously we used RGS4-YFP plasma membrane targeting as a great indicator of RGS4 capacity to inhibit Gq signaling pathway. As these experiments are easy and quick, they will provide a simple procedure for primarily selecting potent cellular external stimuli that control RGS4 localization. If successful these findings will then be adapted to *in vivo* models, where we will attempt observe the effect of the selected stimuli on RGS4 capacity to inhibit G-protein signalling *in vivo*. As described in the introduction of this document, numerous functions of RGS4 have been described using murine model. For example we may use the fact that RGS4 normally inhibits glucose stimulated insulin secretion[95] and, catecholamine release[97] as two robust indicators of RGS4 activity. We plan to analyse these parameters on RGS4WT, RGS4+/- and RGS4-/- mice that our lab successfully used in the past[111]. Our plan also includes checking the potential variation of RGS4 level of expression under external stimuli in different tissues as our team successfully did RT-PCR on endogenous RGS4 expression[111].

In this study, we identified targets for the design of drug therapy aiming at increasing RGS4 activity. We demonstrate the colocalization of RGS4 and Rab11 and the important role of Rab11 in RGS4 plasma membrane targeting and inhibition of Gq signaling pathway. Since RGS4 cys2 palmitoylation seems to occur at Rab11 compartment and has been shown to protect RGS4 function and expression[118-120], we predict that increasing Rab11 activity and expression may significantly increase RGS4 expression, plasma membrane targeting and most importantly inhibition of G-protein signaling. Other proteins present in Rab11 endosomal compartment undergo translocation to the plasma membrane under PI3K/Akt stimulation. For instance GLUTR4 translocates to the plasma membrane under insulin stimulation[224] which is an agonist of insulin receptor: a PI3K/Akt activator[224]. Therefore, insulin-stimulated PI3K activation may be expected to increase RGS4 function in

our cultured cell model. In the case that insulin does indeed increase RGS4 activity, we will search for external stimuli that work upstream of PI3K activation.

Personal Conclusion

Pour en arriver là, l'intelligence n'est pas suffisante. Travail, rigueur et patience sont je pense les valeurs qui font la différence.

La différence, parlons-en. Je suis circonspect d'observer les différences universitaires entre l'Europe et les Amériques. Le système américain pousse tous les bons étudiants à devenir médecin et non chercheur. Lorsqu'un étudiant entre dans un laboratoire, c'est simplement dans l'optique de remplir son CV, merci et au revoir. Il ne sera jamais chercheur. De plus, il ne pense qu'au gros chèque qu'il obtiendra après médecine, d'où le désintérêt du pourquoi être chercheur et une sorte de délaissement de la recherche fondamentale au profit des médecins de ce côté-ci de l'océan. En cela j'adresse un salut à notre système éducatif qui clairement nous valorise et permet d'orienter convenablement les étudiants. De même, la sélection en fac de médecine Française semble beaucoup plus juste tant elle est directement reliées aux notes et non au CV.

Sur le plan personnel, je suis arrivé dans un autre pays, seul, ne parlant que très peu l'anglais. Je pense être très satisfait au regard de mon évolution et de mon parcours en général. Mais ma réflexion ne porte que très peu sur ce genre d'éléments. En outre, devenir international vous confère directement une étiquette, des stéréotypes. Cela vous fait comprendre énormément de choses concernant votre pays, ce qui vous fait êtes Français. Et plus que jamais pourquoi l'histoire du monde se vit jalonné de batailles Franco-British *ad vitam aeternam*. Cette histoire serait longue à expliquer, mais je veux tenter de vous la présenter en quelques phrases. «1. Il est difficile de ne pas être arrogant en étant Français à l'étranger tant nous comprenons ce que nous avons et ce que les autres n'ont pas. 2. Les règles qu'imposent les anglo-saxons sont indéniablement proches de notre model et pourtant tellement éloignées.»

Pour finir, quelques phrases concerneront mes sensations sur la recherche scientifique en tant que telle. Plus le temps passe, plus je comprends la complexité de trouver des solutions aux pathologies. Afin de faciliter la recherche, je pense que le nombre

d'informations biologiques complémentaires et conditionnées devraient être posées sur un format complémentaire aux « reviews ». Explicitement, un outil informatique devrait permettre aux chercheurs de participer mondialement à modéliser l'accumulation de données. Chaque nouvelle donnée pourrait être ajoutée lorsque publiée. Ce model devrait être animé; animer, par exemple : la translocation d'effecteurs ainsi que l'ensemble des phosphorylation/déphosphorylation, changement de nucléotide tel que GDP remplacé par GTP, tout cela suite à l'ajout d'un agoniste/activation d'une voie de signalisation. Par ce biais, l'observation facilitée de phénotypes pourrait ouvrir à une nouvelle dynamique.

References

Reference List

1. **Sjogren B, Blazer LL, Neubig RR. Regulators of G protein signaling proteins as targets for drug discovery. *Prog Mol Biol Transl Sci*. 2010;91:81-119.**

2. **Rasmussen SG, DeVree BT, Zou Y, Kruse AC, Chung KY, Kobilka TS, Thian FS, Chae PS, Pardon E, Calinski D, Mathiesen JM, Shah ST, Lyons JA, Caffrey M, Gellman SH, Steyaert J, Skiniotis G, Weis WI, Sunahara RK, Kobilka BK. Crystal structure of the beta2 adrenergic receptor-Gs protein complex. *Nature*. 2011;477:549-555.**

3. **Strader CD, Fong TM, Tota MR, Underwood D, Dixon RA. Structure and function of G protein-coupled receptors. *Annu Rev Biochem*. 1994;63:101-132.**

4. **Bourne HR, Sanders DA, McCormick F. The GTPase superfamily: conserved structure and molecular mechanism. *Nature*. 1991;349:117-127.**

5. **Lambert NA. Dissociation of heterotrimeric g proteins in cells. *Sci Signal*. 2008;1:re5.**

6. **Cabrera-Vera TM, Vanhauwe J, Thomas TO, Medkova M, Preininger A, Mazzoni MR, Hamm HE. Insights into G protein structure, function, and regulation. *Endocr Rev*. 2003;24:765-781.**

7. **Neves SR, Ram PT, Iyengar R. G protein pathways. *Science*. 2002;296:1636-1639.**

8. **Hu H, O'Mullane LM, Cummins MM, Campbell CR, Hosoda Y, Poronnik P, Dinudom A, Cook DI. Negative regulation of Ca(2+) influx during P2Y(2) purinergic receptor activation is mediated by Gbetagamma-subunits. *Cell Calcium*. 2010;47:55-64.**

9. **Ushio-Fukai M, Alexander RW, Akers M, Lyons PR, Lassegue B, Griendling KK. Angiotensin II receptor coupling to phospholipase D is mediated by the betagamma subunits of heterotrimeric G proteins in vascular smooth muscle cells. *Mol Pharmacol*. 1999;55:142-149.**

10. **Downes GB, Gautam N. The G protein subunit gene families. *Genomics*. 1999;62:544-552.**

11. **Premont RT, Gainetdinov RR. Physiological roles of G protein-coupled receptor kinases and arrestins. *Annu Rev Physiol*. 2007;69:511-534.**

12. **Tesmer JJ. The quest to understand heterotrimeric G protein signaling. *Nat Struct Mol Biol*. 2010;17:650-652.**

13. **Ross EM, Wilkie TM. GTPase-activating proteins for heterotrimeric G proteins: regulators of G protein signaling (RGS) and RGS-like proteins. *Annu Rev Biochem*. 2000;69:795-827.**

14. **Chisari M, Saini DK, Kalyanaraman V, Gautam N. Shuttling of G protein subunits between the plasma membrane and intracellular membranes. *J Biol Chem*. 2007;282:24092-24098.**

15. **Chen CA, Manning DR. Regulation of G proteins by covalent modification. *Oncogene*. 2001;20:1643-1652.**

16. **De Vries L, Mousli M, Wurmser A, Farquhar MG. GAIP, a protein that specifically interacts with the trimeric G protein G alpha i3, is a member of a protein family with a highly conserved core domain. *Proc Natl Acad Sci U S A*. 1995;92:11916-11920.**

17. **Berman DM, Kozasa T, Gilman AG. The GTPase-activating protein RGS4 stabilizes the transition state for nucleotide hydrolysis. *J Biol Chem*. 1996;271:27209-27212.**

18. **Popov S, Yu K, Kozasa T, Wilkie TM. The regulators of G protein signaling (RGS) domains of RGS4, RGS10, and GAIP retain GTPase activating protein activity in vitro. *Proc Natl Acad Sci U S A*. 1997;94:7216-7220.**

19. **De Vries L, Elenko E, Hubler L, Jones TL, Farquhar MG. GAIP is membrane-anchored by palmitoylation and interacts with the activated (GTP-bound) form of G alpha i subunits. *Proc Natl Acad Sci U S A*. 1996;93:15203-15208.**

20. **Glick JL, Meigs TE, Miron A, Casey PJ. RGSZ1, a Gz-selective regulator of G protein signaling whose action is sensitive to the phosphorylation state of Gzalpha. *J Biol Chem*. 1998;273:26008-26013.**

21. **Jordan JD, Carey KD, Stork PJ, Iyengar R. Modulation of rap activity by direct interaction of Galpha(o) with Rap1 GTPase-activating protein. *J Biol Chem*. 1999;274:21507-21510.**

22. Berstein G, Blank JL, Jhon DY, Exton JH, Rhee SG, Ross EM. Phospholipase C-beta 1 is a GTPase-activating protein for Gq/11, its physiologic regulator. *Cell*. 1992;70:411-418.

23. Wang Q, Liu M, Mullah B, Siderovski DP, Neubig RR. Receptor-selective effects of endogenous RGS3 and RGS5 to regulate mitogen-activated protein kinase activation in rat vascular smooth muscle cells. *J Biol Chem*. 2002;277:24949-24958.

24. Ponting CP, Bork P. Pleckstrin's repeat performance: a novel domain in G-protein signaling? *Trends Biochem Sci*. 1996;21:245-246.

25. Snow BE, Betts L, Mangion J, Sondek J, Siderovski DP. Fidelity of G protein beta-subunit association by the G protein gamma-subunit-like domains of RGS6, RGS7, and RGS11. *Proc Natl Acad Sci U S A*. 1999;96:6489-6494.

26. Chen CK, Eversole-Cire P, Zhang H, Mancino V, Chen YJ, He W, Wensel TG, Simon MI. Instability of GGL domain-containing RGS proteins in mice lacking the G protein beta-subunit Gbeta5. *Proc Natl Acad Sci U S A*. 2003;100:6604-6609.

27. Jayaraman M, Zhou H, Jia L, Cain MD, Blumer KJ. R9AP and R7BP: traffic cops for the RGS7 family in phototransduction and neuronal GPCR signaling. *Trends Pharmacol Sci*. 2009;30:17-24.

28. Drenan RM, Doupnik CA, Boyle MP, Muglia LJ, Huettner JE, Linder ME, Blumer KJ. Palmitoylation regulates plasma membrane-nuclear shuttling of R7BP, a novel membrane anchor for the RGS7 family. *J Cell Biol*. 2005;169:623-633.

29. Posner BA, Gilman AG, Harris BA. Regulators of G protein signaling 6 and 7. Purification of complexes with gbeta5 and assessment of their effects on g protein-mediated signaling pathways. *J Biol Chem*. 1999;274:31087-31093.

30. He W, Cowan CW, Wensel TG. RGS9, a GTPase accelerator for phototransduction. *Neuron*. 1998;20:95-102.

31. Chen CK, Burns ME, He W, Wensel TG, Baylor DA, Simon MI. Slowed recovery of rod photoresponse in mice lacking the GTPase accelerating protein RGS9-1. *Nature*. 2000;403:557-560.

32. Anderson GR, Posokhova E, Martemyanov KA. The R7 RGS protein family: multi-subunit regulators of neuronal G protein signaling. *Cell Biochem Biophys*. 2009;54:33-46.

33. Ponting CP. Raf-like Ras/Rap-binding domains in R. *J Mol Med (Berl)*. 1999;77:695-698.

34. Siderovski DP, Diverse-Pierluissi M, De Vries L. The GoLoco motif: a Galphai/o binding motif and potential guanine-nucleotide exchange factor. *Trends Biochem Sci*. 1999;24:340-341.

35. Hollinger S, Taylor JB, Goldman EH, Hepler JR. RGS14 is a bifunctional regulator of Galphai/o activity that exists in multiple populations in brain. *J Neurochem*. 2001;79:941-949.

36. Snow BE, Hall RA, Krumins AM, Brothers GM, Bouchard D, Brothers CA, Chung S, Mangion J, Gilman AG, Lefkowitz RJ, Siderovski DP. GTPase activating specificity of RGS12 and binding specificity of an alternatively spliced PDZ (PSD-95/Dlg/ZO-1) domain. *J Biol Chem*. 1998;273:17749-17755.

37. Schiff ML, Siderovski DP, Jordan JD, Brothers G, Snow B, De Vries L, Ortiz DF, Diverse-Pierluissi M. Tyrosine-kinase-dependent recruitment of RGS12 to the N-type calcium channel. *Nature*. 2000;408:723-727.

38. Mao J, Yuan H, Xie W, Wu D. Guanine nucleotide exchange factor GEF115 specifically mediates activation of Rho and serum response factor by the G protein alpha subunit Galpha13. *Proc Natl Acad Sci U S A*. 1998;95:12973-12976.

39. Krupnick JG, Benovic JL. The role of receptor kinases and arrestins in G protein-coupled receptor regulation. *Annu Rev Pharmacol Toxicol*. 1998;38:289-319.

40. Pitcher JA, Freedman NJ, Lefkowitz RJ. G protein-coupled receptor kinases. *Annu Rev Biochem*. 1998;67:653-692.

41. Carman CV, Parent JL, Day PW, Pronin AN, Sternweis PM, Wedegaertner PB, Gilman AG, Benovic JL, Kozasa T. Selective regulation of Galpha(q/11) by an RGS domain in the G protein-coupled receptor kinase, GRK2. *J Biol Chem*. 1999;274:34483-34492.

42. Tesmer JJ, Berman DM, Gilman AG, Sprang SR. Structure of RGS4 bound to AlF4--activated G(i alpha1): stabilization of the transition state for GTP hydrolysis. *Cell*. 1997;89:251-261.

43. Watson N, Linder ME, Druey KM, Kehrl JH, Blumer KJ. RGS family members: GTPase-activating proteins for heterotrimeric G-protein alpha-subunits. *Nature*. 1996;383:172-175.

44. Xu X, Zeng W, Popov S, Berman DM, Davignon I, Yu K, Yowe D, Offermanns S, Muallem S, Wilkie TM. RGS proteins determine signaling specificity of Gq-coupled receptors. *J Biol Chem*. 1999;274:3549-3556.

45. **Roman DL, Blazer LL, Monroy CA, Neubig RR. Allosteric inhibition of the regulator of G protein signaling-Galpha protein-protein interaction by CCG-4986. *Mol Pharmacol*. 2010;78:360-365.**

46. **Blazer LL, Roman DL, Chung A, Larsen MJ, Greedy BM, Husbands SM, Neubig RR. Reversible, allosteric small-molecule inhibitors of regulator of G protein signaling proteins. *Mol Pharmacol*. 2010;78:524-533.**

47. **Blazer LL, Zhang H, Casey EM, Husbands SM, Neubig RR. A nanomolar-potency small molecule inhibitor of regulator of G-protein signaling proteins. *Biochemistry*. 2011;50:3181-3192.**

48. **Ajit SK, Young KH. Analysis of chimeric RGS proteins in yeast for the functional evaluation of protein domains and their potential use in drug target validation. *Cell Signal*. 2005;17:817-825.**

49. **Kimple AJ, Willard FS, Giguere PM, Johnston CA, Mocanu V, Siderovski DP. The RGS protein inhibitor CCG-4986 is a covalent modifier of the RGS4 Galpha-interaction face. *Biochim Biophys Acta*. 2007;1774:1213-1220.**

50. **Grillet N, Dubreuil V, Dufour HD, Brunet JF. Dynamic expression of RGS4 in the developing nervous system and regulation by the neural type-specific transcription factor Phox2b. *J Neurosci*. 2003;%19;23:10613-10621.**

51. **Ebert PJ, Campbell DB, Levitt P. Bacterial artificial chromosome transgenic analysis of dynamic expression patterns of regulator of G-protein signaling 4 during development. I. Cerebral cortex. *Neuroscience*. 2006;142:1145-1161.**

52. **Erdely HA, Lahti RA, Lopez MB, Myers CS, Roberts RC, Tamminga CA, Vogel MW. Regional expression of RGS4 mRNA in human brain. *Eur J Neurosci*. 2004;19:3125-3128.**

53. **Gold SJ, Han MH, Herman AE, Ni YG, Pudiak CM, Aghajanian GK, Liu RJ, Potts BW, Mumby SM, Nestler EJ. Regulation of RGS proteins by chronic morphine in rat locus coeruleus. *Eur J Neurosci*. 2003;17:971-980.**

54. **Bansal G, Druey KM, Xie Z. R4 RGS proteins: regulation of G-protein signaling and beyond. *Pharmacol Ther*. 2007;116:473-495.**

55. **Ding J, Guzman JN, Tkatch T, Chen S, Goldberg JA, Ebert PJ, Levitt P, Wilson CJ, Hamm HE, Surmeier DJ. RGS4-dependent attenuation of M4 autoreceptor function in striatal cholinergic interneurons following dopamine depletion. *Nat Neurosci*. 2006;9:832-842.**

56. Bowden NA, Scott RJ, Tooney PA. Altered expression of regulator of G-protein signalling 4 (RGS4) mRNA in the superior temporal gyrus in schizophrenia. *Schizophr Res*. 2007;89:165-168.

57. Brzustowicz LM, Hodgkinson KA, Chow EW, Honer WG, Bassett AS. Location of a major susceptibility locus for familial schizophrenia on chromosome 1q21-q22. *Science*. 2000;288:678-682.

58. Grillet N, Pattyn A, Contet C, Kieffer BL, Goridis C, Brunet JF. Generation and characterization of Rgs4 mutant mice. *Mol Cell Biol*. 2005;25:4221-4228.

59. Liu W, Yuen EY, Allen PB, Feng J, Greengard P, Yan Z. Adrenergic modulation of NMDA receptors in prefrontal cortex is differentially regulated by RGS proteins and spinophilin. *Proc Natl Acad Sci U S A*. 2006;103:18338-18343.

60. Ding L, Hegde AN. Expression of RGS4 splice variants in dorsolateral prefrontal cortex of schizophrenic and bipolar disorder patients. *Biol Psychiatry*. 2009;65:541-545.

61. Albig AR, Schiemann WP. Identification and characterization of regulator of G protein signaling 4 (RGS4) as a novel inhibitor of tubulogenesis: RGS4 inhibits mitogen-activated protein kinases and vascular endothelial growth factor signaling. *Mol Biol Cell*. 2005;16:609-625.

62. Carmeliet P. Mechanisms of angiogenesis and arteriogenesis. *Nat Med*. 2000;6:389-395.

63. Folkman J. Role of angiogenesis in tumor growth and metastasis. *Semin Oncol*. 2002;29:15-18.

64. Folkman J. Angiogenesis in cancer, vascular, rheumatoid and other disease. *Nat Med*. 1995;1:27-31.

65. Meier-Kriesche HU, Li S, Gruessner RW, Fung JJ, Bustami RT, Barr ML, Leichtman AB. Immunosuppression: evolution in practice and trends, 1994-2004. *Am J Transplant*. 2006;6:1111-1131.

66. Olyaei AJ, de Mattos AM, Bennett WM. Nephrotoxicity of immunosuppressive drugs: new insight and preventive strategies. *Curr Opin Crit Care*. 2001;7:384-389.

67. Siedlecki A, Anderson JR, Jin X, Garbow JR, Lupu TS, Muslin AJ. RGS4 controls renal blood flow and inhibits cyclosporine-mediated nephrotoxicity. *Am J Transplant*. 2010;10:231-241.

68. Schnitzler MA, Hollenbeak CS, Cohen DS, Woodward RS, Lowell JA, Singer GG, Tesi RJ, Howard TK, Mohanakumar T, Brennan DC. The economic implications of HLA matching in cadaveric renal transplantation. *N Engl J Med*. 1999;341:1440-1446.

69. Cristol JP, Thiemermann C, Mitchell JA, Walder C, Vane JR. Support of renal blood flow after ischaemic-reperfusion injury by endogenous formation of nitric oxide and of cyclo-oxygenase vasodilator metabolites. *Br J Pharmacol*. 1993;109:188-194.

70. Shibouta Y, Suzuki N, Shino A, Matsumoto H, Terashita Z, Kondo K, Nishikawa K. Pathophysiological role of endothelin in acute renal failure. *Life Sci*. 1990;46:1611-1618.

71. Abels, B. C., Branch, R. A., and Sabra, R. Interaction between thromboxane A2 and angiotensin II in postischemic renal vasoconstriction in dogs. J.Pharmacol.Exp.Ther. 264(3), 1285-1292. 1993.

Ref Type: Journal (Full)

72. Siedlecki AM, Jin X, Thomas W, Hruska KA, Muslin AJ. RGS4, a GTPase activator, improves renal function in ischemia-reperfusion injury. *Kidney Int*. 2011;80:263-271.

73. Khan WI, Collins SM. Gut motor function: immunological control in enteric infection and inflammation. *Clin Exp Immunol*. 2006;143:389-397.

74. Salinthone S, Singer CA, Gerthoffer WT. Inflammatory gene expression by human colonic smooth muscle cells. *Am J Physiol Gastrointest Liver Physiol*. 2004;287:G627-G637.

75. Hu W, Mahavadi S, Li F, Murthy KS. Upregulation of RGS4 and downregulation of CPI-17 mediate inhibition of colonic muscle contraction by interleukin-1beta. *Am J Physiol Cell Physiol*. 2007;293:C1991-C2000.

76. Natale L, Piepoli AL, De Salvia MA, De Salvatore G, Mitolo CI, Marzullo A, Portincasa P, Moschetta A, Palasciano G, Mitolo-Chieppa D. Interleukins 1 beta and 6 induce functional alteration of rat colonic motility: an in vitro study. *Eur J Clin Invest*. 2003;33:704-712.

77. Aube AC, Blottiere HM, Scarpignato C, Cherbut C, Roze C, Galmiche JP. Inhibition of acetylcholine induced intestinal motility by interleukin 1 beta in the rat. *Gut*. 1996;39:470-474.

78. Hu W, Li F, Mahavadi S, Murthy KS. Upregulation of RGS4 expression by IL-1beta in colonic smooth muscle is enhanced by ERK1/2 and p38 MAPK and

inhibited by the PI3K/Akt/GSK3beta pathway. *Am J Physiol Cell Physiol*. 2009;296:C1310-C1320.

79. Dragon S, Rahman MS, Yang J, Unruh H, Halayko AJ, Gounni AS. IL-17 enhances IL-1beta-mediated CXCL-8 release from human airway smooth muscle cells. *Am J Physiol Lung Cell Mol Physiol*. 2007;292:L1023-L1029.

80. Cherry J, Karschner V, Jones H, Pekala PH. HuR, an RNA-binding protein, involved in the control of cellular differentiation. *In Vivo*. 2006;20:17-23.

81. Li F, Hu DY, Liu S, Mahavadi S, Yen W, Murthy KS, Khalili K, Hu W. RNA-binding protein HuR regulates RGS4 mRNA stability in rabbit colonic smooth muscle cells. *Am J Physiol Cell Physiol*. 2010;299:C1418-C1429.

82. Moy B, Goss PE. Lapatinib: current status and future directions in breast cancer. *Oncologist*. 2006;11:1047-1057.

83. Dorsam RT, Gutkind JS. G-protein-coupled receptors and cancer. *Nat Rev Cancer*. 2007;7:79-94.

84. Boire A, Covic L, Agarwal A, Jacques S, Sherifi S, Kuliopulos A. PAR1 is a matrix metalloprotease-1 receptor that promotes invasion and tumorigenesis of breast cancer cells. *Cell*. 2005;120:303-313.

85. Guise TA, Yin JJ, Mohammad KS. Role of endothelin-1 in osteoblastic bone metastases. *Cancer*. 2003;97:779-784.

86. Xie Y, Wolff DW, Wei T, Wang B, Deng C, Kirui JK, Jiang H, Qin J, Abel PW, Tu Y. Breast cancer migration and invasion depend on proteasome degradation of regulator of G-protein signaling 4. *Cancer Res*. 2009;69:5743-5751.

87. Boucharaba A, Serre CM, Guglielmi J, Bordet JC, Clezardin P, Peyruchaud O. The type 1 lysophosphatidic acid receptor is a target for therapy in bone metastases. *Proc Natl Acad Sci U S A*. 2006;103:9643-9648.

88. Zhang T, Wang Q, Zhao D, Cui Y, Cao B, Guo L, Lu SH. The oncogenetic role of microRNA-31 as a potential biomarker in oesophageal squamous cell carcinoma. *Clin Sci (Lond)*. 2011;121:437-447.

89. Tatenhorst L, Senner V, Puttmann S, Paulus W. Regulators of G-protein signaling 3 and 4 (RGS3, RGS4) are associated with glioma cell motility. *J Neuropathol Exp Neurol*. 2004;63:210-222.

90. Puiffe ML, Le Page C, Filali-Mouhim A, Zietarska M, Ouellet V, Tonin PN, Chevrette M, Provencher DM, Mes-Masson AM. Characterization of ovarian cancer ascites on cell invasion, proliferation, spheroid formation, and gene

expression in an in vitro model of epithelial ovarian cancer. *Neoplasia*. 2007;9:820-829.

91. Niedergethmann M, Alves F, Neff JK, Heidrich B, Aramin N, Li L, Pilarsky C, Grutzmann R, Allgayer H, Post S, Gretz N. Gene expression profiling of liver metastases and tumour invasion in pancreatic cancer using an orthotopic SCID mouse model. *Br J Cancer*. 2007;97:1432-1440.

92. Serafimidis I, Heximer S, Beis D, Gavalas A. G protein-coupled receptor signaling and sphingosine-1-phosphate play a phylogenetically conserved role in endocrine pancreas morphogenesis. *Mol Cell Biol*. 2011;31:4442-4453.

93. Gradwohl G, Dierich A, LeMeur M, Guillemot F. neurogenin3 is required for the development of the four endocrine cell lineages of the pancreas. *Proc Natl Acad Sci U S A*. 2000;97:1607-1611.

94. Johansson KA, Dursun U, Jordan N, Gu G, Beermann F, Gradwohl G, Grapin-Botton A. Temporal control of neurogenin3 activity in pancreas progenitors reveals competence windows for the generation of different endocrine cell types. *Dev Cell*. 2007;12:457-465.

95. Ruiz dA, I, Scarselli M, Rosemond E, Gautam D, Jou W, Gavrilova O, Ebert PJ, Levitt P, Wess J. RGS4 is a negative regulator of insulin release from pancreatic beta-cells in vitro and in vivo. *Proc Natl Acad Sci U S A*. 2010;107:7999-8004.

96. Ruiz dA, I, Gautam D, Guettier JM, Wess J. Novel insights into the function of beta-cell M3 muscarinic acetylcholine receptors: therapeutic implications. *Trends Endocrinol Metab*. 2011;22:74-80.

97. Iankova I, Chavey C, Clape C, Colomer C, Guerineau NC, Grillet N, Brunet JF, Annicotte JS, Fajas L. Regulator of G protein signaling-4 controls fatty acid and glucose homeostasis. *Endocrinology*. 2008;149:5706-5712.

98. Kanzaki M, Watson RT, Artemyev NO, Pessin JE. The trimeric GTP-binding protein (G(q)/G(11)) alpha subunit is required for insulin-stimulated GLUT4 translocation in 3T3L1 adipocytes. *J Biol Chem*. 2000;275:7167-7175.

99. Zhang S, Watson N, Zahner J, Rottman JN, Blumer KJ, Muslin AJ. RGS3 and RGS4 are GTPase activating proteins in the heart. *J Mol Cell Cardiol*. 1998;30:269-276.

100. Wang X, Adams LD, Pabon LM, Mahoney WM, Jr., Beaudry D, Gunaje J, Geary RL, Deblois D, Schwartz SM. RGS5, RGS4, and RGS2 expression and aortic contractibility are dynamically co-regulated during aortic banding-induced hypertrophy. *J Mol Cell Cardiol*. 2008;44:539-550.

101. Tokudome T, Kishimoto I, Horio T, Arai Y, Schwenke DO, Hino J, Okano I, Kawano Y, Kohno M, Miyazato M, Nakao K, Kangawa K. Regulator of G-protein signaling subtype 4 mediates antihypertrophic effect of locally secreted natriuretic peptides in the heart. *Circulation*. 2008;117:2329-2339.

102. Tamirisa P, Blumer KJ, Muslin AJ. RGS4 inhibits G-protein signaling in cardiomyocytes. *Circulation*. 1999;99:441-447.

103. Rogers JH, Tamirisa P, Kovacs A, Weinheimer C, Courtois M, Blumer KJ, Kelly DP, Muslin AJ. RGS4 causes increased mortality and reduced cardiac hypertrophy in response to pressure overload. *J Clin Invest*. 1999;104:567-576.

104. Rogers JH, Tsirka A, Kovacs A, Blumer KJ, Dorn GW, Muslin AJ. RGS4 reduces contractile dysfunction and hypertrophic gene induction in Galpha q overexpressing mice. *J Mol Cell Cardiol*. 2001;33:209-218.

105. Jaen C, Doupnik CA. RGS3 and RGS4 differentially associate with G protein-coupled receptor-Kir3 channel signaling complexes revealing two modes of RGS modulation. Precoupling and collision coupling. *J Biol Chem*. 2006;281:34549-34560.

106. Ishii M, Inanobe A, Kurachi Y. PIP3 inhibition of RGS protein and its reversal by Ca2+/calmodulin mediate voltage-dependent control of the G protein cycle in a cardiac K+ channel. *Proc Natl Acad Sci U S A*. 2002;99:4325-4330.

107. Doupnik CA, Davidson N, Lester HA, Kofuji P. RGS proteins reconstitute the rapid gating kinetics of gbetagamma-activated inwardly rectifying K+ channels. *Proc Natl Acad Sci U S A*. 1997;94:10461-10466.

108. Doupnik CA, Jaen C, Zhang Q. Measuring the modulatory effects of RGS proteins on GIRK channels. *Methods Enzymol*. 2004;389:131-54.:131-154.

109. Jaen C, Doupnik CA. RGS3 and RGS4 differentially associate with G protein-coupled receptor-Kir3 channel signaling complexes revealing two modes of RGS modulation. Precoupling and collision coupling. *J Biol Chem*. 2006;281:34549-34560.

110. Cifelli C, Rose RA, Zhang H, Voigtlaender-Bolz J, Bolz SS, Backx PH, Heximer SP. RGS4 regulates parasympathetic signaling and heart rate control in the sinoatrial node. *Circ Res*. 2008;103:527-535.

111. Cifelli C, Rose RA, Zhang H, Voigtlaender-Bolz J, Bolz SS, Backx PH, Heximer SP. RGS4 regulates parasympathetic signaling and heart rate control in the sinoatrial node. *Circ Res*. 2008;103:527-535.

112. Harris IS, Treskov I, Rowley MW, Heximer S, Kaltenbronn K, Finck BN, Gross RW, Kelly DP, Blumer KJ, Muslin AJ. G-protein signaling participates in the development of diabetic cardiomyopathy. *Diabetes*. 2004;53:3082-3090.

113. Chen C, Seow KT, Guo K, Yaw LP, Lin SC. The membrane association domain of RGS16 contains unique amphipathic features that are conserved in RGS4 and RGS5. *J Biol Chem*. 1999;274:19799-19806.

114. Bernstein LS, Grillo AA, Loranger SS, Linder ME. RGS4 binds to membranes through an amphipathic alpha -helix. *J Biol Chem*. 2000;275:18520-18526.

115. Osterhout JL, Waheed AA, Hiol A, Ward RJ, Davey PC, Nini L, Wang J, Milligan G, Jones TL, Druey KM. Palmitoylation regulates regulator of G-protein signaling (RGS) 16 function. II. Palmitoylation of a cysteine residue in the RGS box is critical for RGS16 GTPase accelerating activity and regulation of Gi-coupled signalling. *J Biol Chem*. 2003;278:19309-19316.

116. Hiol A, Davey PC, Osterhout JL, Waheed AA, Fischer ER, Chen CK, Milligan G, Druey KM, Jones TL. Palmitoylation regulates regulators of G-protein signaling (RGS) 16 function. I. Mutation of amino-terminal cysteine residues on RGS16 prevents its targeting to lipid rafts and palmitoylation of an internal cysteine residue. *J Biol Chem*. 2003;278:19301-19308.

117. Srinivasa SP, Bernstein LS, Blumer KJ, Linder ME. Plasma membrane localization is required for RGS4 function in Saccharomyces cerevisiae. *Proc Natl Acad Sci U S A*. 1998;95:5584-5589.

118. Lee MJ, Tasaki T, Moroi K, An JY, Kimura S, Davydov IV, Kwon YT. RGS4 and RGS5 are in vivo substrates of the N-end rule pathway. *Proc Natl Acad Sci U S A*. 2005;102:15030-15035.

119. Davydov IV, Varshavsky A. RGS4 is arginylated and degraded by the N-end rule pathway in vitro. *J Biol Chem*. 2000;275:22931-22941.

120. Wang J, Xie Y, Wolff DW, Abel PW, Tu Y. DHHC protein-dependent palmitoylation protects regulator of G-protein signaling 4 from proteasome degradation. *FEBS Lett*. 2010;584:4570-4574.

121. Ouyang YS, Tu Y, Barker SA, Yang F. Regulators of G-protein signaling (RGS) 4, insertion into model membranes and inhibition of activity by phosphatidic acid. *J Biol Chem*. 2003;278:11115-11122.

122. Ou-Yang YS, Tu Y, Yang F. The mutation in the N-terminal domain of RGS4 disrupts PA-conferred inhibitory effect on GAP activity. *Biosci Rep*. 2003;23:213-224.

123. Huang J, Zhou H, Mahavadi S, Sriwai W, Murthy KS. Inhibition of Galphaq-dependent PLC-beta1 activity by PKG and PKA is mediated by phosphorylation of RGS4 and GRK2. *Am J Physiol Cell Physiol*. 2007;292:C200-C208.

124. Tu Y, Popov S, Slaughter C, Ross EM. Palmitoylation of a conserved cysteine in the regulator of G protein signaling (RGS) domain modulates the GTPase-activating activity of RGS4 and RGS10. *J Biol Chem*. 1999;274:38260-38267.

125. Osterhout JL, Waheed AA, Hiol A, Ward RJ, Davey PC, Nini L, Wang J, Milligan G, Jones TL, Druey KM. Palmitoylation regulates regulator of G-protein signaling (RGS) 16 function. II. Palmitoylation of a cysteine residue in the RGS box is critical for RGS16 GTPase accelerating activity and regulation of Gi-coupled signalling. *J Biol Chem*. 2003;278:19309-19316.

126. Popov SG, Krishna UM, Falck JR, Wilkie TM. Ca2+/Calmodulin reverses phosphatidylinositol 3,4, 5-trisphosphate-dependent inhibition of regulators of G protein-signaling GTPase-activating protein activity. *J Biol Chem*. 2000;275:18962-18968.

127. Ishii M, Fujita S, Yamada M, Hosaka Y, Kurachi Y. Phosphatidylinositol 3,4,5-trisphosphate and Ca2+/calmodulin competitively bind to the regulators of G-protein-signalling (RGS) domain of RGS4 and reciprocally regulate its action. *Biochem J*. 2005;385:65-73.

128. Ishii M, Inanobe A, Kurachi Y. PIP3 inhibition of RGS protein and its reversal by Ca2+/calmodulin mediate voltage-dependent control of the G protein cycle in a cardiac K+ channel. *Proc Natl Acad Sci U S A*. 2002;99:4325-4330.

129. Shin DM, Dehoff M, Luo X, Kang SH, Tu J, Nayak SK, Ross EM, Worley PF, Muallem S. Homer 2 tunes G protein-coupled receptors stimulus intensity by regulating RGS proteins and PLCbeta GAP activities. *J Cell Biol*. 2003;162:293-303.

130. Srinivasa SP, Watson N, Overton MC, Blumer KJ. Mechanism of RGS4, a GTPase-activating protein for G protein alpha subunits. *J Biol Chem*. 1998;273:1529-1533.

131. Nadolski MJ, Linder ME. Protein lipidation. *FEBS J*. 2007;274:5202-5210.

132. Smotrys JE, Linder ME. Palmitoylation of intracellular signaling proteins: regulation and function. *Annu Rev Biochem*. 2004;73:559-587.

133. Drisdel RC, Alexander JK, Sayeed A, Green WN. Assays of protein palmitoylation. *Methods*. 2006;40:127-134.

134. Fukata Y, Iwanaga T, Fukata M. Systematic screening for palmitoyl transferase activity of the DHHC protein family in mammalian cells. *Methods*. 2006;40:177-182.

135. Swarthout JT, Lobo S, Farh L, Croke MR, Greentree WK, Deschenes RJ, Linder ME. DHHC9 and GCP16 constitute a human protein fatty acyltransferase with specificity for H- and N-Ras. *J Biol Chem*. 2005;280:31141-31148.

136. Fernandez-Hernando C, Fukata M, Bernatchez PN, Fukata Y, Lin MI, Bredt DS, Sessa WC. Identification of Golgi-localized acyl transferases that palmitoylate and regulate endothelial nitric oxide synthase. *J Cell Biol*. 2006;174:369-377.

137. Mumby SM, Kleuss C, Gilman AG. Receptor regulation of G-protein palmitoylation. *Proc Natl Acad Sci U S A*. 1994;91:2800-2804.

138. Fishburn CS, Herzmark P, Morales J, Bourne HR. Gbetagamma and palmitate target newly synthesized Galphaz to the plasma membrane. *J Biol Chem*. 1999;274:18793-18800.

139. Goddard AD, Watts A. Regulation of G protein-coupled receptors by palmitoylation and cholesterol. *BMC Biol*. 2012;10:27.

140. Greaves J, Carmichael JA, Chamberlain LH. The palmitoyl transferase DHHC2 targets a dynamic membrane cycling pathway: regulation by a C-terminal domain. *Mol Biol Cell*. 2011;22:1887-1895.

141. Komaniwa S, Hayashi H, Kawamoto H, Sato SB, Ikawa T, Katsura Y, Udaka K. Lipid-mediated presentation of MHC class II molecules guides thymocytes to the CD4 lineage. *Eur J Immunol*. 2009;39:96-112.

142. Sato I, Obata Y, Kasahara K, Nakayama Y, Fukumoto Y, Yamasaki T, Yokoyama KK, Saito T, Yamaguchi N. Differential trafficking of Src, Lyn, Yes and Fyn is specified by the state of palmitoylation in the SH4 domain. *J Cell Sci*. 2009;122:965-975.

143. Greaves J, Chamberlain LH. Differential palmitoylation regulates intracellular patterning of SNAP25. *J Cell Sci*. 2011;124:1351-1360.

144. Alvarez E, Girones N, Davis RJ. Inhibition of the receptor-mediated endocytosis of diferric transferrin is associated with the covalent modification of the transferrin receptor with palmitic acid. *J Biol Chem*. 1990;265:16644-16655.

145. Aicart-Ramos C, Valero RA, Rodriguez-Crespo I. Protein palmitoylation and subcellular trafficking. *Biochim Biophys Acta*. 2011;1808:2981-2994.

146. Valdez-Taubas J, Pelham H. Swf1-dependent palmitoylation of the SNARE Tlg1 prevents its ubiquitination and degradation. *EMBO J*. 2005;24:2524-2532.

147. Aittaleb M, Nishimura A, Linder ME, Tesmer JJ. Plasma membrane association of p63 Rho guanine nucleotide exchange factor (p63RhoGEF) is mediated by palmitoylation and is required for basal activity in cells. *J Biol Chem*. 2011;286:34448-34456.

148. Delint-Ramirez I, Willoughby D, Hammond GV, Ayling LJ, Cooper DM. Palmitoylation targets AKAP79 protein to lipid rafts and promotes its regulation of calcium-sensitive adenylyl cyclase type 8. *J Biol Chem*. 2011;286:32962-32975.

149. Taguchi T, Misaki R. Palmitoylation pilots ras to recycling endosomes. *Small Gtpases*. 2011;2:82-84.

150. Resh MD. Palmitoylation of ligands, receptors, and intracellular signaling molecules. *Sci STKE*. 2006;2006:re14.

151. Mueller GM, Maarouf AB, Kinlough CL, Sheng N, Kashlan OB, Okumura S, Luthy S, Kleyman TR, Hughey RP. Cys palmitoylation of the beta subunit modulates gating of the epithelial sodium channel. *J Biol Chem*. 2010;285:30453-30462.

152. McCormick PJ, Dumaresq-Doiron K, Pluviose AS, Pichette V, Tosato G, Lefrancois S. Palmitoylation controls recycling in lysosomal sorting and trafficking. *Traffic*. 2008;9:1984-1997.

153. Lobo S, Greentree WK, Linder ME, Deschenes RJ. Identification of a Ras palmitoyltransferase in Saccharomyces cerevisiae. *J Biol Chem*. 2002;277:41268-41273.

154. Roth AF, Feng Y, Chen L, Davis NG. The yeast DHHC cysteine-rich domain protein Akr1p is a palmitoyl transferase. *J Cell Biol*. 2002;159:23-28.

155. Bartels DJ, Mitchell DA, Dong X, Deschenes RJ. Erf2, a novel gene product that affects the localization and palmitoylation of Ras2 in Saccharomyces cerevisiae. *Mol Cell Biol*. 1999;19:6775-6787.

156. Greaves J, Chamberlain LH. DHHC palmitoyl transferases: substrate interactions and (patho)physiology. *Trends Biochem Sci*. 2011;36:245-253.

157. Putilina T, Wong P, Gentleman S. The DHHC domain: a new highly conserved cysteine-rich motif. *Mol Cell Biochem*. 1999;195:219-226.

158. Mitchell DA, Vasudevan A, Linder ME, Deschenes RJ. Protein palmitoylation by a family of DHHC protein S-acyltransferases. *J Lipid Res*. 2006;47:1118-1127.

159. Fukata Y, Fukata M. Protein palmitoylation in neuronal development and synaptic plasticity. *Nat Rev Neurosci*. 2010;11:161-175.

160. Ohno Y, Kihara A, Sano T, Igarashi Y. Intracellular localization and tissue-specific distribution of human and yeast DHHC cysteine-rich domain-containing proteins. *Biochim Biophys Acta*. 2006;1761:474-483.

161. Zhou F, Xue Y, Yao X, Xu Y. CSS-Palm: palmitoylation site prediction with a clustering and scoring strategy (CSS). *Bioinformatics*. 2006;22:894-896.

162. Ren J, Wen L, Gao X, Jin C, Xue Y, Yao X. CSS-Palm 2.0: an updated software for palmitoylation sites prediction. *Protein Eng Des Sel*. 2008;21:639-644.

163. Tsutsumi R, Fukata Y, Noritake J, Iwanaga T, Perez F, Fukata M. Identification of G protein alpha subunit-palmitoylating enzyme. *Mol Cell Biol*. 2009;29:435-447.

164. Lumb JH, Connell JW, Allison R, Reid E. The AAA ATPase spastin links microtubule severing to membrane modelling. *Biochim Biophys Acta*. 2012;1823:192-197.

165. Epp N, Rethmeier R, Kramer L, Ungermann C. Membrane dynamics and fusion at late endosomes and vacuoles--Rab regulation, multisubunit tethering complexes and SNAREs. *Eur J Cell Biol*. 2011;90:779-785.

166. Zerial M, McBride H. Rab proteins as membrane organizers. *Nat Rev Mol Cell Biol*. 2001;2:107-117.

167. D'Souza-Schorey C, Chavrier P. ARF proteins: roles in membrane traffic and beyond. *Nat Rev Mol Cell Biol*. 2006;7:347-358.

168. Shin HW, Hayashi M, Christoforidis S, Lacas-Gervais S, Hoepfner S, Wenk MR, Modregger J, Uttenweiler-Joseph S, Wilm M, Nystuen A, Frankel WN, Solimena M, De Camilli P, Zerial M. An enzymatic cascade of Rab5 effectors regulates phosphoinositide turnover in the endocytic pathway. *J Cell Biol*. 2005;170:607-618.

169. Brown FC, Pfeffer SR. An update on transport vesicle tethering. *Mol Membr Biol*. 2010;27:457-461.

170. Horgan CP, McCaffrey MW. The dynamic Rab11-FIPs. *Biochem Soc Trans*. 2009;37:1032-1036.

171. Zylbersztejn K, Galli T. Vesicular traffic in cell navigation. *FEBS J*. 2011;278:4497-4505.

172. Hunt SD, Stephens DJ. The role of motor proteins in endosomal sorting. *Biochem Soc Trans*. 2011;39:1179-1184.

173. Sandilands E, Frame MC. Endosomal trafficking of Src tyrosine kinase. *Trends Cell Biol*. 2008;18:322-329.

174. Maxfield FR, McGraw TE. Endocytic recycling. *Nat Rev Mol Cell Biol*. 2004;5:121-132.

175. Bonifacino JS, Rojas R. Retrograde transport from endosomes to the trans-Golgi network. *Nat Rev Mol Cell Biol*. 2006;7:568-579.

176. Hutagalung AH, Novick PJ. Role of Rab GTPases in membrane traffic and cell physiology. *Physiol Rev*. 2011;91:119-149.

177. Andres DA, Seabra MC, Brown MS, Armstrong SA, Smeland TE, Cremers FP, Goldstein JL. cDNA cloning of component A of Rab geranylgeranyl transferase and demonstration of its role as a Rab escort protein. *Cell*. 1993;73:1091-1099.

178. Alexandrov K, Horiuchi H, Steele-Mortimer O, Seabra MC, Zerial M. Rab escort protein-1 is a multifunctional protein that accompanies newly prenylated rab proteins to their target membranes. *EMBO J*. 1994;13:5262-5273.

179. Barr F, Lambright DG. Rab GEFs and GAPs. *Curr Opin Cell Biol*. 2010;22:461-470.

180. Pfeffer SR. Rab GTPases: specifying and deciphering organelle identity and function. *Trends Cell Biol*. 2001;11:487-491.

181. Mir A, Kaufman L, Noor A, Motazacker MM, Jamil T, Azam M, Kahrizi K, Rafiq MA, Weksberg R, Nasr T, Naeem F, Tzschach A, Kuss AW, Ishak GE, Doherty D, Ropers HH, Barkovich AJ, Najmabadi H, Ayub M, Vincent JB. Identification of mutations in TRAPPC9, which encodes the NIK- and IKK-beta-binding protein, in nonsyndromic autosomal-recessive mental retardation. *Am J Hum Genet*. 2009;85:909-915.

182. Di Pietro SM, Dell'Angelica EC. The cell biology of Hermansky-Pudlak syndrome: recent advances. *Traffic*. 2005;6:525-533.

183. Aligianis IA, Morgan NV, Mione M, Johnson CA, Rosser E, Hennekam RC, Adams G, Trembath RC, Pilz DT, Stoodley N, Moore AT, Wilson S, Maher ER. Mutation in Rab3 GTPase-activating protein (RAB3GAP) noncatalytic subunit in a kindred with Martsolf syndrome. *Am J Hum Genet*. 2006;78:702-707.

184. MacDonald IM, Smaoui N, Seabra MC. Choroideremia. 1993.

185. Nielsen E, Severin F, Backer JM, Hyman AA, Zerial M. Rab5 regulates motility of early endosomes on microtubules. *Nat Cell Biol*. 1999;1:376-382.

186. Sandvig K, Pust S, Skotland T, van Deurs B. Clathrin-independent endocytosis: mechanisms and function. *Curr Opin Cell Biol*. 2011;23:413-420.

187. Wang T, Ming Z, Xiaochun W, Hong W. Rab7: role of its protein interaction cascades in endo-lysosomal traffic. *Cell Signal*. 2011;23:516-521.

188. Poteryaev D, Datta S, Ackema K, Zerial M, Spang A. Identification of the switch in early-to-late endosome transition. *Cell*. 2010;141:497-508.

189. Mohrmann K, van der SP. Regulation of membrane transport through the endocytic pathway by rabGTPases. *Mol Membr Biol*. 1999;16:81-87.

190. Jing J, Junutula JR, Wu C, Burden J, Matern H, Peden AA, Prekeris R. FIP1/RCP binding to Golgin-97 regulates retrograde transport from recycling endosomes to the trans-Golgi network. *Mol Biol Cell*. 2010;21:3041-3053.

191. Ren M, Xu G, Zeng J, Lemos-Chiarandini C, Adesnik M, Sabatini DD. Hydrolysis of GTP on rab11 is required for the direct delivery of transferrin from the pericentriolar recycling compartment to the cell surface but not from sorting endosomes. *Proc Natl Acad Sci U S A*. 1998;95:6187-6192.

192. Stenmark H, Parton RG, Steele-Mortimer O, Lutcke A, Gruenberg J, Zerial M. Inhibition of rab5 GTPase activity stimulates membrane fusion in endocytosis. *EMBO J*. 1994;13:1287-1296.

193. van der SP, Hull M, Webster P, Male P, Goud B, Mellman I. The small GTP-binding protein rab4 controls an early sorting event on the endocytic pathway. *Cell*. 1992;70:729-740.

194. Tachiyama R, Ishikawa D, Matsumoto M, Nakayama KI, Yoshimori T, Yokota S, Himeno M, Tanaka Y, Fujita H. Proteome of ubiquitin/MVB pathway: possible involvement of iron-induced ubiquitylation of transferrin receptor in lysosomal degradation. *Genes Cells*. 2011;16:448-466.

195. Druey KM, Ugur O, Caron JM, Chen CK, Backlund PS, Jones TL. Amino-terminal cysteine residues of RGS16 are required for palmitoylation and modulation of Gi- and Gq-mediated signaling. *J Biol Chem*. 1999;274:18836-18842.

196. Gu S, He J, Ho WT, Ramineni S, Thal DM, Natesh R, Tesmer JJ, Hepler JR, Heximer SP. Unique hydrophobic extension of the RGS2 amphipathic helix domain imparts increased plasma membrane binding and function relative to other RGS R4/B subfamily members. *J Biol Chem*. 2007;282:33064-33075.

197. Reaves B, Horn M, Banting G. TGN38/41 recycles between the cell surface and the TGN: brefeldin A affects its rate of return to the TGN. *Mol Biol Cell*. 1993;4:93-105.

198. Kaveesh Dissanayake. Defining the Mechanisms by which Palmitoylation Regulates the Localization and Function of RGS4. 2010.

Ref Type: Generic

199. Rose JJ, Taylor JB, Shi J, Cockett MI, Jones PG, Hepler JR. RGS7 is palmitoylated and exists as biochemically distinct forms. *J Neurochem*. 2000;75:2103-2112.

200. Jia L, Linder ME, Blumer KJ. Gi/o signaling and the palmitoyltransferase DHHC2 regulate palmitate cycling and shuttling of RGS7 family-binding protein. *J Biol Chem*. 2011;286:13695-13703.

201. Sullivan BM, Harrison-Lavoie KJ, Marshansky V, Lin HY, Kehrl JH, Ausiello DA, Brown D, Druey KM. RGS4 and RGS2 bind coatomer and inhibit COPI association with Golgi membranes and intracellular transport. *Mol Biol Cell*. 2000;11:3155-3168.

202. Pfeffer SR. Multiple routes of protein transport from endosomes to the trans Golgi network. *FEBS Lett*. 2009;583:3811-3816.

203. Gardner LA, Hajjhussein H, Frederick-Dyer KC, Bahouth SW. Rab11a and its binding partners regulate the recycling of the ss1-adrenergic receptor. *Cell Signal*. 2011;23:46-57.

204. Zimmermann L, Paster W, Weghuber J, Eckerstorfer P, Stockinger H, Schutz GJ. Direct observation and quantitative analysis of Lck exchange between plasma membrane and cytosol in living T cells. *J Biol Chem*. 2010;285:6063-6070.

205. Koegl M, Zlatkine P, Ley SC, Courtneidge SA, Magee AI. Palmitoylation of multiple Src-family kinases at a homologous N-terminal motif. *Biochem J*. 1994;303 (Pt 3):749-753.

206. Apolloni A, Prior IA, Lindsay M, Parton RG, Hancock JF. H-ras but not K-ras traffics to the plasma membrane through the exocytic pathway. *Mol Cell Biol*. 2000;20:2475-2487.

207. Misaki R, Morimatsu M, Uemura T, Waguri S, Miyoshi E, Taniguchi N, Matsuda M, Taguchi T. Palmitoylated Ras proteins traffic through recycling endosomes to the plasma membrane during exocytosis. *J Cell Biol*. 2010;191:23-29.

208. Gonzalez MA, Quiroga R, Maccioni HJ, Valdez TJ. A novel motif at the C-terminus of palmitoyltransferases is essential for Swf1 and Pfa3 function in vivo. *Biochem J*. 2009;419:301-308.

209. Paspalas CD, Selemon LD, Arnsten AF. Mapping the regulator of G protein signaling 4 (RGS4): presynaptic and postsynaptic substrates for neuroregulation in prefrontal cortex. *Cereb Cortex*. 2009;19:2145-2155.

210. Lawe DC, Chawla A, Merithew E, Dumas J, Carrington W, Fogarty K, Lifshitz L, Tuft R, Lambright D, Corvera S. Sequential roles for phosphatidylinositol 3-phosphate and Rab5 in tethering and fusion of early endosomes via their interaction with EEA1. *J Biol Chem*. 2002;277:8611-8617.

211. Mills IG, Urbe S, Clague MJ. Relationships between EEA1 binding partners and their role in endosome fusion. *J Cell Sci*. 2001;114:1959-1965.

212. Shapiro MS, Gomeza J, Hamilton SE, Hille B, Loose MD, Nathanson NM, Roche JP, Wess J. Identification of subtypes of muscarinic receptors that regulate Ca2+ and K+ channel activity in sympathetic neurons. *Life Sci*. 2001;68:2481-2487.

213. Jimenez E, Montiel M. Activation of MAP kinase by muscarinic cholinergic receptors induces cell proliferation and protein synthesis in human breast cancer cells. *J Cell Physiol*. 2005;204:678-686.

214. Montiel M, Quesada J, Jimenez E. Activation of calcium-dependent kinases and epidermal growth factor receptor regulate muscarinic acetylcholine receptor-mediated MAPK/ERK activation in thyroid epithelial cells. *Cell Signal*. 2007;19:2138-2146.

215. Veeraragavan S, Bui N, Perkins JR, Yuva-Paylor LA, Carpenter RL, Paylor R. Modulation of behavioral phenotypes by a muscarinic M1 antagonist in a mouse model of fragile X syndrome. *Psychopharmacology (Berl)*. 2011;217:143-151.

216. Almasieh M, Zhou Y, Kelly ME, Casanova C, Di Polo A. Structural and functional neuroprotection in glaucoma: role of galantamine-mediated activation of muscarinic acetylcholine receptors. *Cell Death Dis*. 2010;1:e27.

217. Barak S, Weiner I. The M/M preferring agonist xanomeline reverses amphetamine-, M. *Int J Neuropsychopharmacol*. 2011;14:1233-1246.

218. Shirey JK, Brady AE, Jones PJ, Davis AA, Bridges TM, Kennedy JP, Jadhav SB, Menon UN, Xiang Z, Watson ML, Christian EP, Doherty JJ, Quirk MC, Snyder DH, Lah JJ, Levey AI, Nicolle MM, Lindsley CW, Conn PJ. A selective allosteric potentiator of the M1 muscarinic acetylcholine receptor increases activity of

medial prefrontal cortical neurons and restores impairments in reversal learning. *J Neurosci*. 2009;29:14271-14286.

219. Giguere P, Rochdi MD, Laroche G, Dupre E, Whorton MR, Sunahara RK, Claing A, Dupuis G, Parent JL. ARF6 activation by Galpha q signaling: Galpha q forms molecular complexes with ARNO and ARF6. *Cell Signal*. 2006;18:1988-1994.

220. Reiner C, Nathanson NM. The internalization of the M2 and M4 muscarinic acetylcholine receptors involves distinct subsets of small G-proteins. *Life Sci*. 2008;82:718-727.

221. Hurst JH, Mendpara N, Hooks SB. Regulator of G-protein signalling expression and function in ovarian cancer cell lines. *Cell Mol Biol Lett*. 2009;14:153-174.

222. Hao J, Michalek C, Zhang W, Zhu M, Xu X, Mende U. Regulation of cardiomyocyte signaling by RGS proteins: differential selectivity towards G proteins and susceptibility to regulation. *J Mol Cell Cardiol*. 2006;41:51-61.

223. Sato M, Ishikawa Y. Accessory proteins for heterotrimeric G-protein: Implication in the cardiovascular system. *Pathophysiology*. 2010;17:89-99.

224. Ishikura S, Koshkina A, Klip A. Small G proteins in insulin action: Rab and Rho families at the crossroads of signal transduction and GLUT4 vesicle traffic. *Acta Physiol (Oxf)*. 2008;192:61-74.

Annexe I

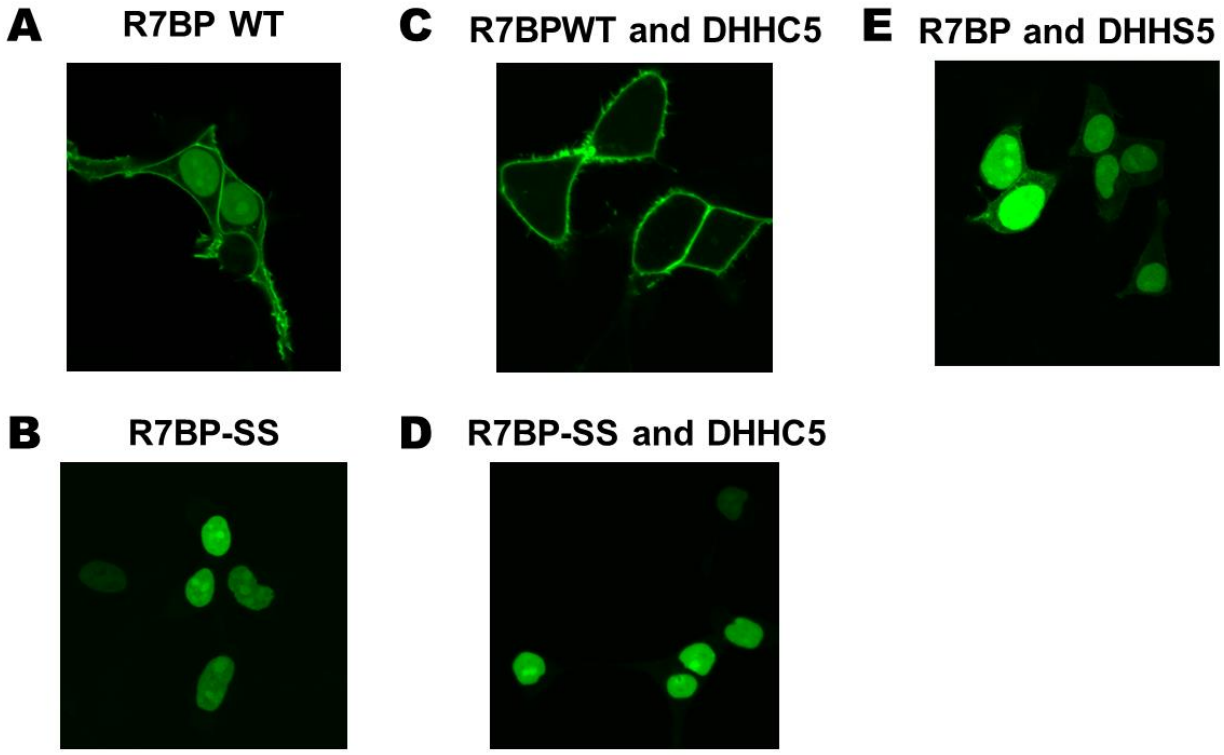

Figure Annexe1: DHHC5 mediates R7BP cellular localization. (**A**) Steady state level of wild-type R7BP indicated an approximately equal localization between the nucleus and plasma membrane. (**B**) The C252S/C253S double mutant or R7BP-SS, which lacks the conserved sites for palmitoylation, accumulates in the nucleus. (**C**) Co-expression of R7BP-WT with the palmitoylating enzyme, DHHC5 drives the localization of R7BP almost exclusively to the plasma membrane. (**D**) Co-expression of R7BP-SS and DHHC5results in the accumulation of R7BP in the nucleus. (**E**) Co-expression of R7BP-WT with a mutant palmitoylating, DHHS-5 results in increased localization to the nucleus and none to the plasma membrane. Bastin, G. Unpublished results.

AnnexeII

I investigated proteomic approach for characterizing RGS4's post translational modifications and interactome. Briefly, two tags were added to RGS4, Streptavidin binding domain and Calmodulin binding domain in order to purify RGS4 from HEK293 cell culture by tap tag (Tandem Affinity Purification). The tags were added at the C-terminal side of the protein to avoid any interference with its intracellular localization. RGS4 was purified under gentle conditions (neutral pH, weak detergent) to keep weakly bound interactors bound to RGS4. The purified fraction was then concentrated by speed vacuum, re-suspended with an appropriate buffer and digested with ArgC. No desalting step was performed. Samples have been analyzed by ESI-Q-FT-ICR downstream of a 50cm Reverse phase column.

On two duplicated attempts: after the transfection of 50 time 10cm plates of HEK293 cells and addition of proteasome inhibitor, RGS4 signal remained very low on the spectrum, only 2peptides could be detected. The low number of peptides obtained decreased my level of confidence on the capacity of our method to study RGS4 post translational modifications by this approach. Moreover, RGS4 is known to interact with heterotrimeric G-proteins which, in my hand, are not appearing on the list of potential interacting proteins. This absence of positive known interactants also decreased my confidence in the used approach to study RGS4's interactome. I enclosed the list of potential interactants in the table of AnnexeII and underlined proteins that could be linked with RGS4. It is important to address that the list of reported proteins were not present in the controls: untransfected HEK293 prepared in similar conditions.

Hits		Number of peptide						Accession number
Experiment1	Experiment2							
26		7	40S ribosomal protein S3a OS=Homo sapiens GN=RPS3A PE=1 SV=2					P61247|RS3A_HUMAN
21		5	Histone H4 OS=Homo sapiens GN=HIST1H4A PE=1 SV=2					P62805|H4_HUMAN
16		2	Histone H2B type 1-B OS=Homo sapiens GN=HIST1H2BB PE=1 SV=2					P33778|H2B1B_HUMAN
13		3	Histone H2A type 1-B/E OS=Homo sapiens GN=HIST1H2AB PE=1 SV=2					P04908|H2A1B_HUMAN
12		5	Ribosome biogenesis protein BOP1 OS=Homo sapiens GN=BOP1 PE=1 SV=2					Q14137|BOP1_HUMAN
11		2	40S ribosomal protein S15a OS=Homo sapiens GN=RPS15A PE=1 SV=2					P62244|RS15A_HUMAN
10		3	Transcription intermediary factor 1-beta OS=Homo sapiens GN=TRIM28 PE=1 SV=5					Q13263|TIF1B_HUMAN
9		2	Histone H3.1 OS=Homo sapiens GN=HIST1H3A PE=1 SV=2					P68431|H31_HUMAN
5	5	2	Septin-8 OS=Homo sapiens GN=SEPT8 PE=1 SV=4					
8	8	3	Mitogen-activated protein kinase kinase kinase 4 OS=Homo sapiens GN=MAP4K4 PE=1 SV=2					O95819|M4K4_HUMAN
8	8	2	Regulator of G-protein signaling 4 OS=Homo sapiens GN=RGS4 PE=1 SV=1					P49798|RGS4_HUMAN
7		4	40S ribosomal protein S13 OS=Homo sapiens GN=RPS13 PE=1 SV=2					P62277|RS13_HUMAN
7		6	Pre-mRNA-splicing factor ATP-dependent RNA helicase PRP16 OS=Homo sapiens GN=DHX38 PE=1 SV=2					Q92620|PRP16_HUMAN
7		4	YTH domain-containing protein 1 OS=Homo sapiens GN=YTHDC1 PE=1 SV=3					Q96MU7|YTDC1_HUMAN
7		3	Zinc finger CCCH domain-containing protein 4 OS=Homo sapiens GN=ZC3H4 PE=1 SV=3					Q9UPT8|ZC3H4_HUMAN
6		2	60S ribosomal protein L27a OS=Homo sapiens GN=RPL27A PE=1 SV=2					P46776|RL27A_HUMAN
6		2	Translation initiation factor eIF-2B subunit beta OS=Homo sapiens GN=EIF2B2 PE=1 SV=3					P49770|E2BB_HUMAN
6		3	60S ribosomal protein L10 OS=Homo sapiens GN=RPL10 PE=1 SV=4					P27635|RL10_HUMAN
6		4	CAD protein OS=Homo sapiens GN=CAD PE=1 SV=3					P27708|PYR1_HUMAN
6	6	2	Filamin-A OS=Homo sapiens GN=FLNA PE=1 SV=4					P21333|FLNA_HUMAN
5		2	Serine/threonine-protein kinase 6 OS=Homo sapiens GN=AURKA PE=1 SV=2					O14965|STK6_HUMAN
5		4	Scaffold attachment factor B2 OS=Homo sapiens GN=SAFB2 PE=1 SV=1					Q14151|SAFB2_HUMAN
5	5	2	Actin-binding LIM protein 1 OS=Homo sapiens GN=ABLIM1 PE=1 SV=3					O14639|ABLM1_HUMAN
5		2	Anion exchange protein 2 OS=Homo sapiens GN=SLC4A2 PE=1 SV=4					P04920|B3A2_HUMAN
5		3	Heat shock 70 kDa protein 1L OS=Homo sapiens GN=HSPA1L PE=2 SV=2					P34931|HS71L_HUMAN
4	4	4	E3 ubiquitin-protein ligase HUWE1 OS=Homo sapiens GN=HUWE1 PE=1 SV=3					Q7Z6Z7|HUWE1_HUMAN
4	4	2	Brain-specific angiogenesis inhibitor 1-associated protein 2-like protein 1 OS=Homo sapiens GN=BAIAP2L1 PE=1 SV=2					Q9UHR4|IB2L1_HUMAN
2	2	1	G-protein-signaling modulator 1 OS=Homo sapiens GN=GPSM1 PE=1 SV=1					Q86YR5|GPSM1_HUMAN
1	1	1	G patch domain-containing protein 4 OS=Homo sapiens GN=GPATCH4 PE=1 SV=2					Q5T3I0|GPTC4_HUMAN
1	1	1	Rho GTPase-activating protein 17 OS=Homo sapiens GN=ARHGAP17 PE=1 SV=1					
1	1	1	Rho guanine nucleotide exchange factor 11 OS=Homo sapiens GN=ARHGEF11 PE=1 SV=1					

Published paper related to my work

Amino terminal cysteine residues differentially influence RGS4 plasma membrane targeting, intracellular trafficking, and function.

Guillaume Bastin[1,2], Kevin Singh[1], Kaveesh Dissanayake[1], Alexandra S. Mighiu[1], Aliya Nurmohamed[1] & Scott P. Heximer[1]*

[1] Department of Physiology, Heart and Stroke/Richard Lewar Centre of Excellence in Cardiovascular Research, University of Toronto, 1 King's College Circle, Toronto, Ontario M5S 1A8.

[2] Université de Lille 1, Sciences et Technologies, USR CNRS 3290 Miniaturisation pour Synthèse, l'Analyse & Protéomique, 59655 Villeneuve d'Ascq, France

*Canada Research Chair in Cardiovascular Physiology, to whom all correspondence should be addressed:

scott.heximer@utoronto.ca

Phone (416) 978-6048

Fax (416) 978-4373

Running Title: Cys2 and Cys12 direct RGS4 to different cellular compartments.

Corresponding author:

Scott P. Heximer

scott.heximer@utoronto.ca

Phone (416) 978-6048

Fax (416) 978-4940

Word Count:

Abstract: 254

Introduction: 493

Results : 1419

Discussion: 1380

Pages: 23

Tables: 0

Figures: 8

References: 33

Data Supplement: 1

Supplemental Movie Files: 3

List of Abbreviations: G-protein; guanine nucleotide binding protein, GPCR; G-protein coupled receptor, RGS; regulator of G-protein signaling; GAP; GTPase activating protein, YFP; yellow fluorescent protein, CFP; cyan fluorescent protein, TGN; trans-Golgi network, aa; amino acid, HEK; Human Embryonic Kidney, 2-BP; 2-Bromo Palmitate, PM; Plasma Membrane, PCC; Pearson Correlation Coefficient, DHHC; Palmitoyl-CoA transferase active site motif.

Background: Intracellular trafficking of RGS proteins is an important determinant of their function as G-protein inhibitors.

Results: Amino-terminal cysteine residues in RGS4 confer previously uncharacterized localization and trafficking activities.

Conclusion: Cys12 is required for plasma membrane targeting whereas Cys2 is required for localization to endosomal pools.

Significance: Understanding the mechanisms governing cellular distribution of RGS4 may lead to novel strategies for regulation of its function.

SUMMARY

RGS proteins are potent inhibitors of heterotrimeric G-protein signaling. RGS4 attenuates G-protein activity in several tissues. Previous work demonstrated that cysteine palmitoylation on residues in the amino terminal (Cys2 and Cys12) and core domains (Cys95) of RGS4 is important for protein stability, plasma membrane targeting, and GTPase activating function. To date, Cys2 has been the priority target for RGS4 regulation by palmitoylation based on its putative role in stabilizing the RGS4 protein. We here investigate differences in the contribution of Cys2 and Cys12 to the intracellular localization and function of RGS4. Inhibition of RGS4 palmitoylation with 2-bromopalmitate dramatically reduced its localization to the plasma membrane. Similarly, mutation of the RGS4 amphipathic helix (L23D) prevented membrane localization and its Gq inhibitory function. Together, these data suggest that both RGS4 palmitoylation and the amphipathic helix domain are required for optimal plasma membrane targeting and function of RGS4. Mutation of Cys12 decreased RGS4 membrane targeting to a similar extent as 2-bromopalmitate resulting in complete loss of its Gq inhibitory function. Mutation of Cys2 did not impair plasma membrane targeting but did partially impair its function as a Gq inhibitor. Comparison of the endosomal distribution pattern of wild type and mutant RGS4 proteins with TGN38 indicated that palmitoylation of

these two cysteines contributes differentially to the intracellular trafficking of RGS4. These data show for the first time that Cys2 and Cys12 play markedly different roles in the regulation of RGS4 membrane localization, intracellular trafficking, and Gq inhibitory function via mechanisms that are unrelated to RGS4 protein stabilization.

Heterotrimeric G-protein coupled receptors mediate the responses of a wide array of hormones and neurotransmitters. In many circumstances, increased G-protein activity is associated with pathophysiologic processes and disease progression. Thus, understanding the cellular mechanisms whereby G-protein signaling can be attenuated is an important step toward designing therapeutic strategies for the control and prevention of such diseases. Regulator of G-protein signaling (RGS) proteins comprise a family of > 35 G-protein inhibitors (1). RGS proteins function as GTPase activating proteins (GAPs) for Gα subunits (2,3) thereby decreasing the lifetime of activated G-protein complexes. One member of the RGS protein superfamily, RGS4, has been shown to be critical for regulation of G-protein signaling in the brain (4), sinoatrial node (5), pancreas (6) and during tumor cell metastasis (7). Thus, defining intracellular pathways that modulate RGS4 function may have important implications for understanding its role in the modulation of neural function, heart rate regulation, insulin release and cancer.

The RGS4 protein is comprised of two primary functional domains that are both regulated by palmitoylation. First, the carboxyl-terminus contains the ~120 aa GAP domain capable of inhibiting both Gi- and Gq-mediated signaling. Palmitoylation of Cys95 within the GAP domain is believed to be important for its function (8). Second, the ~ 50 aa amino-terminus contains an amphipathic α helix membrane targeting domain that is found adjacent to two palmitoylatable cysteine residues (Cys2 and Cys12). Simultaneous mutagenesis of both Cys2 and Cys12 or mutagenesis of the amphipathic α helix domain alone (9,10) have been shown to

modulate protein function and plasma membrane targeting.

Until recently however, the relative contributions of Cys2 and Cys12 were not independently examined. Some studies suggest that Cys2 is the primary site of palmitoylation in RGS4 and that palmitoylation of this residue enhances RGS4 function by preventing oxidation/arginylation and subsequent degradation via the N-end rule ubiquitin-mediated proteasomal pathway (11,12). Recently Tu and coworkers showed that palmitoylation of Cys2 by the palmitoyl acyltransferases DHHC3 (and DHHC7) can increase the half-life of RGS4 and thereby showing better G-protein inhibitory potential (13).

In contrast to the large amount of information known about Cys2 palmitoylation and its contribution to RGS4 stabilization, very little information is available concerning the relative roles of Cys2 and Cys12 as determinants of RGS4 localization and intracellular trafficking. We here investigate the extent to which Cys12 palmitoylation, regardless of the palmitoylation status of Cys2, may be an important regulator of RGS4 intracellular localization and function. Our data show for the first time that Cys12 is more important than Cys2 as a determinant of RGS4 plasma membrane targeting and Gq inhibitory function and we propose that this is due to its proximity to the amphipathic α helix plasma membrane targeting domain. Although Cys2 is largely dispensable for plasma membrane targeting, it does appear to play a role in the trafficking of RGS4 through different intracellular membrane compartments and thus its palmitoylation status may be important for regulating its normal trafficking and recycling within the cell.

METHODS AND MATERIALS

Materials- The pEYFP-C1 plasmid (Clontech/ BD Biosciences, Mississauga, ON) and pQE Trisystem1 (Qiagen, Mississauga, ON) expression vectors were used for expression of all RGS protein constructs. HA-tagged Gq-R183C was generously provided by P. Waedegartner (Thomas Jefferson University, Philadelphia, PA). Fluorescently tagged

versions of the Trans Golgi Network marker protein TGN38 were a kind gift from J. Lippincott-Schwartz (National Institutes of Health, Bethesda, MD). The monoclonal anti-His tag antibody was from Clontech (# 631212), anti-HA antibody was from Roche Scientific, Mississauga, ON, (# 11666606001) and the anti- mouse secondary antibody was from GE Healthcare, Mississauga, ON (# NXA931). All tissue culture media and transfection reagents were from Invitrogen (Burlington, ON) and Roche Scientific respectively. HEK293 cells (tsA-201 derivative) were a kind gift from Z-P. Feng (University of Toronto, Toronto, ON). Unless otherwise stated all other reagents and chemicals were from Sigma (Oakville, ON).

Cell culture – HEK293 cells were grown in Dulbecco's modified Eagle's medium (DMEM): Ham's F12 medium (1:1), supplemented with 10% (v/v) heat-inactivated fetal bovine serum, 2 mM glutamine, 10 µg/ml streptomycin, 100 units/ml penicillin) at 37 °C in a humidified atmosphere with 5% CO_2.

RGS4 expression constructs – For subcellular localization studies RGS4-YFP expression plasmids were generated in the pEYFP-C1 vector by cloning the human RGS4 cDNA into the NheI/AgeI sites to generate a carboxyl terminal YFP fusion. Robust expression was ensured by inclusion of an optimized translation initiation signal in the context of the first methionine codon (GCCACCATGGCG).For functional studies RGS4-His expression constructs were generated in the pQE Trisystem1 vector by cloning RGS4 coding sequences into the NcoI/BamHI polylinker sites. Cysteine point mutations were introduced by site-directed mutagenesis and primer sequences are available as supplemental data. All plasmid constructs were purified using the Endofree Maxi kit (Qiagen) and verified by sequencing of the complete protein-coding region. The expression of the pQE trysistem clones were analyzed by Western blotting using anti-His-tag antibody and ECL detection.

Assays of Gq-dependent Phosphoinositide Hydrolysis—HEK293 cells (2.0 x10^6 in 6-well plates) were transfected in triplicate using of Fugene 6™ transfection reagent

according to the manufacturer's specifications. DNA amounts used in transfection were determined empirically to ensure similar expression levels of all RGS4 constructs tested. Specifically we used 0.5 μg of Gq(R183C); 3 μg of RGS4WT-His, 0.5 μg of RGS4C2A-His, 3 μg of RGS4C12A-His, 0.5 μg of RGS4C2AC12A-His, 1 μg of RGS4L23D-His and an appropriate amount of empty HisStrep vector to ensure 4.0 μg of total plasmid DNA/well. After 24h cells were trypsinized, pooled and replated in 6-well plates for analysis of inositol phosphate production (n= 3 wells /construct) and corresponding protein expression determination by Western blotting. Inositol phosphate production was measured 48 h after transfection as described previously (14). Briefly, 5h after plating cells were washed with phosphate buffered saline and labeled in complete Dulbecco's modified Eagle's medium (without inositol) containing 10 mM LiCl and 1.4 μCi/mL myo-[^{3}H]-inositol (Perkin Elmer, Vaughan, ON) for exactly 15h. Then cells were washed with phosphate buffered saline and the inositol phosphate production was stopped with 750 μL of ice-cold 20 mM formic acid. The entire contents of the wells were collected and spun at 13,000 x g for 15 min in a microcentrifuge at 4°C. The supernatant fraction (700μL) was neutralized with 214 μL of 0.7M NH_4OH before proceeding to the ion exchange chromatography steps. For each well to be measured, a 3-mL Dowex resin (AG 1-X8, 200-400-mesh, formate form) column was prepared. The entire sample was added to the column, and unbound ^{3}H-labeled material consisting of the total inositol-containing fraction was collected, after, the phosphate inositol-containing fraction was eluted into collection tubes with 5mL of 1.2M ammonium formate. 0.5mL of each sample from total inositol-containing and inositol phosphate-containing fractions was added to 10mL of scintillation fluid and counted. Inositol phosphate levels were expressed as the fraction of the total soluble ^{3}H-labeled inositol material (inositol phosphate total/inositol-containing fraction) for each sample.

Confocal microscopy- For most experiments HEK293 cells were plated at 50% in tissue culture-treated microsopy dishes (Ibidi, #81156) and transfected

with 1 μg of each construct to be tested using Fugene 6 transfection reagent as describe above. For localization of RGS4 during phosphoinositol hydrolysis experiments, constructs were transfected in the identical ratios that were used for functional analysis (outlined above). Following 20h incubation dishes were sent for confocal microscopy to determine their plasma membrane/cytosol localization ratio containing transfected cells. Confocal microscopy was performed on ~70% confluence live cells at 37°C using an Olympus FluoView 1000 laser-scanning confocal microscope. Images represent single equatorial plane on the basal side of the cell obtained with a 60x oil objective, 1.4 numerical aperture. Confocal images were processed with Microsoft Office 2010. Quantification of plasma and endo-membrane localization was performed in a blinded manner, with membrane/cytosol ratios measured using the Image J software package and Pearson Correlation Coefficient (PCC) for each endosome was calculated by the Fluo-View software. For movie data, the cells were visualized on a WaveFX Spinning-Disk confocal microscope (Quorum Technologies, Guelph, Canada), which comprises an Olympus IX81 microscope stand, a Yokogawa CSU10 spinning-disk unit, and a Hamamatsu

C9100-13 EM-CCD camera, all controlled with Volocity software. Imaging was performed using a 60x/1.42NA oil immersion objective lens, 488nm solid-state laser illumination, and an EGFP bandpass filter. .

Palmitate Labeling and Detection by Click Chemistry - 10 x 10 cm plates of HEK293 cells stably transfected with either wild type or the C2A:C12A mutant of RGS4 were plated to ~70 % confluence. To increase final RGS4 protein yield, each plate was transiently transfected with the same RGS4 clone that was used to make the stable lines (RGS4WT- 6 μg or C2AC12A -2 mg in 6 μl X-tremegene HP, Roche). The RGS4 expression constructs contained a carboxyl-terminal Streptavidin Binding Peptide (SBP) tag. 12 h post-transfection medium was changed to 1:1 DMEM: F12 with 5% charcoal-treated fatty acid free serum. After 24 h, cells were serum starved for 1h in DMEM:F12, and then incubated for 8 hours in palmitic acid labeling medium

(DMEM containing 10% charcoal-treated serum, 0.4% of 25 mM alkyl-17-ODYA - palmitate analogue). Cells were collected and lysed at 4°C, using lysis buffer containing 20 mM HEPES, 150 mM NaCl, 3 mM $MgCl_2$, 1% Triton-X, pH 7.4, and protease Complete Mini™ protease inhibitors (Roche). Samples were briefly sonicated and lysates incubated with Streptavidin Sepharose High Performace beads (GE Healthcare), overnight at 4°C. Beads were washed five times with lysis buffer, and once with acidic lysis buffer (pH 4.0). For click chemistry reaction, beads were mixed with lysis buffer containing 1 mM $CuSO_4$, 1 mM TCEP, 100 μM TBTA, and 20 μM Alexa-488 azide (Invitrogen) at room temperature for 1.5 hours. Following the click-mediated addition of Alexa-488 to palmitoylated proteins, the beads were washed three times with lysis buffer, and RGS4 eluted in SDS PAGE loading buffer before running on 12% gels. Gels were fixed in 40% methanol, 10% acetic acid for in gel fluorescent detection of in Alexa-488 on the Typhoon imaging station. The relative amount of RGS4 protein in the eluates was examined by Western blotting for the HA epitope tag.

Western Blotting- Proteins were transferred to (Trans-Blot, BioRad) nitrocellulose membrane. Membranes were blocked for 1 hr in 0.1% Tween-20 and 5% bovine serum albumin. Primary antibodies were added to 5% BSA at concentrations provided by the vendor's instructions and incubated with membranes overnight at 4°C before removing by washing. Horseradish peroxidase linked-secondary mouse or rabbit antibody in 5%BSA was added for 2 hr, before washing and signal detection using Super Signal West Pico Chemiluminscent Substrate (Thermo Scientific).

Statistical Analysis – One-way ANOVA with a Tukey's post hoc test was used to determine statistical significance between the groups. Where correlation coefficients were compared Fisher's r to z' transformation was employed. *$P<0.05$.

RESULTS

The N-terminal domain of RGS4 was previously shown to be important for

its plasma membrane targeting in yeast cells (9,10). This domain contains an amphipathic α helical domain and two palmitoylatable cysteine residues (Cys2 and Cys12) as potential plasma membrane targeting motifs. In a heterologous yeast system, the amphipathic helix domain of RGS4 was shown to be necessary and sufficient for plasma membrane targeting and G-protein inhibition. These data suggested a diminutive role for amino terminal palmitoylation in regulating RGS4 function in lower eukaryotes. In a more autologous human cell line, however, the determinants that control human RGS4 plasma membrane targeting, function, and intracellular trafficking have not been carefully examined. In particular, very little is known about the intracellular trafficking of RGS4 between plasma membrane and endosomal or cytosolic pools.

Wild type RGS4-YFP strongly localized to the plasma membrane as well at bright endosome-like structures (~ 40% of HEK293 cells examined) in laser-scanning confocal microscopy experiments (Figure 1A). Spinning-disc confocal analysis of the wild type clone also revealed a high level of RGS4-containing endosome activity including the slower-moving structures described above and numerous less fluorescent rapidly-moving endosomes that were not readily discernible by the laser-scanning technique (Supplemental Movie 1). Mutation of L23 within the amphipathic helix domain (L23D) resulted in complete redistribution of RGS4 from the plasma membrane to the cytosol and an apparent loss of RGS4 localization to the endosomal compartment. Spinning-disc confocal microscopy of L23D confirmed loss of RGS4 within both the bright slow moving and rapidly-moving endosome pools. (Supplemental Movie 2)

Compared to controls, expression of Gq(R183C) markedly increased the production of inositol phosphates in HEK293 cells. Co-expression of wild type RGS4 with Gq(R183C) resulted in an ~ 80% reduction in inositol phosphate production. Consistent with the notion that proper plasma membrane targeting is required for its function, the mislocalized L23D mutant was unable to inhibit Gq(R183C)-mediated inositol

phosphate production compared to wild type RGS4 (Figure 1B). Thus, the L23D mutant could be used as a nonfunctional RGS transfection control for other mutants to be analysed.

We focused first on whether palmitoylation of the amino terminus was an important determinant of its plasma membrane localization and function in mammalian cells. Indeed, inhibition of endogenous palmitoyl-CoA transferases with 2-bromopalmitate (2-BP) resulted in marked redistribution of RGS4 from the plasma membrane to the cytosol (Figure 2A). To determine the potential contribution of Cys2- and Cys12-palmitoylation to the membrane localization of RGS4, we studied the localization of individual (C2A or C12A) and combined (C2A; C12A) alanine mutations. Supporting the notion that palmitoylation of the amino terminus is a key determinant of human RGS4 localization in human cells, the combined mutation of Cys2 and Cys12 dramatically decreased plasma membrane:cytosol localization ratio (Figures 2B & 2C). Indeed, the extent of mislocalization of the combined mutant approached that of the L23D clone. Evidence that a loss of palmitoylation may explain the mislocalization of the mutant RGS4 protein came from palmitate-labeling studies, where introduction of the C2A;C12A mutant all but abolished incorporation of the palmitic acid analogue 17-octadecynoic acid (Figure 2D). Also of interest was the observation that, like L23D, the C2A:C12A mutant show dramatically reduced endosomal localization when it was examined by spinning disk microscopy (Supplemental Movie 3). Surprisingly, mutation of Cys12 alone (C12A), but not Cys2 (C2A) was sufficient to disrupt the plasma membrane targeting of RGS4. Notably, the effect of the cysteine mutations on plasma membrane:cytosol ratio was similar in both the absence (Figure 2) and the presence (Figure 3) of coexpressed GqR183C. It did appear, however, that active Gq modestly increased plasma membrane:cytosol ratio of all the wild type and cysteine mutants , presumably via its ability to recruit some RGS4 from the cytosolic pool.

Functional studies for the RGS4 cysteine mutant series mostly paralleled

the plasma membrane localization data. Specifically, compared to the wild type protein the mislocalized C12A and C2A;C12A proteins showed virtually no Gq-inhibitory function whereas the C2A protein retained some Gq inhibitory function (Figure 4). In an attempt to explain the differential importance of Cys2 and Cys12 with respect to RGS4 localization and function we used a helical net projection to map the positions of Cys2 and Cys12 relative to the stretch of amino acids in RGS4 containing its amphipathic helix domain (amino acid residues 12-30) (Figure 5). Based on the relative proximity of Cys12 to this helix domain and its position immediately adjacent to the putative membrane-binding surface, it seems likely that palmitoylation of Cys12 would have a greater impact on the length of the hydrophobic interface of the helix than would palmitoylation of Cys2. Previous work on the RGS2 protein showed that the length of the aliphatic interface had a profound effect on its plasma membrane localization and Gq-inhibitory function (15).

Since palmitoylation regulates intracellular trafficking of multiple components of the GPCR signaling pathways including G-protein α subunits (16), RGS proteins (17), and some RGS protein-binding proteins (18) we next examined the extent to which palmitoylation on Cys2 or Cys12 affects the intracellular trafficking of RGS4. The spinning-disk confocal data discussed above provided preliminary evidence that mutation of C2 and C12 may alter endosomal localization of RGS4. We next used laser scanning confocal to more carefully quantify this effect. RGS4-YFP was observed in discreet intracellular compartments in ~ 40% of the cells examined (Figure 6). Addition of 2-BP dramatically reduced targeting of RGS4 to the endosome compartment (data not shown). Notably, Cys2 and Cys12 seem to contribute differentially to the distribution of RGS4 within the intracellular pool. Mutation of Cys12 reduced the percentage of cells showing endosomes to ~15% while mutation of Cys2 nearly completely disrupted RGS4 localization to endosomal structures (Figure 6).

G-protein alpha subunits cycle between the plasma membrane and the Golgi compartment. Palmitoylation at the level of the Golgi is a key step in this process (16). We wondered whether the Cys2 and Cys12 palmitoylation sites on RGS4 may likewise be a component of its cycling between the PM and Golgi. Indeed RGS4 was reported to be associated with both the PM and Golgi compartments (19). We thus examined the potential for RGS4 to colocalize with TGN38, a trans-Golgi compartment marker known to traffic constitutively between the Golgi and plasma membrane(20). In cells expressing TGN38-CFP, it is localized primarily to the trans-Golgi region as expected, but its expression was also observed in endosomal structures proximal to the Golgi. Although strong trans-Golgi colocalization was not observed for wild type RGS4-YFP, the fluorescent endosomes containing RGS4 frequently coincided with vesicles containing TGN38-CFP (Figure7A). Indeed, when the entire RGS4-YFP endosome population was examined for its colocalization with TGN38-CFP, a Pearson correlation coefficient (PCC) of 0.32 was obtained. Consistent with a differential role for Cys2 and Cys12 in the intracellular trafficking of RGS4, endosomes containing the C12A mutant showed a high extent of colocalization with TGN38-CFP (PCC = 0.75) whereas endosomes containing C2A or the double mutant C2A:C12A were poorly colocalized with the TGN38 pool (PCC values of -0.1 and -0.3 respectively) (Figure7B). Together, these data suggest that putative palmitoylation of Cys2 or Cys12 differentially affects the trafficking of RGS4 along endosome recycling circuits that normally allow the traffic of RGS4 and other similarly recycled proteins such as TGN38 between the plasma membrane and Golgi.

The potential significance of the difference in TGN38 colocalization between wild type RGS4- and C12A-containing endosomes was examined in Figure 8. When scatter plots of endosome colocalization coefficient versus diameter were examined, two interesting patterns emerged. First, the wild type protein has a vastly different endosome size distribution profile compared to C12A. In particular, the wild type protein is observed much more commonly in small sized (< 1 μm) endosomes than is the

C12A protein (73% versus 35% of total endosomes respectively). Secondly, when the size distribution of endosomes with high and low TGN38 colocalization coefficients is compared we observe that for the wild type clone there is a large (39% of total endosomes) pool of small sized endosomes that does not colocalize with TGN38. The mutation of Cys12 seems to prevent the localization of RGS4 to this small sized TGN38-deficient pool since most Cys12 containing endosomes contain TGN38 irrespective of their size (Figure 8). Taken together, these data are consistent with a model where palmitoylation at either Cys2 or Cys12 can differentially regulate the intracellular trafficking of RGS4. Mutation at Cys2 almost completely eliminates its endosomal localization whereas mutation at Cys12 impairs its localization to TGN-38-refractory endosomes without affecting its targeting to a TGN38 containing endosomal compartment.

DISCUSSION

Over the last decade, palmitoylation has been shown to be a key regulator of signaling protein localization and function. Specifically, this reversible post-translational modification of cysteine residues regulates the intracellular trafficking of proteins such as ras, Gαi, Gαq and Src-family kinases and helps promote their proper intracellular trafficking (19,21). Potential sites of palmitoylation are often clustered together within protein domains and in many cases they are believed to work in concert to promote proper intracellular targeting. Such is believed to be the case for the tyrosine kinases Fyn, Yes (21) and Lck (22) that undergo palmitoylation at cysteine residues 3 and 6 in their amino terminal targeting domain (23). It has been similarly suggested that a pair of closely spaced cysteines (Cys 2 and Cys 12) found in the amino terminal domains of RGS4, RGS5, and RGS16 may work in concert to promote their proper localization and G-protein inhibitory function (24). We here show the surprising result however, that Cys2 and Cys12 appear to act independently to modulate plasma membrane targeting, intracellular trafficking and function of RGS4 in mammalian cells.

We set out to characterize the relative contribution of determinants within RGS4 that are necessary for its plasma membrane targeting and function in mammalian cells. Consistent with previous studies that showed the relative importance of the amphipathic helical domain (9); the L23D mutant remained completely cytosolic with no detectable membrane localization. It was interesting to observe that inhibition of RGS4 palmitoylation by 2-bromoplamitate also results in a complete disruption of plasma membrane targeting. Thus, the amphipathic helix domain and cysteine palmitoylation both appear necessary but not sufficient for optimal plasma membrane targeting of human RGS4 in human cells. Together these data indicate that the G-protein binding domain (RGS box) with its previously reported palmitoylation site at Cys95 may not be a primary determinant of RGS4 plasma membrane localization. However, the observation that C2A:C12A shows low, but appreciable levels of tonic membrane localization compared to L23D and WT following 2-BP addition suggests that Cys95 may contribute a minor component of RGS4's membrane targeting capacity.

The data herein show that Cys12, the palmitoylatable residue adjacent to the amphipathic helix domain, is the most important cysteine residue for plasma membrane targeting of RGS4. By contrast, Cys2 residue appears to be dispensable for membrane localization of RGS4. The simplest explanation for these data is that palmitoylation of Cys12 increases the length of hydrophobic surface of the amphipathic alpha helix to promote greater steady-state association with the inner leaflet of the plasma membrane. In an analogous situation, an extended hydrophobic surface of the RGS2 amphipathic helix was shown to be critical for its strong localization to the cell membrane (15). Circular dichroism studies have shown that peptides containing the amphipathic helical domain of RGS4 maintain a disordered (random coil) structure until presented with lipid vesicles whose phospholipid composition resembles the anionic plasma membrane inner leaflet (9). Whereas Cys12 palmitoylation may be able to cooperate with the adjacent hydrophobic amino acids to promote formation of an extended helix domain

(one additional turn), it may be that Cys2 palmitoylation is located at too great a distance from the core helix to promote extended helix formation. It is prudent, however, to consider the alternative possibility that Cys12, in its palmitoylated or non-palmitoylated state, is working independently from the amphipathic helix to promote association with an unknown plasma membrane protein or protein complex. Consistent with the notion that membrane targeting is necessary for RGS4 function, mutation of Cys12 in the context of both the C12A and C2A; C12A reduced RGS4 Gq inhibitory function to a level similar to that of the L23D mutation. Functional data for the C2A mutant, however, suggest that membrane localization alone may not be sufficient for optimal RGS4 activity. Specifically, despite the strong membrane localization of the C2A, this clone also showed a measurable decrease in its Gq inhibitory function suggesting that Cys2 may contribute to an additional previously uncharacterized functional activity to RGS4. It is important to note that this novel activity appears to be independent from the known protein-stabilizing effects of Cys2 palmitoylation (11,12) since protein expression levels were normalized at the transfection stage for these experiments. Instead, it may be that Cys2 in its palmitoylated or non-palmitoylated states promotes interaction between RGS4 and Homer2 (25) or a similar docking protein that might increase its G-protein inhibitory activity. It will be interesting to determine the residues on RGS4 that are required for its interaction with Homer2 and whether palmitoylation enhances this interaction.

Many palmitoylated proteins shuttle continuously between the plasma membrane and other intracellular compartments (16, 21, 26-28). Since 2-BP treatment of RGS4-transfected cells completely prevented its localization to the endosomal compartment, we asked whether Cys2 and Cys12 may contribute to endosomal trafficking and localization of RGS4. The C2A mutant showed dramatically impaired localization to the endosomes population consistent with the idea that endosome localization is dependent on Cys2 palmitoylation. If endosome localization is required for a posttranslational modification or protein interaction that serves to increase RGS4 function, then its impaired localization to

the endosome pool could explain its impaired inhibition of Gq signalling. It will be of future interest to determine whether RGS4 activity promoting modifications such as PKG/PKA-dependent phosphorylation (29), Ca2+/calmodulin-binding (30), spinophilin (31) and/or Homer2 interaction (25) require recycling of RGS4 through an endosomal compartment. By contrast, the C12A mutation had a quite distinct effect on endosomal localization. Although this mutant targeted TGN38-containing endosomes with a similar efficiency as the wild type protein, it was completely absent from the TGN38-deficient pool of small-sized endosomes that is normally populated by the wild type protein. To the extent that trafficking of RGS4 through endosome compartments that do not contain TGN38 may be important for its G-protein function, this observation might further serve to explain the lack of inhibitory activity that we observed for the C12A mutants.

The fact that the L23D amphipathic α-helix mutant did not populate either endosomal compartment is consistent with the possibility that these previously unreported structures are bounded by lipid bilayers. The nature of the compartment that is populated by both wild type and C12A mutant proteins is of much interest. Its high TGN38 expression and localization deep within the cytosol suggest that it may be an intracellular sorting compartment related to the trans-Golgi network. To our knowledge no such compartments have been previously described for fluorescently tagged TGN38 constructs. Clearly, Cys12 is not required for localization to this endosomal structure. Taken together these data are consistent with a model whereby sequential palmitoylation of Cys2 and Cys12 may be required to promote proper trafficking of RGS4 between the plasma membrane, Golgi and endosomal compartments. Specifically, Cys2 palmitoylation would allow access to the endosomal TGN38-containing pool and Cys12 palmitoylation presumably occurring within that compartment would be required for exiting that TGN38 containing pool. The precedent for this type of sequential trafficking model are proteins such as H- or N-Ras where palmitoylation was shown to be required for them to migrate

out of the Golgi (32,33). This model would also suggest that the different Golgi-associated and endosomal compartments through which RGS4 and other palmitoylated proteins traffic may contain palmitoyl-transferases (DHHC family members) with different substrate specificities or compartmentalizations to facilitate efficient movement of proteins from one compartment to another.

In summary, we show here for the first time that two putative palmitoylation sites in the RGS4 amino terminus, Cys2 and Cys12, may have unique and complementary activities with respect to mediating intracellular localization and Gq inhibitory function. Cys12 appears to be more important for plasma membrane targeting and endosomal trafficking whereas Cys2 appears more important for trafficking within intracellular pathways. It will, therefore, be of future interest to characterize the effects of the two palmitoyl-CoA transferases known to palmitoylate RGS4 (DHHC3 and DHHC7) on its localization trafficking and function to determine whether there may exist a specificity of these enzymes for Cys2 or Cys12. Moreover extending the characterization of the endosomal pools of RGS4 might be critical for understanding their importance in the functionality of RGS4. Lastly, given the similarity of the amino terminal domains of RGS5 and RGS16, it will be of interest to determine whether Cys2 and Cys12 play similar complimentary roles in the regulation of these closely related RGS protein family members.

ACKNOWLEDGEMENTS:

We are grateful to Dr. Hangjun Zhang and David Cowieson for their technical support on this project. We would also like to acknowledge Dr. Christian Rolando at “La Plateforme Proteomique de Lille”, University of Lille 1 in France for his generous support, mentorship (G.B.), and critical evaluation of this work. This work was funded by the Heart and Stroke Foundation of Canada Grant-in-Aid Program (S.P.H., #T6799).

REFERENCES:

1. Wilkie, T. M. (2000) *Annu Rev Biochem* **69**, 795-827
2. Berman, D. M., Wilkie, T. M., and Gilman, A. G. (1996) *Cell* **86**, 445-452
3. Watson, N., Linder, M. E., Druey, K. M., Kehrl, J. H., and Blumer, K. J. (1996) *Nature* **383**, 172-175
4. Pacey, L. K., Heximer, S. P., and Hampson, D. R. (2009) *Mol Pharmacol* **76**(1), 18-24
5. Cifelli, C., Rose, R. A., Zhang, H., Voigtlaender-Bolz, J., Bolz, S. S., Backx, P. H., and Heximer, S. P. (2008) *Circ Res* **103**(5), 527-535
6. Ruiz de Azua, I., Scarselli, M., Rosemond, E., Gautam, D., Jou, W., Gavrilova, O., Ebert, P. J., Levitt, P., and Wess, J. *Proc Natl Acad Sci U S A* **107**(17), 7999-8004
7. Xie, Y., Wolff, D. W., Wei, T., Wang, B., Deng, C., Kirui, J. K., Jiang, H., Qin, J., Abel, P. W., and Tu, Y. (2009) *Cancer research* **69**(14), 5743-5751
8. Tu, Y., Popov, S., Slaughter, C., and Ross, E. M. (1999) *J Biol Chem* **274**(53), 38260-38267
9. Bernstein, L. S., Grillo, A. A., Loranger, S. S., and Linder, M. E. (2000) *J Biol Chem* **275**(24), 18520-18526
10. Srinivasa, S. P., Bernstein, L. S., Blumer, K. J., and Linder, M. E. (1998) *Proc Natl Acad Sci U S A* **95**(10), 5584-5589
11. Davydov, I. V., and Varshavsky, A. (2000) *J Biol Chem* **275**(30), 22931-22941
12. Bodenstein, J., Sunahara, R. K., and Neubig, R. R. (2007) *Mol Pharmacol* **12**, 12

13. Wang, J., Xie, Y., Wolff, D. W., Abel, P. W., and Tu, Y. (2010) *FEBS Lett* **584**(22), 4570-4574

14. Heximer, S. P. (2004) *Methods Enzymol* **390**, 65-82.

15. Gu, S., He, J., Ho, W. T., Ramineni, S., Thal, D. M., Natesh, R., Tesmer, J. J., Hepler, J. R., and Heximer, S. P. (2007) *J.Biol.Chem.* **282**(45), 33064-33075

16. Tsutsumi, R., Fukata, Y., Noritake, J., Iwanaga, T., Perez, F., and Fukata, M. (2009) *Mol Cell Biol* **29**(2), 435-447

17. Rose, J. J., Taylor, J. B., Shi, J., Cockett, M. I., Jones, P. G., and Hepler, J. R. (2000) *J Neurochem* **75**(5), 2103-2112

18. Jia, L., Linder, M. E., and Blumer, K. J. (2011) *J Biol Chem* **286**(15), 13695-13703

19. Sullivan, B. M., Harrison-Lavoie, K. J., Marshansky, V., Lin, H. Y., Kehrl, J. H., Ausiello, D. A., Brown, D., and Druey, K. M. (2000) *Mol Biol Cell* **11**(9), 3155-3168

20. Reaves, B., Horn, M., and Banting, G. (1993) *Mol Biol Cell* **4**(1), 93-105

21. Sato, I., Obata, Y., Kasahara, K., Nakayama, Y., Fukumoto, Y., Yamasaki, T., Yokoyama, K. K., Saito, T., and Yamaguchi, N. (2009) *J Cell Sci* **122**(Pt 7), 965-975

22. Zimmermann, L., Paster, W., Weghuber, J., Eckerstorfer, P., Stockinger, H., and Schutz, G. J. (2009) *J Biol Chem* **285**(9), 6063-6070

23. Koegl, M., Zlatkine, P., Ley, S. C., Courtneidge, S. A., and Magee, A. I. (1994) *Biochem J* **303 (Pt 3)**, 749-753

24. Osterhout, J. L., Waheed, A. A., Hiol, A., Ward, R. J., Davey, P. C., Nini, L., Wang, J., Milligan, G., Jones, T. L., and Druey, K. M. (2003) *J Biol Chem* **278**(21), 19309-19316

25. Shin, D. M., Dehoff, M., Luo, X., Kang, S. H., Tu, J., Nayak, S. K., Ross, E. M., Worley, P. F., and Muallem, S. (2003) *J Cell Biol* **162**(2), 293-303

26. Aicart-Ramos, C., Valero, R. A., and Rodriguez-Crespo, I. *Biochim Biophys Acta* **1808**(12), 2981-2994

27. Lu, W., and Roche, K. W. *Curr Opin Neurobiol*

28. Rush, D., Leon, R., McCollum, M., Treu, R., and Wei, J. *Biochem J*

29. Huang, J., Zhou, H., Mahavadi, S., Sriwai, W., and Murthy, K. S. (2007) *Am J Physiol Cell Physiol* **292**(1), C200-208

30. Popov, S. G., Krishna, U. M., Falck, J. R., and Wilkie, T. M. (2000) *J Biol Chem* **275**(25), 18962-18968

31. Liu, W., Yuen, E. Y., Allen, P. B., Feng, J., Greengard, P., and Yan, Z. (2006) *Proc Natl Acad Sci U S A* **103**(48), 18338-18343

32. Apolloni, A., Prior, I. A., Lindsay, M., Parton, R. G., and Hancock, J. F. (2000) *Mol Cell Biol* **20**(7), 2475-2487

33. Misaki, R., Morimatsu, M., Uemura, T., Waguri, S., Miyoshi, E., Taniguchi, N., Matsuda, M., and Taguchi, T. *J Cell Biol* **191**(1), 23-29

FIGURE LEGENDS:

Figure 1: Disruption of RGS4 plasma membrane targeting domain abrogates its Gq inhibitory function in HEK293 cells. *A*. Localization of YFP fusion constructs was examined by transient transfection and confocal microscopy in live HEK293 cells. Shown are YFP fluorescence images of the basal side (relative to the nuclear equator) of the cells with low to intermediated fluorescence. Images are representative of at least 80 cells examined in each of 3 independent experiments. *Scale bars* represent 1 μm. *B*. Inositol phosphate production was measured using ^{3}H-myoinositol labeling of transfected cultures. HEK293 cells were co-transfected with vector control or constitutively active Gq(R183C) and the indicated HisStrep-tagged RGS4 construct. Relative expression levels of RGS4-HisStrep proteins and Gq(R183C) were determined by immunoblotting (*inset*). Following overnight labeling, inositol phosphate production was measured as described in the "Experimental Procedures". Values indicate absolute inositol phosphate/total soluble inositol ratios and are the mean of 5 independent experiments each performed in triplicate. Raw cpm data is presented in Supplemental Table IA. S.E. are indicated by *error bars*. One-way ANOVA with a Tukey's post hoc test was used to determine differences between groups ($*p < 0.001$).

Figure 2: Defining the effect of palmitoylation and N-terminal cysteine residues mutation on the plasma membrane targeting of RGS4. *A*. Localization of the wild type RGS4-YFP construct in the presence and absence of the palmitoyl-CoA transferase inhibitor 2-bromopalmitate (2-BP) was examined by confocal microscopy as described above. *B*. Localization of different YFP-tagged cysteine mutants of RGS4 fusion constructs in HEK293 cells. *Scale bars* represent 1 μm. *C.* The ratio of the RGS4-YFP signal between the cytosol and plasma membrane was analyzed by densitometry using ImageJ software. Shown are means ratio of n >80 cells. S.E. are indicated by *error bars.* D. ODYA-17 (palmitic acid analog)-labelling of wild type and cysteine mutants of RGS4. *Upper panel* shows the extent of palmitoylation labeling in the indicated RGS4 constructs as measured by epitope-tag

pulldown, click chemistry adduction of Alexa-488 and in-gel fluorescence. Control sample is from HEK cells not transfected with RGS4. *Lower panel* shows Western blot analysis of the pulldown eluates analyzed in the panel above. Where necessary, one-way ANOVA with a Tukey's post hoc test was used to determine differences between groups (*$p < 0.01$).

Figure 3: Localization of RGS4 wild type and mutant constructs is relatively unaffected by Gq(R183C). *A.* Localization of different YFP-tagged cysteine mutants of RGS4 fusion constructs in HEK293 cells in the presence of co-expressed Gq(R183C) was examined by confocal microscopy as described above. *Scale bars* represent 1 μm. *B.* The ratio of the RGS4-YFP signal between the cytosol and plasma membrane was analyzed as above (n >30). One-way ANOVA with a Tukey's post hoc test was used to determine differences between groups S.E are indicated by *arrow bars* (*$p < 0.05$).

Figure 4: Mutation of Cys2 and Cys12 exert differential effects on RGS4 Gq inhibitory activity. Inositol phosphate production was measured using ^{3}H-myoinositol labeling from triplicate wells for each transfection condition. Briefly, HEK293 cells were co-transfected with constitutively active Gq(R183C) and the indicated HisStrep-tagged RGS4 construct. Relative expression levels of RGS4-HisStrep proteins and Gq(R183C) were determined by immunoblotting (*inset*). Following overnight labeling, inositol phosphate production was measured as described in the "Experimental Procedures". Values indicate the mean inositol phosphate/total soluble inositol ratio relative to that for the internal RGS4-inactive control (L23D) and are the mean of 5 independent experiments performed on separate days. Raw cpm data is presented in Supplemental Table IB. S.E. are indicated by *error bars*. One-way ANOVA with a Tukey's post hoc test was used to determine differences between groups (*$p < 0.05$).

Figure 5: Helical net modeling of the hydrophobic surface on the RGS4 amphipathic helix in non-palmitoylated (left) and mono-palmitoylated states. Shown is a 2D schematic

representation of the alpha helical RGS4 membrane association domain. Arrows denote putative palmitoylation sites (Cys2 and Cys12) in the RGS4 amino terminus. *Shading* indicates the length of the hydrophobic surface on the amphipathic α-helix of RGS4. Aliphatic and nonpolar aromatic residues are shown as *black*, polar residues in *white* and palmitoylated cysteine residues in *yellow*. Note how Cys12 palmitoylation may be predicted to increase the length of the hydrophobic surface by at least one turn of the helix.

Figure 6: RGS4 requires the N-terminal amphipathic α-helix and amino-terminal cysteine residues for endosome localization. The indicated RGS4-YFP fusion constructs were examined for the presence of RGS4-containing endosomes. For each construct, cells with low to intermediate fluorescence intensity were scored for the presence or absence of endosome structures. Shown are the mean of the percentage of cells with RGS4-containing endosomes determined during 4 independent experiments (n > 40 cells/experiment, n > 180 total cells/construct). One-way ANOVA with a Tukey's post hoc test was used to determine differences between groups (*$p < 0.01$). S.E. are indicated by *error bars.*

Figure 7: Colocalization of RGS4–containing endosomes with TGN38 is differentially affected by Cys2 and Cys12. Localization of RGS4-containing endosomal structures with the trans-Golgi-endosome marker TGN38 (TGN38-CFP) was examined by co-transfection in HEK293 cells followed by fluorescent microscopy of live cells. *A*. WT (*upper* and *lower panels* highlight the existence of both strongly (cell #1) and poorly (cell #2) colocalized endosomes in different cells), *B*. C2A (show typically poorly colocalized endosomes), *C*. C12A (show typically well-colocalized endosomes). Using the excitation and emission discrimination capabilities of the Olympus FV1000 confocal microscope, RGS4 (*red pseudocolor*) and TGN38 (*green pseudocolor*) images were collected from the same confocal plane. Merged images indicate areas of potential colocalization (shown in yellow). *Scale bars* represent 1μm. *D.* Pearson correlation coefficients (PCCs) for RGS4-containing endosomes with TGN38 expression were determined using Olympus Fluo-View software. Shown are mean PCC values (WT; n=84, C12A; n=70, C2A; n=12, and C2AC12A; n=12)

pooled from 4 independent experiments. Fisher's r to z' transformation was employed to determine differences between correlation coefficients of RGS4WT and C12A. (*$p < 0.0001$). S.E. are indicated by *error bars.*

Figure 8: Distribution of RGS4-containing endosomes by endosome size and TGN38 colocalization coefficient. Scatter plot for RGS4-containing endosomes comparing diameter and extent of colocalization with TGN38 colocalization (PCC). Plotted data were only available for WT and C12A as C2A and C2AC12A constructs localized very poorly to the endosome pool. The plot represents pooled data from 4 independent experiments. Each data point represents a single endosome. All RGS4-containing endosomes identified by microscopy were examined for their colocalization with TGN38. RGS4-containing endosomes were arbitrarily sorted into strongly (PCC > 0.4) and weakly (PCC < 0.2) TGN38-colocalized pools. Pool distribution profiles of RGS4-containing endosomes varied greatly between the WT and C12A constructs.

Figure1

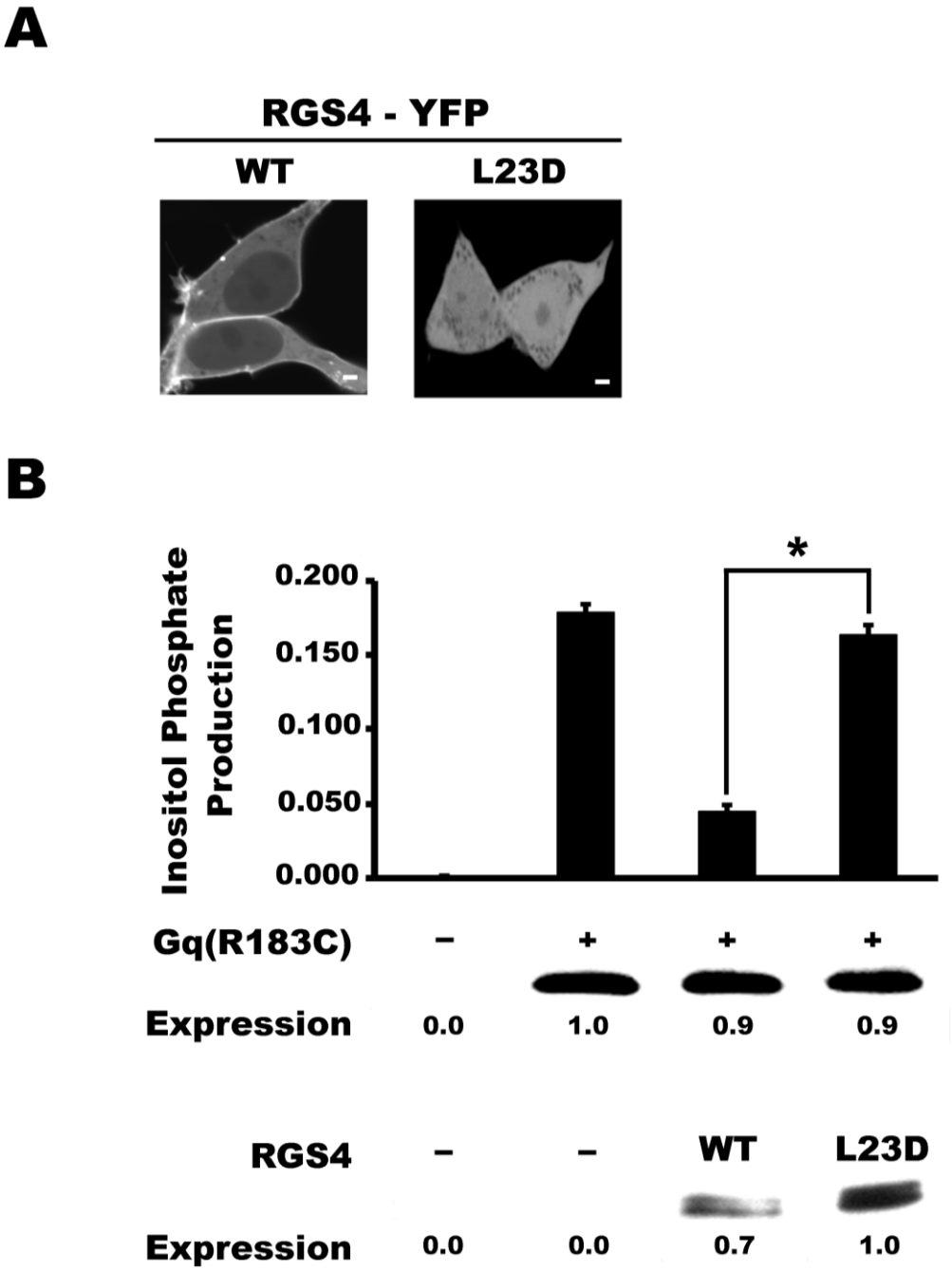

Figure2

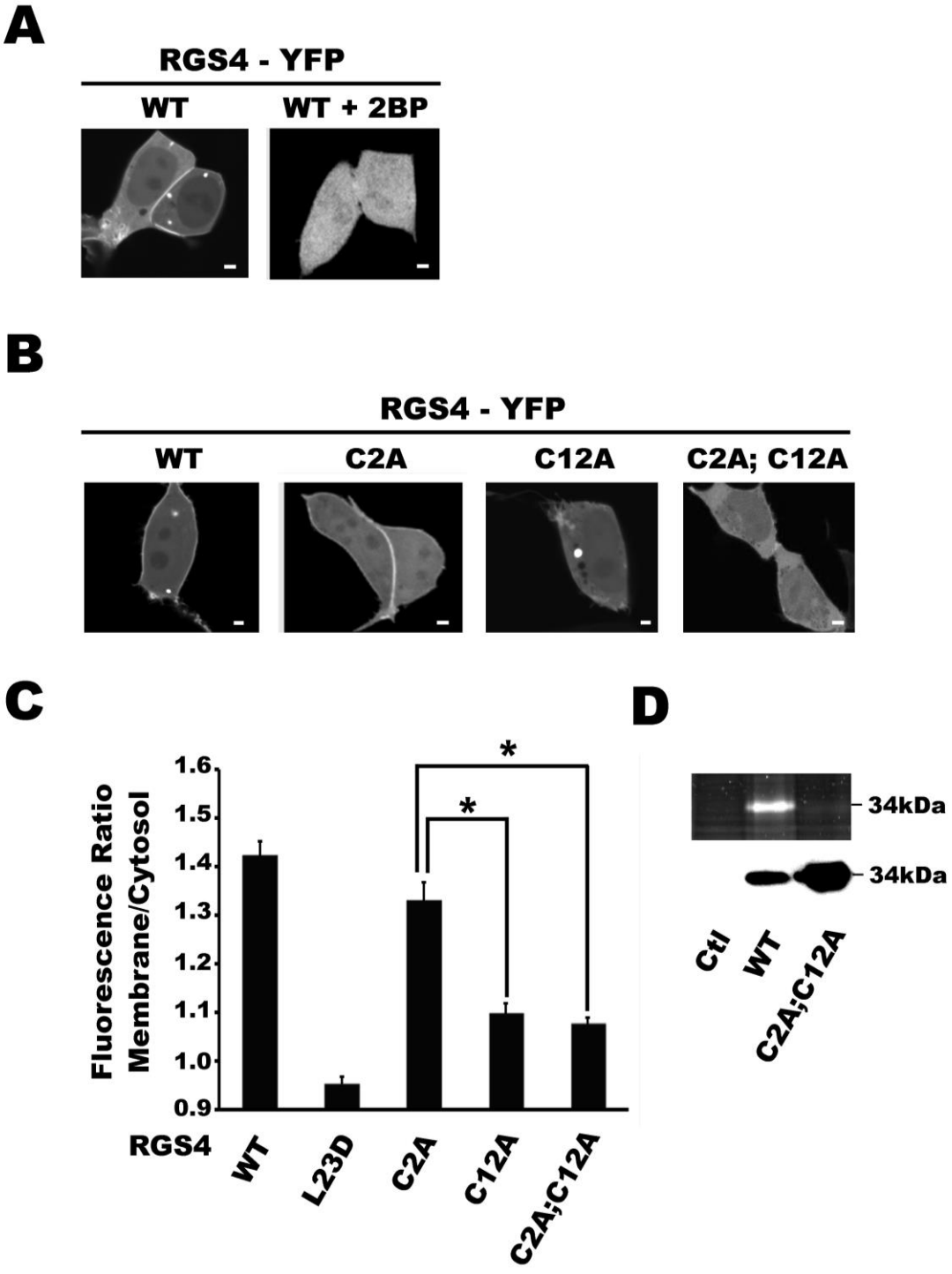

Figure3

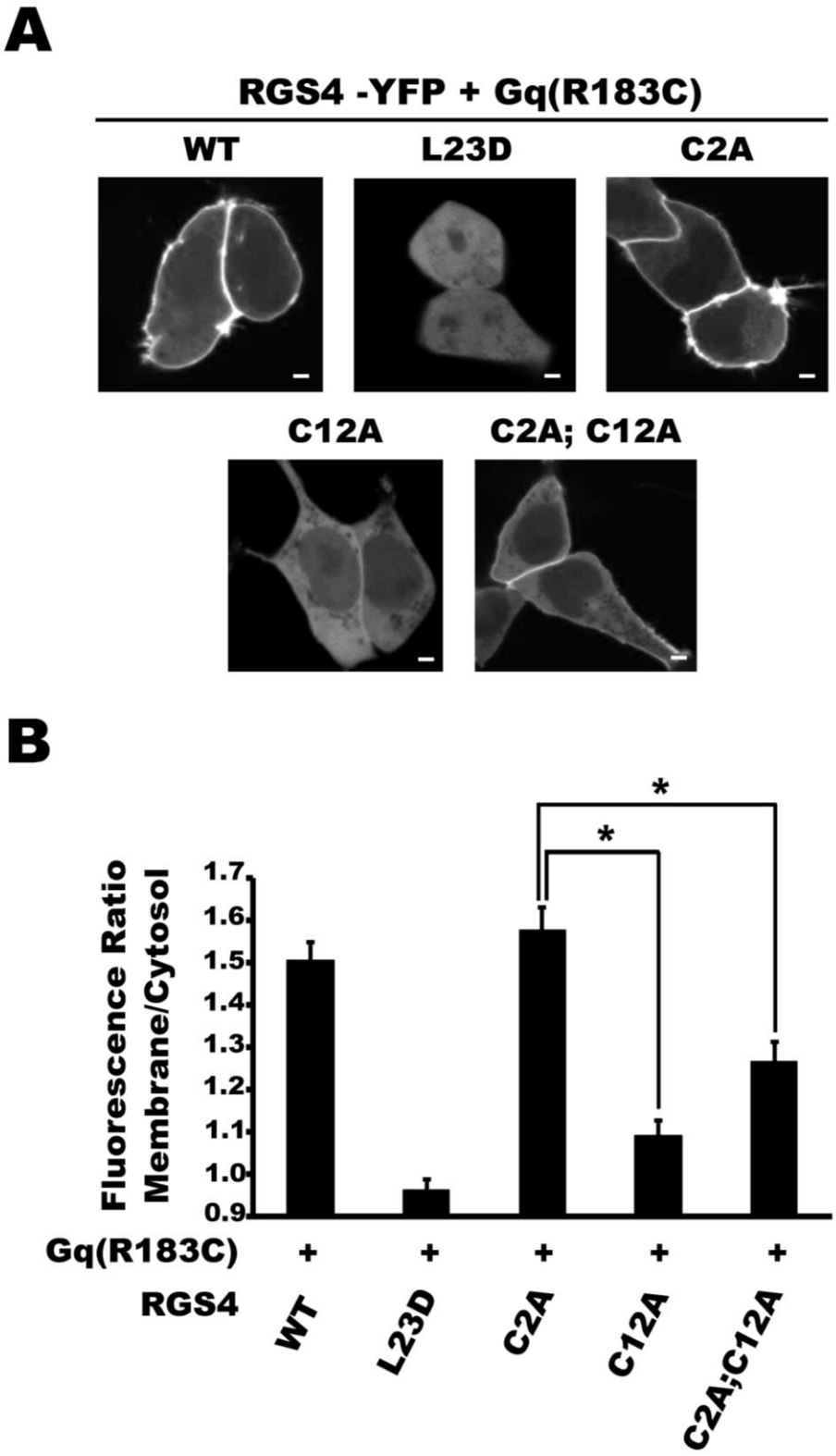

Figure4

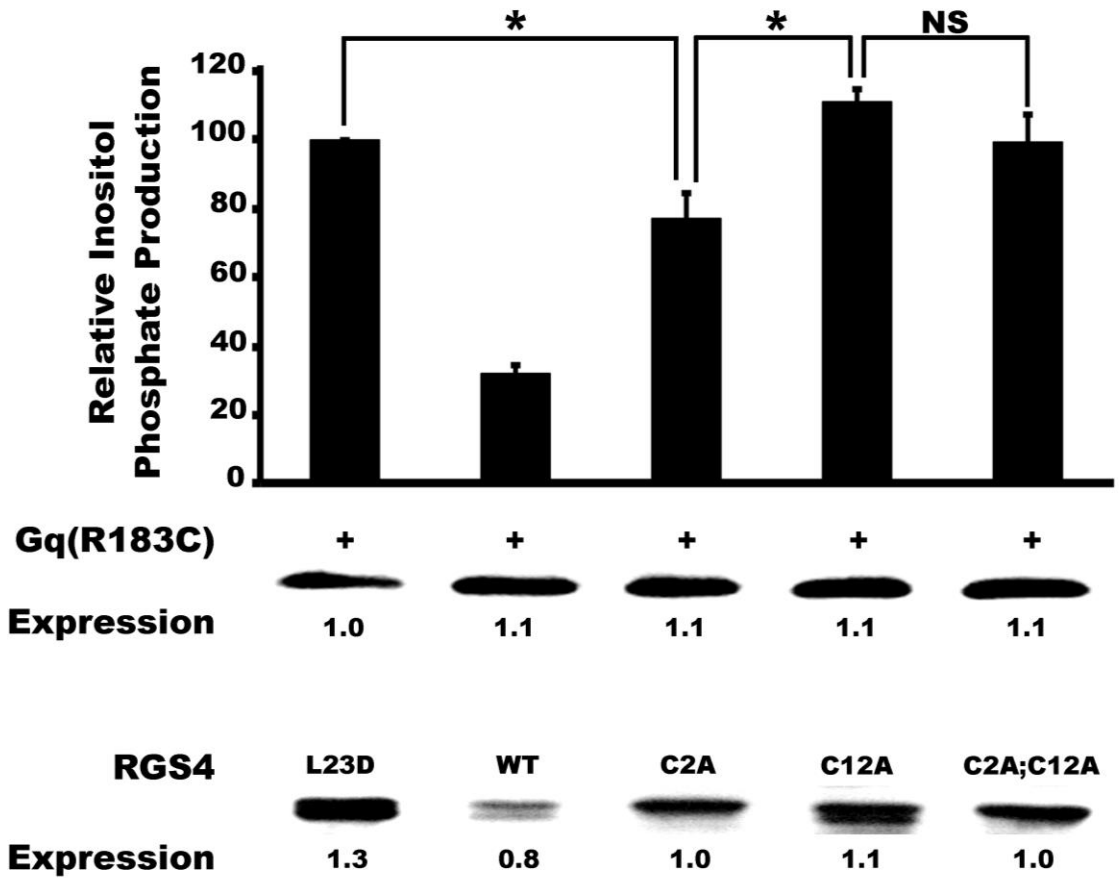

Figure5

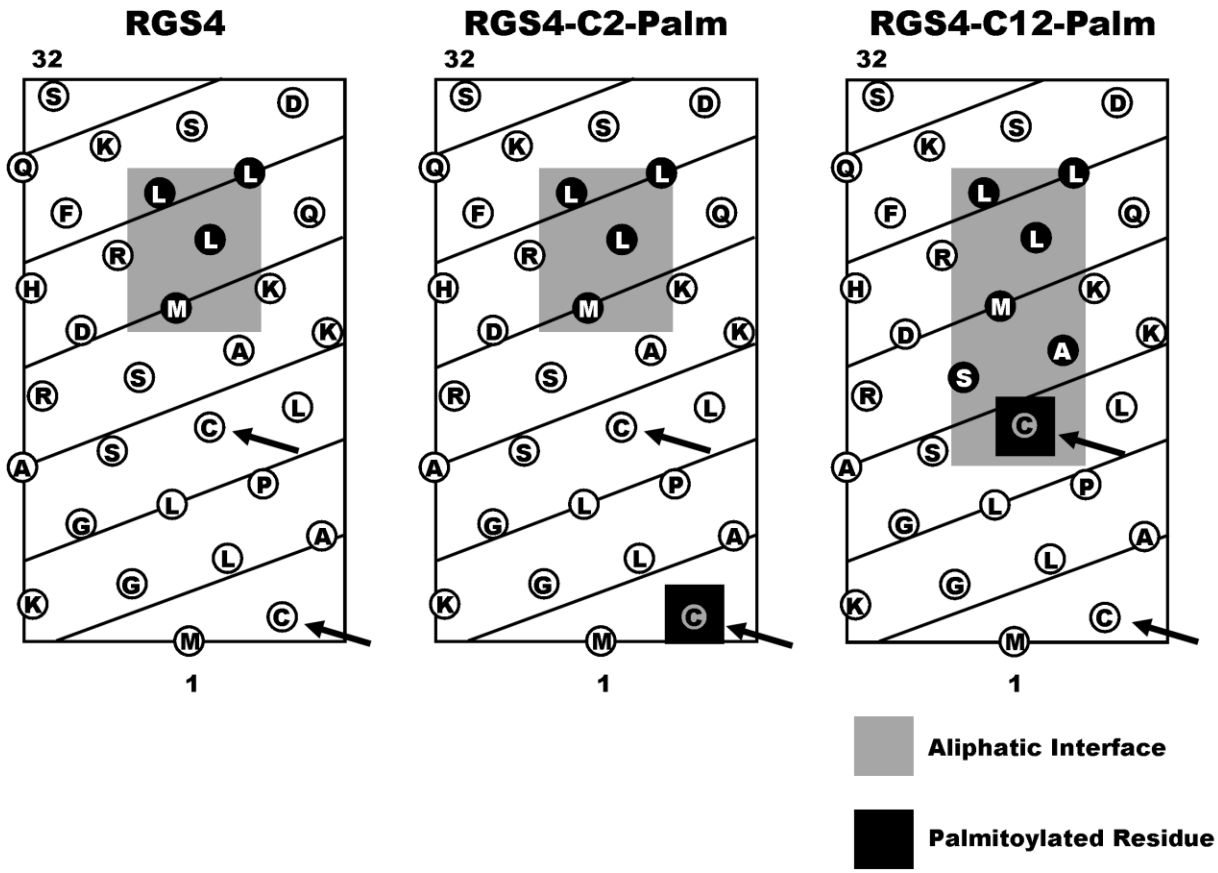

Figure6

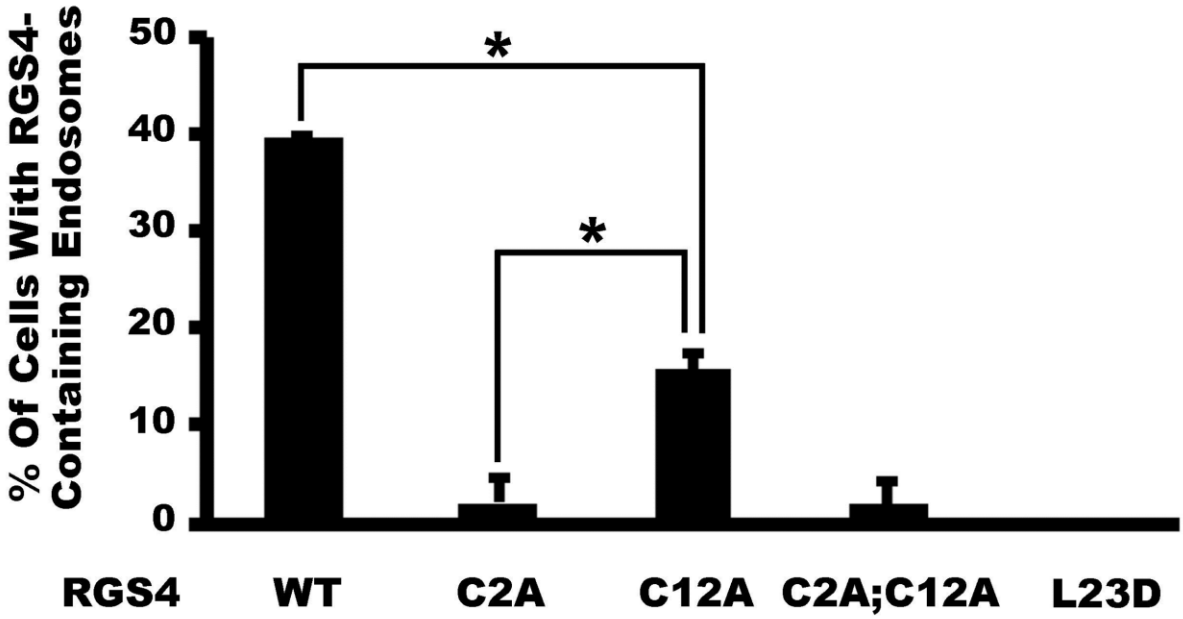

Figure7

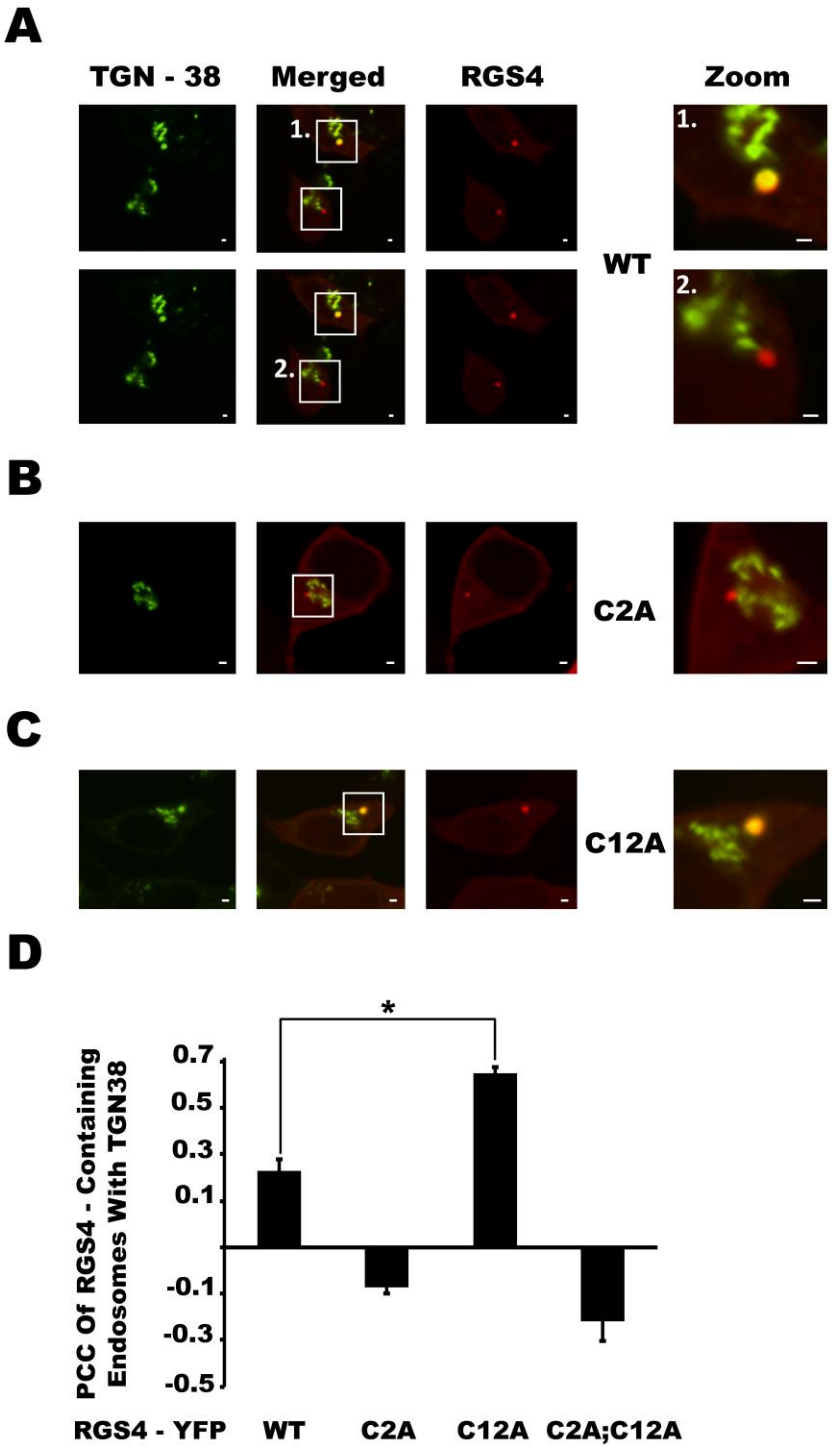

Figure8

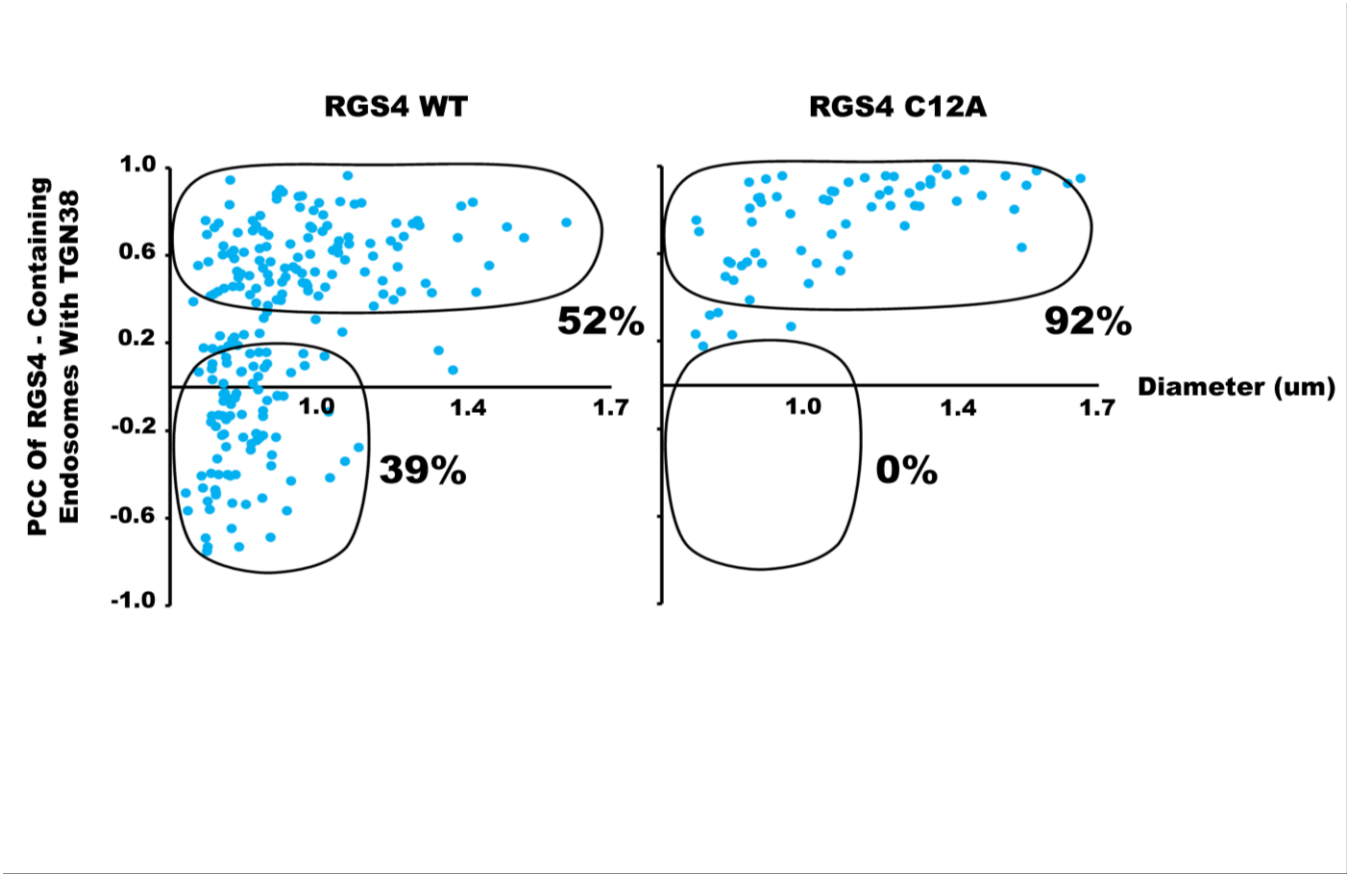

Supplemental Data

Primers for site directed mutagenesis:

RGS4 (C12A)

FWD 5'-gcaggtctgccggctagcgcgctgaggagtgcaaaagata-3'

REV 5'-tatcttttgcactcctcagcgcgctagccggcagacctgc-3'

RGS4 (C2A)

FWD 5'-agctagctagcgccaccatggccaaagggcttgcaggtctgcc-3'

REV 5'-ggcagacctgcaagccctttggccatggtggcgctagctagct-3'

RGS4 (L23D)

FWD 5'-aaaagatatgaaacaccgggacggtttcctgctgcaa-3'

REV 5'-ttgcagcaggaaaccgtcccggtgtttcatatctttt-3'

Supplemental Tables:

Supplemental Data Tables IA and IB: Mean CPM data for experiments to measure inositol phosphate production experiments from cells expressing the indicated RGS4 clones (WT, L23D, C2A, C12A, C2A;C12A) with and without GqR183C (n=5 separate experiments

performed on 5 separate days). All conditions were simultaneously examined in each of the 5 experiments. Data in Table IA corresponds to raw data used to produce Figure 1B whereas data in Table IB corresponds to raw data used to produce Figure 4. *for purposes of standardization WT and L23D control data were used as functional comparators in both data sets.

Table IA: Loss of RGS4 plasma membrane targeting reduces its Gq inhibitory function

RGS4 clone	No RGS	No RGS	WT	L23D
GqR183C	-	+	+	+
Total (cpm +/- S.E.)	9768.8 +/- 891.2	10391.5+/-808.9	11855.6+/- 1009.8	13981.3 +/- 907.6
IP3 (cpm+/- S.E.)	27.0 +/- 8.0	1107.4 +/-116.2	343.3 +/- 34.2	1282.9 +/- 94.2
IP3/total	0.003	0,107	0,029	0,092

Table IB: Mutation of amino-terminal cysteine residues in RGS4 reduces its Gq inhibitory function

RGS4 clone	L23D*	WT*	C2A	C12A	C2A;C12A
GqRC	+	+	+	+	+
Total (cpm +/- S.E.)	13981.3 +/- 907.6	11855.6+/- 1009.8	13047.4+/- 862.7	12704.3 +/- 896.2	13168,6 +/- 878.2
IP3 (cpm+/- S.E.)	1282.9 +/- 94.2	343.3 +/- 34.2	935.4 +/- 79.9	1279.2 +/- 96.9	1185.5 +/- 53.7
IP3/total	0,092	0,029	0,072	0,101	0,090

Supplemental Figure Legends:

Supplemental Movie 1. RGS4 WT shows dynamic endosome pool. Spinning-disk confocal was used to capture the endosome dynamics of transiently transfected wild-type RGS4-YFP in living cells. Image sequences were collected using aYokogawa CSU10 spinning-disk unit and processed using the Volocity software package.

Supplemental Movie 2. RGS4 L23D shows reduced endosome dynamics. Spinning-disk confocal was used to capture the endosome dynamics of transiently transfected RGS4-YFP (L23D) in living cells. Image sequences were collected using aYokogawa CSU10 spinning-disk unit and processed using the Volocity software package.

Supplemental Movie 3. RGS4 C2A;C12A shows reduced endosome dynamics. Spinning-disk confocal was used to capture the endosome dynamics of transiently transfected wild-type RGS4-YFP (C2A; C12A) in living cells. Image sequences were collected using aYokogawa CSU10 spinning-disk unit and processed using the Volocity software package.